

SAMPLE PREPARATION FOR, AND CURRENT STATUS OF, THE ARGONNE PREMIUM COAL SAMPLE PROGRAM*

Karl S. Vorres
Chemistry Division, Building 211
Argonne National Laboratory
Argonne, IL 60439

ABSTRACT

The Argonne Premium Coal Sample Program includes eight coals (Upper Freeport, Wyodak-Anderson, Illinois #6, Pittsburgh, Pocahontas #3, Utah Blind Canyon, Lewiston-Stockton and Beulah-Zap seams) chosen to provide a range of chemical composition, including sulfur content, maceral content and geographic distribution. One of the purposes is to provide a set of pristine samples for comparison and correlation. They have been collected in ton-sized batches and processed to provide a minimal exposure to oxygen, thoroughly mixed, and packaged in borosilicate glass ampoules containing either 5 grams of -100 mesh or 10 grams of -20 mesh material. This material has been analyzed by a number of laboratories, including a round robin with Commercial Testing and Engineering Co. Further data are being added to an analytical data base as they become available. Over 190 shipments have been made to over 110 different users. Research is currently being carried out in almost every area of coal science with these samples.

* This work was supported by the Office of Basic Energy Sciences, Division of Chemical Sciences, U. S. Department of Energy, under contract number W-31-109-ENG-38.

INTRODUCTION

Goals:

The Premium Coal Sample Program was initiated at the Argonne National Laboratory about five years ago to provide the basic coal research community with a small number of carefully selected, collected, processed packaged and analyzed samples. The techniques of mixing, sealing and storage are intended to provide a large number of uniform samples that will be stable over a long time, and will permit reproducible experiments to be carried out at different times and laboratories.

Selection of Samples:

The coals included in the program were selected to give a range of composition in terms of the carbon, sulfur, hydrogen and oxygen contents. A cluster analysis involving data from over 200 channel samples in the existing Pennsylvania State University database was used to provide eight ranges of composition, from which the chemical composition characteristics of the eight samples were chosen. In addition they were selected to give a range of rank, geographical distribution, and maceral content.

In the order collected, these eight coals are:

#	Seam	Origin	Rank
1	Upper Freeport	PA	MVB
2	Wyodak-Anderson	WY	SUB
3	Illinois #6	IL	HVB
4	Pittsburgh	PA	HVB
5	Pocahontas #3	VA	LVB
6	Utah Blind Canyon	UT	HVB
7	Lewiston-Stockton	WV	HVB
8	Beulah-Zap	ND	LIG

The abbreviations are: LIG = lignite, SUB = subbituminous, HVB = high volatile bituminous, MVB = medium volatile bituminous, LVB = low volatile bituminous.

Collection:

Details of the procedures for collection have been given in earlier reports (1-8). In brief, the samples from underground mines were collected from freshly exposed blocks of coal, the thickness of the seam. Typical samples were about 1 1/2 tons. For thick underground seams (#3,4,5,6,7), the 55 gallon stainless steel drums were taken to the seam face, and representative samples were placed directly into the drums. For the thinner seam (#1) the sample was taken to the surface in double plastic bags. Surface mine samples (#2 and 8) were obtained from core samples.

Processing and Packaging:

At the surface the drums were purged with enough argon to reduce the oxygen content to 100 ppm, and quickly transported in a temperature-controlled semi-trailer to Argonne National Laboratory (ANL) for processing. AT ANL, the drums were weighed, placed into airlocks, purged, the contents were crushed, pulverized to -20 mesh, thoroughly mixed, and the contents were packaged. Half the batch was reground to -100 mesh, and then packaged. Packaging included placing about 80% of the coal in carboys of borosilicate glass for long term storage. The balance went into amber borosilicate glass ampoules of 10 grams of -20 mesh or 5 grams of -100 mesh material. The oxygen content of the packaging facility was maintained below 100 ppm at all times, and was typically about 30 ppm.

CURRENT STATUS

Inventory - Long Term Supply:

The ampoules and carboys are kept in a dark air-conditioned storage room. About 10,000 of the 5 gram ampoules and 5,000 of the 10 gram ampoules were made for each sample. Initially about 120,000 samples were placed in storage with about 550 of the 5 gallon carboys. As shipments deplete the inventory, then carboys can be placed in the packaging facility and additional ampoules filled and sealed to replenish the inventory. The current demand is such that the supply of ampoules should not need replenishing for another 6 years. The Illinois #6 sample is the most frequently requested.

Homogeneity:

Samples were taken during the processing to be irradiated and counted for homogeneity analysis. The results indicate that the samples were well mixed. Additional samples have been sent to a number of laboratories for analysis. Commercial Testing and Engineering Company performed a round robin analysis for the proximate analysis, and also carried out a number of ultimate, ash and other analyses as well.

Stability:

Stability analyses are carried out in two ways. The ampoules are routinely sent to the Analytical Chemistry Laboratory at ANL for gas analyses. The gas inside of the ampoules is analyzed for oxygen, hydrogen, nitrogen, carbon dioxide, methane, and other hydrocarbon gases. The results have indicated that no oxygen is entering the ampoules and the interior gas has a generally stable composition, with some tendency to liberate methane and carbon dioxide. The other stability study involves the gieseler plasticity analysis for the bituminous samples. These samples are sent at half year intervals for continued monitoring.

Analyses:

Other laboratories are encouraged to make the results of their analytical efforts known to the author so that they may be incorporated into a compendium of results for the benefit of all of the sample users. Table 1 gives a listing of the results for the analyses done by CT&E. The modified Parr formula used for the Dry mineral matter free content calculations was:

$$\text{Mineral matter(dry)} = 1.13 \text{ Ash} + 0.47 \text{ Pyritic S(dry)} + 0.50 \text{ Cl (dry)}$$

Other Studies:

This unique set of samples can advantageously be used to carry out a number of studies in a "round-robin" type of effort to help different laboratories compare their results, and develop an understanding of the differences in the coal samples. A study of the NMR characteristics of the samples is being planned, with the results to be shared near the end of 1989.

Shipments:

The acceptance and popularity of the samples may be gauged by the number of shipments, re-ordering and scope of work done with them. At the time of the writing, over 190 shipments had been made. These included over 110 different laboratories and investigators. Several of these have requested four different batches of samples. The shipments have gone approximately about 2/3 to academic institutions, and the rest about evenly divided between industrial and governmentally supported laboratories. About 5% of the shipments have gone to countries other than the U. S. A. The number of ampoules shipped has exceeded 6,000.

USGS Circulars - Geology and Geography:

In addition, the United States Geological Survey, which supervised the collection of the samples, is preparing a series of USGS Circulars, which will summarize the geological and geographical information of general interest about these samples. These may be obtained directly from the USGS.

Newsletter:

A newsletter has been initiated to provide current information of value to all recipients of the samples. The quarterly publication gave the contents of this symposium, and announced the development of a bibliography of references to the use of the Argonne Premium Coal Samples. All recipients of samples are asked to provide references to reports, journal articles and other public information so that this information may be shared with other investigators.

Types of Research Work:

The types of research being done with the samples are about as diverse as the research being done on coal. The symposia that follows will give a representative sample, but certainly does not include all of the work that is being done. The major fields include: structural studies, determination of the functional groups qualitatively and quantitatively in the coal, coalification, pyrolysis, liquefaction and gasification, sulfur removal, new methods of analysis and others.

Symposia:

This symposium is the second in a series devoted to research done with the Argonne Premium Coal Samples. The first, held in New Orleans in September, 1987 had 23 papers on a variety of topics. The organization this year is based on the subject matter of the individual papers. The range of work is such that a number of papers are finding their way into symposia on topics of special interest such as coal liquefaction, and this trend will probably continue.

Future Activities:

The APCSP will continue to provide samples and information about these samples to the users. It is planned to provide a data handbook to give in one document the most frequently requested information. This will include the results of the analytical work that is reported to the author, and special studies which have been arranged to provide for a reasonably complete set of information.

Further, individual studies may be initiated to respond to certain findings of potential interest to the user community. The observation of increased concentrations of methane and carbon dioxide in some of the ampoules led to speculation that anaerobic bacteria may be present with the samples. An effort is underway

to culture bacteria from samples of coal from each of the batches. The results of this effort will be described at a future meeting.

REFERENCES

1. Vorres, K. S., Preprints of the Fuel Chem. Div., Am. Chem. Soc., 32(4) 221-6(1987), *ibid.*, 32(1) 492(1987) (with S. K. Janikowski), 31(3), 304-9(1986) (with S. K. Janikowski), *ibid.*, 30(4), 193-6(1985), *ibid.*, 29(6) 230-3(1984).
2. Vorres, K. S., Proc. , Fourth Annual Pittsburgh Coal Conf., pp. 160-5, Sept 28-Oct. 2, 1987. Univ. of Pittsburgh.
3. Vorres, K. S., 1987 Intl. Conf. on Coal Science, pp. 937-40, Elsevier Science Publishers, BV., Amsterdam, 1987, ed. J. A. Moulijn, H. A. G. Chermin and K. A. Nater.
4. Vorres, K. S., 1985 Intl. Conf. on Coal Science, International Energy Agency, pp 640, October 28-31, Sydney, Australia.
5. Vorres, K. S. SME-AIME Annual Meeting, New York, February 1985, Paper #85-12.
6. Vorres, K. S., J. Coal Quality, 3(4), 31 (1984).
7. Vorres, K. S., Proc. of Workshop on Standards in Biomass for Energy and Chemicals, National Bureau of Standards, Gaithersburg, MD, 1-3 Aug. 1984, pp. 27-33. Ed. T. A. Milne, SERI/CP-234-2506.
8. Anon., Chem. Engr. News, 62(1)24(1984).

ACKNOWLEDGMENTS

The author gratefully acknowledges the support of the Office of Basic Energy Sciences, Division of Chemical Sciences of the U. S. Department of Energy. The efforts of many individuals who contributed at each stage of the program is deeply appreciated. Among these is the glass-blowing done by Joe Gregar.

Table 1. As-received and maf values Calculated from Dry Data from CT&E

Coal	UF	WY	IL	PITT	POC	UT	WV	ND
AR N2O	1.13	28.09	7.97	1.65	0.65	4.63	2.42	32.24
AR Ash	13.03	6.31	14.25	9.10	4.74	4.49	19.36	6.59
AR VM	27.14	32.17	36.86	37.20	18.48	43.72	29.44	30.45
AR S	2.29	0.45	4.45	2.15	0.66	0.59	0.69	0.54
AR Btu	13315	8426	10999	13404	14926	13280	11524	7454
Dry Ash	13.18	8.77	15.48	9.25	4.77	4.71	19.84	9.72
Dry VM	27.45	44.73	40.05	37.82	18.60	45.84	30.17	44.94
Dry S	2.32	0.63	4.83	2.19	0.66	0.62	0.71	0.80
Dry Btu	13467	11717	11951	13629	15024	13925	11810	11001
Dry C	74.23	68.43	65.65	75.50	86.71	76.89	66.20	65.85
Dry H	4.08	4.88	4.23	4.83	4.23	5.49	4.21	4.36
Dry N	1.35	1.02	1.16	1.49	1.27	1.50	1.25	1.04
Dry Cl	0.00	0.03	0.05	0.11	0.19	0.03	0.10	0.04
Dry F	0.00	0.00	0.00	0.00	0.00	0.00	0.00	0.00
Pyritic S	1.77	0.17	2.47	1.32	0.15	0.24	0.16	0.14
Sulfate S	0.00	0.03	0.01	0.01	0.03	0.03	0.03	0.03
Organic S	0.64	0.43	2.01	0.81	0.48	0.35	0.52	0.63
MAF C	85.50	75.01	77.67	83.20	91.05	80.69	82.58	72.94
MAF H	4.70	5.35	5.00	5.32	4.44	5.76	5.25	4.83
MAF N	1.55	1.12	1.37	1.64	1.33	1.57	1.56	1.15
MAF Org S	0.74	0.47	2.38	0.89	0.50	0.37	0.65	0.70
MAF Cl	0.00	0.03	0.06	0.12	0.20	0.03	0.12	0.04
MAF F	0.00	0.00	0.00	0.00	0.00	0.00	0.00	0.00
MAF O	7.51	18.02	13.51	8.83	2.47	11.58	9.83	20.34
MAF Btu	15511	12843	14140	15018	15777	14613	14733	12185

Dmmf values based on modified Parr formulas

Coal	UF	WY	IL	PITT	POC	UT	WV	ND
Dry Ash	13.18	8.77	15.48	9.25	4.77	4.71	19.84	9.72
Dry VM	27.45	44.73	40.05	37.82	18.60	45.84	30.17	44.94
Dry S	2.32	0.63	4.83	2.19	0.66	0.62	0.71	0.80
Dry Btu	13467	11717	11951	13629	15024	13925	11810	11001
MM Parr	15.73	10.00	18.68	11.13	5.56	5.45	22.54	11.07
Dry C	74.23	68.43	65.65	75.50	86.71	76.89	66.20	65.85
Dry H	4.08	4.88	4.23	4.83	4.23	5.49	4.21	4.36
Dry N	1.35	1.02	1.16	1.49	1.27	1.50	1.25	1.04
Dry Cl	0.00	0.03	0.05	0.11	0.19	0.03	0.10	0.04
Dry F	0.00	0.00	0.00	0.00	0.00	0.00	0.00	0.00
Pyritic S	1.77	0.17	2.47	1.32	0.15	0.24	0.16	0.14
Sulfate S	0.00	0.03	0.01	0.01	0.03	0.03	0.03	0.03
Organic S	0.64	0.43	2.01	0.81	0.48	0.35	0.52	0.63
Dmmf C	88.08	76.04	80.73	84.95	91.81	81.32	85.47	74.05
Dmmf H	4.84	5.42	5.20	5.43	4.48	5.81	5.44	4.90
Dmmf N	1.60	1.13	1.43	1.68	1.34	1.59	1.61	1.17
Dmmf Org	0.76	0.48	2.47	0.91	0.51	0.37	0.67	0.71
Dmmf Cl	0.00	0.03	0.06	0.12	0.20	0.03	0.13	0.04
Dmmf F	0.00	0.00	0.00	0.00	0.00	0.00	0.00	0.00
Dmmf O	4.72	16.90	10.11	6.90	1.66	10.88	6.68	19.13
Dmmf Btu	15980	13020	14696	15336	15908	14728	15247	12370

KINETICS OF VACUUM DRYING AND REHYDRATION IN NITROGEN OF COALS FROM THE ARGONNE PREMIUM COAL SAMPLE PROGRAM*

Karl S. Vorres and Roger Kolman
Chemistry Division, Building 211
Argonne National Laboratory
Argonne, IL 60439

ABSTRACT

The kinetics of vacuum drying and rehydration in nitrogen of Wyodak-Anderson subbituminous, and Illinois #6 and Utah Blind Canyon high volatile bituminous coal samples have been studied at room temperature. Some samples were oxidized at room temperature. Several cycles of drying and rehydration were carried out on the same sample. The drying rates depended on particle size and moisture content of the sample. Several different mechanisms of moisture loss and rehydration were indicated by the kinetic data. The mechanism depended on particle size, coal rank, and degree of oxidation.

* This work was supported by the Office of Basic Energy Sciences, Division of Chemical Sciences, U. S. Department of Energy, under contract number W-31-109-ENG-38.

INTRODUCTION

Drying and rehydration of a porous material can give some insight into the surface properties and the internal structure of the material. The rate of moisture removal or replacement will depend upon the coal surface, the macromolecular network of the coal particles and the structure of the pores through which the moisture flows.

An earlier study (1) reported the results of drying and rehydration studies on Illinois #6 Argonne Premium Coal Samples. The work involved different particle sizes and indicated that the mechanisms of drying and rehydration changed, depending on the coal particle size. The samples were fresh and aged, which also affected the results.

In general four mechanisms were observed (1). One involves a diffusion limited process of migration through a uniform barrier, and is observed with a parabolic curve. This is also referred to as Fickian diffusion. A second mechanism, obeying first order kinetics, similar to radioactive decay, would imply that the probability of a given water molecule being removed or adsorbed was a random probability event, and that all surface sites from which the water molecules depart or the water molecules in the sample were apparently equivalent. The third mechanism gives a plot following an adsorption isotherm curve. The mechanism here depends on the degree of surface coverage. A fourth mechanism, sometimes associated with the parabolic curve, is a linear mechanism implying a uniform barrier for diffusion.

The equation for the diffusion through a growing uniform barrier is:

$$W^2 = kt$$

where W is the mass change, k is a rate constant and t is the elapsed time.

The equation for the first order kinetics is:

$$\log W = k t$$

A characteristic half-time or half-life is associated with this reaction such that half the reaction is over in the half life, 3/4 is over in two half lives, 7/8 is over in three half lives etc.

For the adsorption or desorption reaction, the equation is:

$$W = k(t/t + 1)$$

A characteristic half time or half life is also associated with this reaction. The half time is the time for half of the observed change to take place. Then 2/3 of the reaction takes place in two half times, 3/4 takes place in three half times, 4/5 takes place in four half times etc.

The equation for the linear reaction is:

$$W = kt$$

This study extended the earlier work and involved examination of the drying and rehydration behavior of a lower rank Wyodak-Anderson sample, and a similar rank (but lower moisture content) sample from a different coal basin (Utah Blind Canyon seam).

APPARATUS, MATERIAL AND PROCEDURES

The studies were carried out with an Ainsworth recording thermobalance (described earlier (1)). The samples were weighed on a quartz pan and suspended from the balance. A quartz envelope was placed around the sample to control the gaseous environment. A water bath was placed around the sample to provide for temperature control to about 1° C. Initially the gas atmosphere was removed with a vacuum pump for dehydration. After dehydration, the samples were rehydrated by stopping the vacuum pump, backfilling with nitrogen, removing the quartz envelope, inserting an ice cube, re-evacuating to remove air, and backfilling with nitrogen. The ice cube was melted with warm water, and the water bath was replaced. The cycle was repeated by removing the quartz envelope and water, drying the envelope and replacing it and the water bath. From two to four cycles of dehydration and rehydration with the same sample were obtained in this way.

Sample weights varied between 0.100 and 1.112 grams. The weights used were:

IL #6 Block	1.112 grams
IL #6 -20 mesh	0.100 gram
IL #6 -100 mesh	0.239 gram
Wyodak -20 mesh	0.100 gram
UT Blind Canyon -100 mesh	0.346 gram

The data were recorded on chart paper and estimated to the nearest .01 mg. Buoyancy corrections for going between vacuum and atmospheric pressure were made. Due to some difficulties in establishing the initial weight during the conversions from vacuum to moist nitrogen and vice-versa (due to the rapidity of the change and the sensitivity of the sample to the change in conditions) the nature of the initial mass change is considered somewhat uncertain for some of the pulverized samples.

Data were transferred to a Lotus 1-2-3 file and analyzed on an IBM PC-XT microcomputer. Initial plots were generated from the program.

Some of the analytical data on the samples are as follows:

Sample	Moisture	Ash	Carbon (maf)
Wyodak-Anderson	28.09	6.31	75.01
Illinois #6	7.97	14.25	77.67
Utah Blind Canyon	4.63	4.49	80.69

RESULTS

The data for the samples was placed on a common basis of mass change in milligrams per gram of sample. The results for the Illinois #6 sample are given in Figures 1-6 for cycles of dehydration or of rehydration for the block, -20 mesh and -100 mesh material, respectively, at room temperature. Figures 7-8 indicate the data for the Wyodak sample at room temperature, while the Figures 9-10 indicate the data for the Utah Blind Canyon for room temperature. The points represent observed data, and continuous lines represent calculated results using the equations for the mechanisms which gave the best fit to the data. Numbers on the figures refer to the cycle of dehydration or rehydration to which the points correspond.

The mechanisms observed are summarized in Table 1.

DISCUSSION

The dehydration of the Illinois # 6 block followed a set of desorption curves. The amount of water desorbed depended on the amount initially present or returned during the rehydration step. The rehydration #2 was allowed to continue for 3 weeks and indicated that the amount of water which can be adsorbed under those conditions significantly exceeds the ASTM moisture value. The adsorption process is slow and probably would require a number of weeks for a one gram block to reach equilibrium. The desorption mechanism indicates that the rate controlling step involves a loss of moisture from the surface, rather than diffusion from the bulk of the particle to the surface.

The rehydration of the Illinois # 6 block followed a set of parabolic curves, of the type indicating a growing uniform barrier to further diffusion of moisture. This could indicate that the moisture swells the macromolecular network in a manner that uniformly impedes further increase of moisture. The effect of pores for this process is not noticeable.

The dehydration of the -20 mesh material is unique for the samples which have been studied. The initial loss was very low due to the small amount of moisture in the sample at the start. Subsequent runs followed a combination of linear and parabolic segments. The mass change for the initial linear segments increased from cycle 2 to cycle 3. The surface of this sample was oxidized which would provide a number of hydrophilic sites, in contrast to the hydrophobic sites to be expected on pristine samples. The moisture loss is significantly greater than the ASTM moisture value, and a large part takes place in the initial linear segment. This suggests that some moisture may be caught in the interstices of the particles. The ASTM moisture should be the sum of the moisture held in pores and in the macromolecular network. The pore moisture can be approximated by subtracting the amount taken up during the parabolic portion and the final linear part from the ASTM moisture. The amount in excess of the ASTM moisture may approximate the amount held in the interstices between the particles. The interstitial water is expected to be released quickly and following the linear mechanism.

The rehydration of the -20 mesh material was observed to largely follow the adsorption mechanism.

The dehydration of the -100 mesh sample followed the desorption model. The sample had initially been equilibrated with distilled water at room temperature and lost about 11 % moisture. The subsequent rehydration allowed only about 8 % moisture (the ASTM moisture) and that was lost in the following dehydration.

The rehydration curves initially followed an adsorption model and then showed evidence of multilayer formation. However, the subsequent dehydration did not show evidence of separate layers being desorbed.

A comparison of the rates of the reactions showed that the block is the slowest to change mass per gram. The initial rate for the -20 mesh reflects the low initial moisture content of that sample. The intermediate rate was indicated for the -100 mesh material, and the fastest rate for the oxidized -20 mesh material after the initial dehydration. This comparison is valid for both the dehydration and the rehydration mechanisms.

The dehydration data for the Wyodak sample indicated a desorption model.

The rehydration of the Wyodak sample indicated the formation of several layers of moisture following an initial layer of moisture adsorption. Nevertheless, the subsequent dehydration did not show any significant or comparable deviation from the normal desorption curve. The mass loss on the second dehydration indicated that only about 15 % moisture was lost, compared to the 28 % moisture determined by the ASTM method.

The dehydration of the Utah Blind Canyon sample followed the desorption model. The rehydration of the sample also followed the adsorption curve. There was no evidence of multilayer formation.

CONCLUSIONS

The mechanisms of dehydration and rehydration vary depending on the sample size and history. The behavior of an individual particle is best approximated by the block of Illinois #6 which indicated the desorption mechanism for dehydration and the parabolic mechanism or Fickian diffusion for rehydration. In general pristine samples followed an adsorption or desorption mechanism. Aged or oxidized samples showed combinations of linear and parabolic mechanisms which probably reflect a change in the surface properties in going from a hydrophobic behavior for the more pristine to hydrophilic for the more aged or oxidized material. Multilayer adsorption was observed on the lower rank materials which implies that the functional groups present on the surface facilitate this type of phenomenon.

ACKNOWLEDGMENTS

The authors gratefully acknowledge the support of the Office of Basic Energy Sciences, Chemical Sciences Division, and the Argonne National Laboratory Division of Educational Programs. Tim Griswold helped obtain the data and do some of the data reduction. The glassblowing by Joe Gregar was extremely helpful. Useful discussions with Anthony Fraioli are also acknowledged.

REFERENCE

1. Vorres, K. S., Kolman, R. and Griswold, T., Preprints, Fuel Chem. Div., Am. Chem. Soc., 33(2), 333(1988)

TABLE 1.

MECHANISMS FOR THE DEHYDRATION AND REHYDRATION OF COAL SAMPLES.

Sample		Dehydration	Rehydration
Illinois #6	Block	Desorption	Parabolic
	-20 mesh	L - P - L	Adsorption
	-100 mesh	Desorption	Adsorption
Wyodak-Anderson	-20 mesh	Desorption	Adsorption
Utah Blind Canyon	-100 mesh	Desorption	Adsorption

Vacuum Dehydration of IL #6 Coal Block

22 C., IL0012&3, IBDGAL

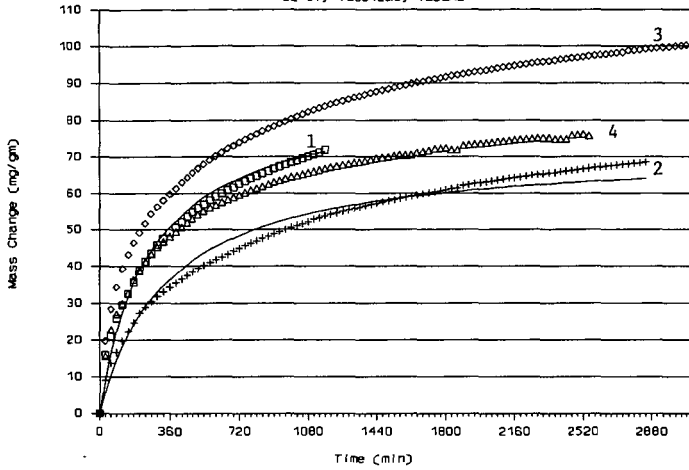


Figure 1.

Rehydration of IL #6 Coal Block

22 C., IL0012R, IBDGAL

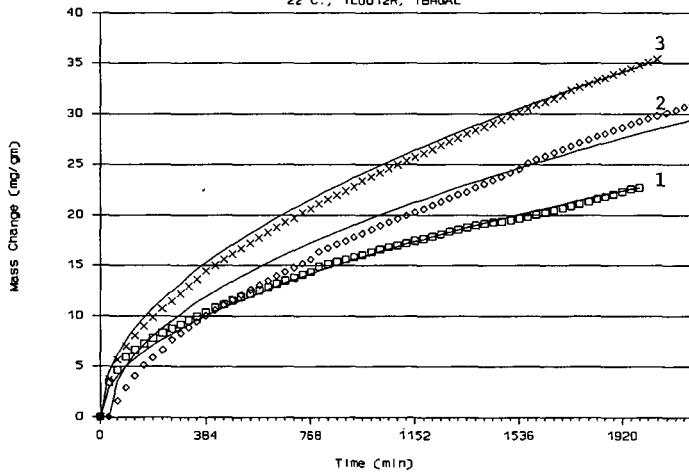


Figure 2.

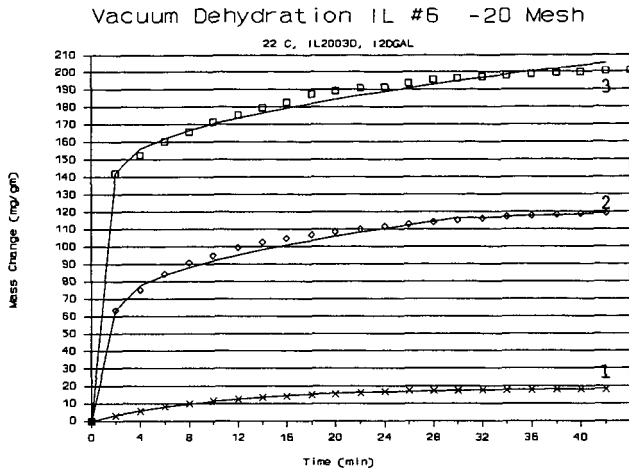


Figure 3.

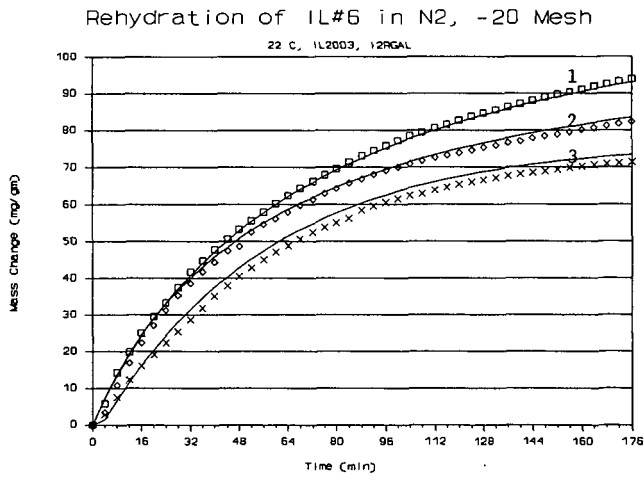


Figure 4.

Vac. Dehydration of IL #6 -100 Mesh

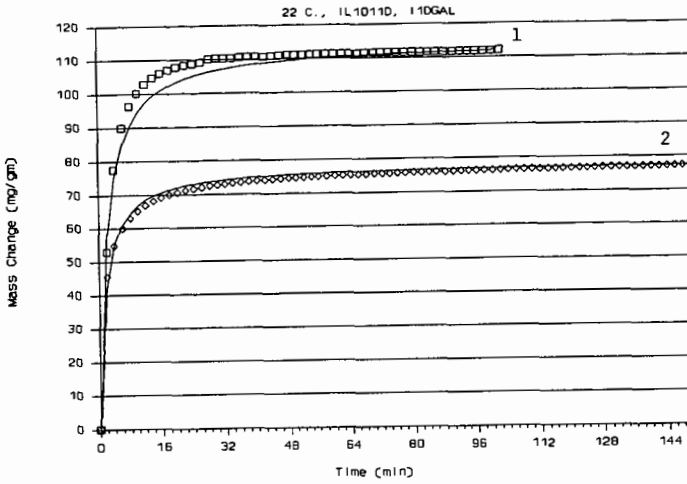


Figure 5.

Rehydration of IL #6 -100 Mesh in N2

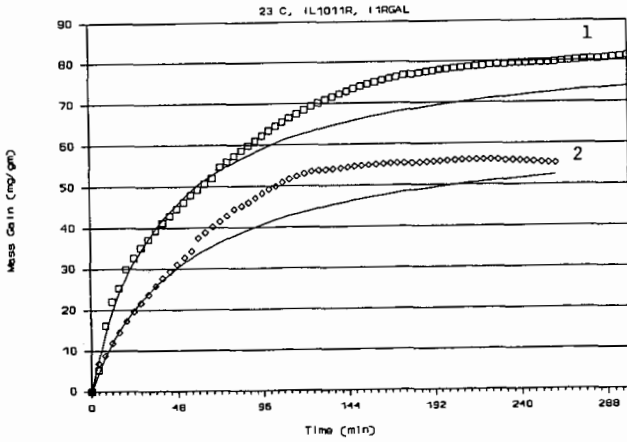


Figure 6.

Vacuum Dehydration of Wyodak -20 mesh

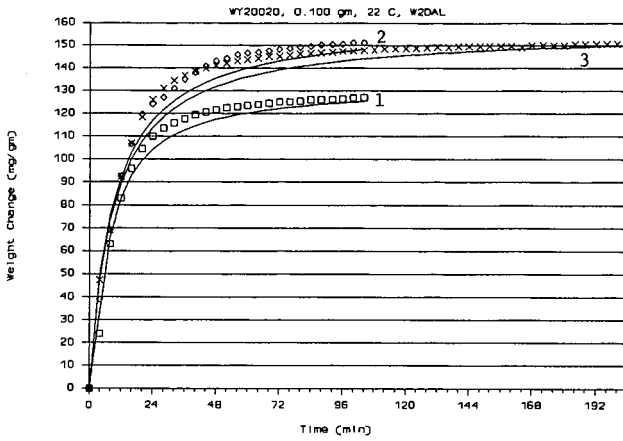


Figure 7.

Rehydration of Wyodak -20 mesh in N2

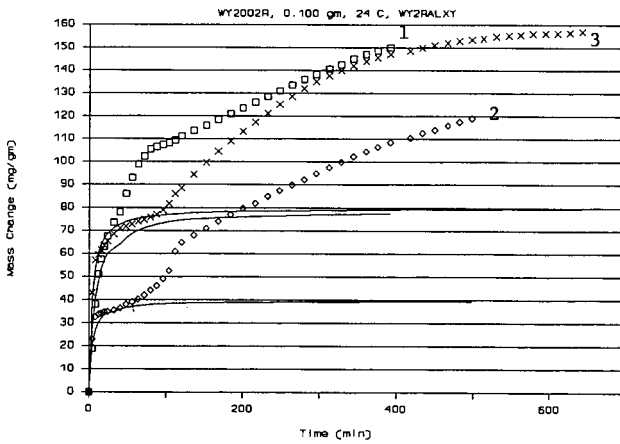


Figure 8.

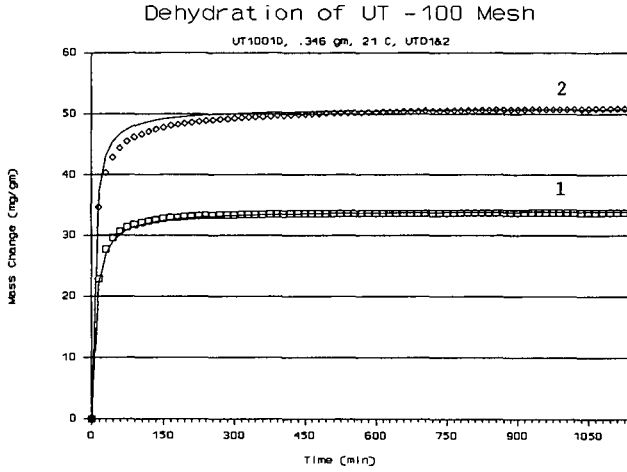


Figure 9.

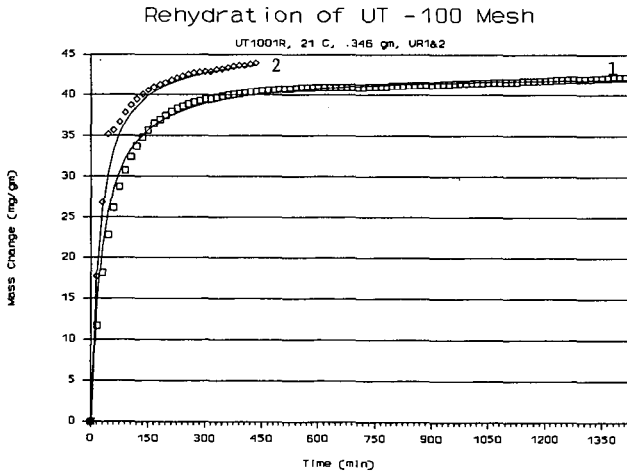


Figure 10.

STRUCTURAL GROUP ANALYSIS OF ARGONNE PREMIUM
COALS BY FTIR SPECTROSCOPY

K.A. Martin
S.S. Chao

Institute of Gas Technology
Chicago, Illinois 60616

INTRODUCTION

Infrared spectroscopy is a well-established method of coal characterization (1-12). Aspects of coal structure such as functional groups and hydrogen-bonding (11) and changes in structure during pyrolysis (6,7) and oxidation (4,5,9,10) have been described through infrared analysis and related to macromolecular processes. In particular, Painter *et. al.* (2), have proposed an FTIR procedure for a fairly exhaustive analysis of coal functional groups. Many of these suggestions are incorporated into the present study for the development of a functional group analysis data base for a set of standard coals.

EXPERIMENTAL

Eight Argonne premium coal samples were studied: Pennsylvania Upper Freeport, Wyodak, Illinois #6, Pittsburgh #8, Pocahontas #3, Utah Blind Canyon, West Virginia Stockton-Lewiston, and Beulah-Zap. Each ampoule of -100 mesh coal was mixed, opened, and the contents dried in a vacuum oven at 40°C for two hours. The dried samples were stored under vacuum until used. Diffuse reflectance infrared (DRIFT) spectra were obtained on neat dried samples with a Nicolet 60SXB FTIR with 500 scans at 4 cm^{-1} resolution. KBr pellets were also prepared (about 0.3% coal by weight) and spectra collected with 128 scans at 4 cm^{-1} resolution. Carbon, hydrogen and nitrogen analyses were performed with a LECO CHN-600 analyzer, and oxygen analyses were performed on a Carlo ERBA 1106 elemental analyzer. The low temperature ash of each coal was obtained with 0.5 g sample in an International Plasma Machine 1101B at 130 watts for several days. Another 0.5 g of each coal was acetylated by heating the coal at 100°C in a 2:1 mixture of pyridine and acetic anhydride for eight hours followed by filtering and vacuum drying.

RESULTS AND DISCUSSION

Each of the two sampling methods employed here, DRIFT and KBr pellets, have advantages and drawbacks in coal analysis. DRIFT suffers from a lower signal-to-noise ratio, but is very sensitive to some infrared bands which do not appear well in transmission spectra. Figure 1 compares the C-H stretching region of the Blind Canyon coal from DRIFT and KBr pellet spectra. Absorbance units are used rather than Kubelka-Munk units because the latter result in intensities too weak to resolve well. A weak band at 2732 cm^{-1} is apparent in the DRIFT spectrum, but barely observed in the transmission spectrum. The relative intensities of the C-H bands also change, with the symmetric and asymmetric CH_3 modes enhanced in the DRIFT spectrum. DRIFT is especially useful because coal can be sampled without an interfering matrix, which is important in determinations of OH and water content. KBr pellets, on the other hand, offer the advantages of a high signal-to-noise ratio and better

control over sample concentration for quantitative work. The strengths of both methods have been exploited in this study.

A common method for determining relative aromatic and aliphatic hydrogen concentrations has been to compare the absorbances or integrated areas of the 3100-3000 and 3000-2800 cm^{-1} regions (2,7). Table 1 gives the results of using conversion factors obtained from model compounds to determine the relative amounts of aliphatic and aromatic hydrogen from the integrated areas of the CH regions. As expected, the ratio of aliphatic to aromatic hydrogen increases as the C/H ratio decreases. A pitfall in this procedure is the assumption of a single average conversion factor for all of the coals. Individual C-H groups have different extinction coefficients and variations in the composition of the aliphatic moiety would affect the average absorption coefficient. Inspection of the asymmetric CH stretch of these coals indicates that the ratio of CH_3 to CH_2 groups increases as the coal rank increases. Also, the second derivative and deconvoluted spectra show that the Beulah-Zap, Wyodak and Blind Canyon coals have very few CH_3 bands, while the other coals have a more diverse composition. In spite of this variation, a single conversion factor applied to all coals should result in a good approximation of the relative abundance of the aliphatic and aromatic hydrogens.

The out-of-plane aromatic CH region, 900-700 cm^{-1} , has three major bands in each of the coal spectra after subtraction of the low-temperature ash spectrum at 870-855 cm^{-1} , 816-812 cm^{-1} , and 754-748 cm^{-1} (Figure 2). These can be assigned to the bending modes of an isolated hydrogen, two adjacent hydrogens, and three or more adjacent hydrogens, respectively. From curve-fitting results, the coals with the highest C/H ratio, Pocahontas and Pennsylvania, have the largest contribution from the band due to lone hydrogen, along with the Illinois and Lewiston-Stockton coals, indicating a higher degree of substitution or cross-linking in these coals. The Wyodak, Blind Canyon and Beulah-Zap coals, with the lowest C/H ratios, have the largest contribution from the 815 cm^{-1} band and a much smaller contribution from the 870 cm^{-1} band, but also fewer aromatic hydrogens overall. This implies a less aromatic structure with less substitution and less cross-linking.

Another facet of aromatic substitution may be the weak band at 2732 cm^{-1} which appears in all but the Wyodak and Beulah-Zap coals. Painter (2) has assigned this as an overtone of methyl groups attached directly to an aromatic ring. The increased intensity of this band as the aromaticity and CH_3 concentration increase supports this assignment. The integrated peak area of this band compared to the total aliphatic CH area can be converted into the percentage of aliphatic hydrogens in methyl groups attached to aromatic rings, using factors obtained from model compounds. The results for the six coals are given in Table 2. These results indicate that over half of the aliphatic hydrogens in the Pocahontas coal are in methyl groups attached to aromatic groups. This leaves few hydrogens which can form methylenic linkages. Blind Canyon coal, on the other hand, has very few hydrogens in this form. This is compatible with the observation that the Blind Canyon coal is less highly substituted.

The prominent band at 1600 cm^{-1} in the spectra of all coals has been attributed to an aromatic ring mode, highly conjugated carbonyls, electron transfer between aromatic planes, to a non-crystalline, non-aromatic graphite-like phase, or to combinations of these (12). Figure 3 shows the spectra of

the eight coals between 1700 and 1500 cm^{-1} after subtraction of the low-temperature ash spectrum. It can be seen that the shape and maxima of the bands shift for the different coals, suggesting a different underlying character. The most intense 1600 cm^{-1} band is found in the Beulah-Zap coal, with the intensity of this band in the other coals decreasing in the same order as the oxygen content decreases. Deconvolution, second derivative and curve-fitted spectra showed that the composition of this band varies. The Wyodak and Beulah-Zap coals have major bands at 1655 and 1562 cm^{-1} , usually assigned to conjugated carbonyls and carboxylate groups (2), but only weak features near 1600 cm^{-1} where the aromatic ring mode is expected. The Pocahontas and Pittsburgh coals, however, have their strongest contribution from a band at 1611 cm^{-1} .

In order to measure the phenolic and alcoholic content of the coals, acetylated derivatives were prepared. The subtracted spectra of the acetylated and initial coals were curve-fit between 1800 and 1500 cm^{-1} . Figure 4 shows the subtracted spectra for the Illinois, Pennsylvania, Wyodak and Pocahontas coals. The bands at 1770, 1740 and 1685 cm^{-1} have been assigned to acetylated phenolic, alkyl OH, and NH groups (2). Conversion factors were obtained from model compounds. Because of the inconsistency in the amine results, only the phenolic and alcoholic results are reported. Table 3 gives the relative abundance of phenolic and alkyl OH groups in the coals. Contrary to Painter's findings (2), this ratio is not very consistent, but increases significantly for the low rank coals. However, this discrepancy could be due to incomplete acetylation of less accessible OH groups.

ACKNOWLEDGMENT

The authors thank Dr. Karl Vorres of Argonne National Laboratory for the coal samples.

REFERENCES

1. J. K. Brown, J. Chem. Soc., 744 (1955).
2. P. Painter, M. Starsinic and M. Coleman, in "Fourier Transform Infrared Spectroscopy", Vol. 4, J. R. Ferraro and L. J. Basile, Eds., Academic Press, Orlando (Fla.), Chap. 5, 1985.
3. S. H. Wang and P. R. Griffiths, Fuel **64**, 229 (1985).
4. M. P. Fuller, I. M. Hamadeh, P. R. Griffiths and D. E. Lowenhaupt, Fuel **61**, 529 (1982).
5. N. R. Smyrl and E. L. Fuller, in "Coal and Coal Products: Analytical Characterization Techniques", E. L. Fuller, Ed., ACS Symposium Series 205, American Chemical Society, Washington, D.C., Chap. 5, 1982.
6. C. J. Chu, S. A. Cannon, R. H. Hauge and J. L. Margrave, Fuel **65**, 1740 (1986).
7. P. R. Solomon, D. G. Hambley and R. M. Carangelo, in "Coal and Coal Products: Analytical Characterization Techniques", E. L. Fuller, Ed., ACS Symposium Series 205, American Chemical Society, Washington, D.C., Chap. 4, 1982.

8. P. C. Painter, S. M. Rimmer, R. W. Snyder and A. Davis, Appl. Spec. 35, 271 (1981).
9. J. S. Gethner, Appl. Spec. 41, 50 (1987).
10. R. Liotta, G. Brons and J. Isaacs, Fuel 62, 781 (1983).
11. P. C. Painter, M. Sobkowiak and J. Youtcheff, Fuel 66, 973 (1987).
12. N. Berkowitz, "An Introduction to Coal Technology", Academic Press, New York, 1979.

RPP/kate2/PF

Table 1. Relative Ratios of the Number of Aliphatic and Aromatic Hydrogens

	<u>Aliphatic Hydrogens/ Aromatic Hydrogens</u>	<u>C/H Ratio</u>
Pocahontas	1.1	20.03
Pennsylvania	2.75	16.54
Lewiston-Stockton	3.9	15.30
Pittsburgh No. 8	5.1	14.99
Illinois No. 6	7.4	14.23
Beulah-Zap	10.9	14.89
Blind Canyon	13.1	13.33
Wyodak	13.8	13.80

Table 2. Concentration of Aliphatic Hydrogens in ϕ -CH₃ Groups

	<u>%</u>
Pocahontas	56.4
Pennsylvania	42.9
Pittsburgh	26.4
Lewiston-Stockton	24.9
Illinois	14.7
Blind Canyon	12.9

Table 3. Ratio of Phenolic to Alkyl OH Groups in Coal

Pocahontas	3.3
Blind Canyon	3.7
Lewiston-Stockton	4.5
Pittsburgh	5.0
Pennsylvania	5.6
Beulah-Zap	9.1
Wyodak	10
Illinois	11

RPP/kate2/PF

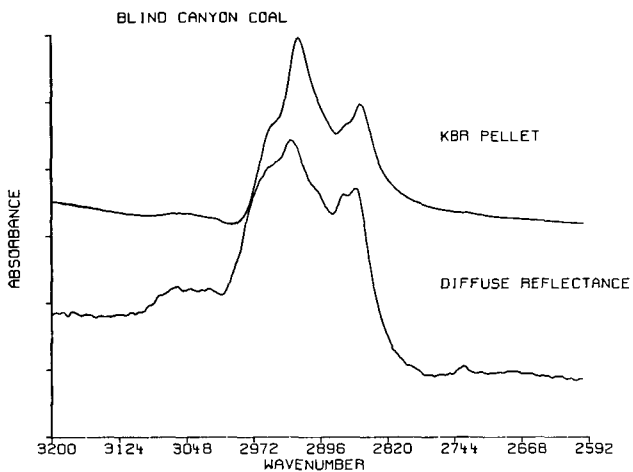


Figure 1. Comparison of KBr pellet and diffuse reflectance spectra of Blind Canyon coal.

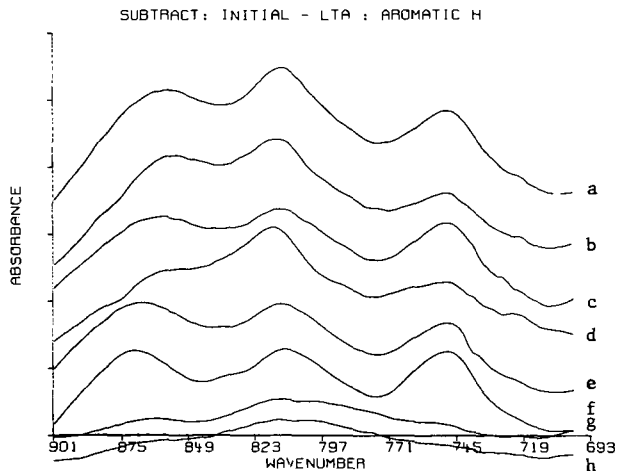


Figure 2. Aromatic hydrogen out-of-plane bending modes (a = Pittsburgh, b = Illinois, c = Lewiston-Stockton, d = Blind Canyon, e = Pennsylvania, f = Pocahontas, g = Wyodak, h = Beulah-Zap).

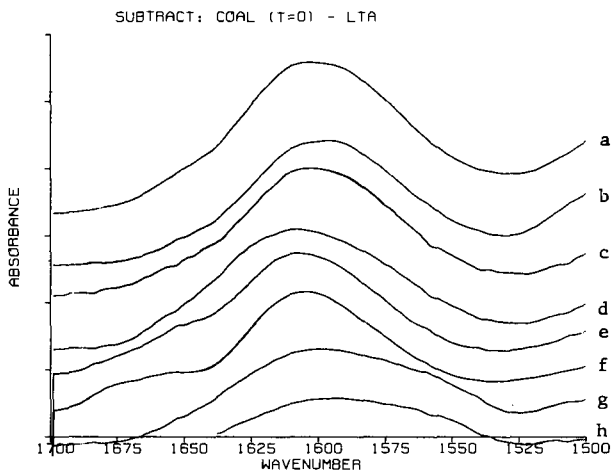


Figure 3. Comparison of 1600 cm^{-1} band for the different coals (a = Pittsburgh, b = Illinois, c = Lewiston-Stockton, d = Blind Canyon, e = Pennsylvania, f = Pocahontas, g = Wyodak, h = Beulah-Zap).

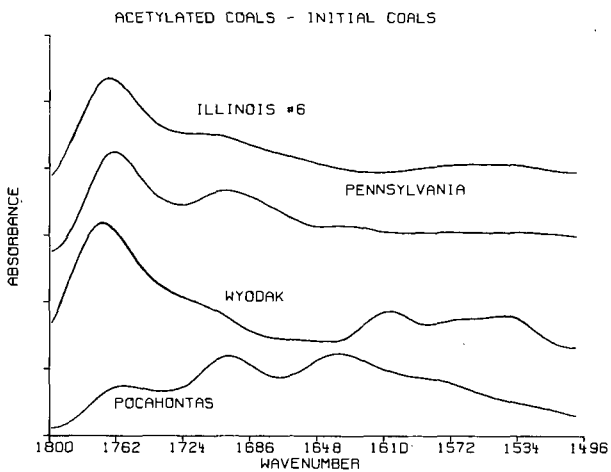


Figure 4. Spectra of Acetylated OH and NH groups for Illinois, Pennsylvania, Wyodak and Pocahontas coals.

SURFACE AND PORE PROPERTIES OF ANL AND PETC COALS.

C. H. Bartholomew, W. E. White, D. Thornock, W. F. Wells, W. C. Hecker, and L. D. Smoot,
Department of Chemical Engineering and Advanced Combustion Engineering Research Center,
Brigham Young University, Provo, Utah 84602

and
D. M. Smith and F. L. Williams
Department of Chemical and Nuclear Engineering
and UNM Powders and Granular Materials Laboratory
University of New Mexico
Albuquerque, New Mexico 87131

ABSTRACT

Surface areas, pore volumes, pore size distributions, and solid densities were measured for three ANL coals (Pittsburgh No. 8, Wyodak, and Beulah Zap Lignite), two PETC coals (Lower Wilcox, and Dietz) and a Utah Scofield coal and for chars derived from these coals. Surface areas were measured using nitrogen and carbon dioxide adsorptions; pore volumes were determined using nitrogen adsorption, mercury porosimetry, and NMR spin-lattice relaxation measurements of samples saturated with water. Solid densities were obtained using helium displacement. The results indicate that chars have larger surface areas and pores relative to coals; large fractions of the internal surfaces of coals are not penetrated by nitrogen molecules but are penetrated by carbon dioxide suggesting that the pores are mostly smaller than 1 nm.

INTRODUCTION

Coals are highly-aged biomaterials (with mineral inclusions) of high surface area and high porosity. These surface properties play an important role in their application as fuels. For example, in pulverized coal combustion the removal of volatile matter and the oxidation of the remaining char are processes the kinetics of which are governed at least in part by diffusion of materials in and out of the pores. Moreover, char oxidation rates depend upon the surface properties of the char, such as total surface area, active surface area and pore structure.

The work reported here is part of an ongoing collaborative study of the surface properties and pore structure of U.S. coals and in particular of a suite of 11 coals selected for comprehensive study by the Advanced Combustion Engineering Research Center (ACERC) of which 8 are ANL coals and 3 are PETC coals [1]. The principal objective is to correlate the surface, pore, and chemical properties of coals and chars with their rates of combustion. Ultimately these correlations will be developed into a computerized mathematical model of char oxidation which relates reactivity with structure [2].

This paper reports surface areas and pore volumes of 6 coals (3 ANL, 2 PETC, and one Utah coal) and of high temperature chars derived from three of these coals. It includes the results of studies of the precision of surface area and pore volume measurements on a given sample and on different samples by different adsorption techniques and by different laboratories. Comparisons are made of the results of this study with those reported in the literature for the same coals and similar chars derived from these coals.

EXPERIMENTAL

Materials. The coals studied are listed in Table 1 according to rank and source.

Table 1
Rank and Source of Coals Studied

<u>Coal Name</u>	<u>Rank</u>	<u>Location</u>	<u>Coal Bank Source</u>
1. Pittsburgh #8	H.V. A Bituminous	Greene Co., PA	ANL
2. Utah Scofield	H.V. C Bituminous	Scofield, UT	Valley Camp Mn
3. Dietz	Subbituminous B	Bighorn Co., MT	PETC
4. Wyodak	Subbituminous C	Gillette, WY	ANL
5. Beulah-Zap	Lignite A	Mercer Co., ND	ANL
6. Lower Wilcox	Lignite A	Titus Co., TX	PETC

Coal Preparation. The parent coals were air-classified and sieved. The lignite coals agglomerate easily and therefore, to facilitate the sieving process, they were first separated into wide size fractions using a cyclone particle classifier. The coal was processed through the separator two times. The first time, the apparatus removed the largest particles which were reground. The reground coal was then fed through the classifier again along with the smaller fraction from the first separation to remove the smallest size fraction. The larger size fraction was then classified using sieve screens to obtain the -200/+230 mesh size fraction. Sieving was performed to collect 200–300 grams of each coal using a RoTap sieve shaker; every fifteen minutes the screens were blown clean. The number of 15-minute periods for completion was greatly dependent on the individual sample, but was generally 4–6. The sieving was considered complete when the percentage passing through the 230 mesh screen remained constant. Both -325/+400 mesh (37–44 μm) and -200/+230 mesh (63–74 μm) size fractions were collected so that the effects of particle size could be studied.

Char Preparation. Details of the char preparation unit are described elsewhere [3]. The apparatus consists of a vibrating annular coal feeder, air/methane delivery system, a flat flame burner, and a cooled probe collection system. The coal feed rate is generally about 30 grams per hour. The flat-flame burner is fabricated from a ceramic monolith support (Cordierite, Corning Glass Works) with 300 square cells per square inch. The monolith is divided into two halves, and glass capillary tubes are inserted in every other hole in every other row. This arrangement gives a flame composed of many diffusion flamelets (at about 2000 K). Flows are controlled by high-accuracy rotameters and pressures are maintained constant by low-pressure line regulators to ensure a stable flame. Typical flow rates (SCFH) are: N₂ feed, 0.632; N₂ quench, 6; methane, 5.867; and air, 59.4. The collection system consists of a water-cooled, nitrogen-quenched probe, a cyclone separator, and a household vacuum. The particle residence time may be changed by varying the height of the collection probe above the burner. The cyclone separator is designed to collect 20 micron particles with greater than 90% efficiency.

Surface Area/Pore Volume Measurements. Total surface areas were measured by means of carbon dioxide adsorption at 273 or 298 K and nitrogen adsorption at 77 K, using either volumetric [4,5] or flow (Quantasorb) adsorption systems. Carbon dioxide adsorption measurements at UNM were conducted at 273 K and three relative pressures using a Quantasorb flow adsorption analyzer, after samples had been outgassed in a dry helium stream at 373 K. CO₂ adsorption measurements at BYU were conducted at 298 K and 3-7 relative pressures using either flow or static, volumetric systems on samples previously outgassed *in vacuo* for 12 hours at 378 K or outgassed in helium at 373 K. In both cases, the data were analyzed using the Dubinin-Polyani (DP) or Dubinin-Radushkevich (DR) equation using an area for the CO₂ molecule of 0.201 nm² based on good agreement between nitrogen adsorption and carbon dioxide adsorption measurements on a graphite carbon [6]. Nitrogen adsorption and desorption experiments were conducted over the relative pressure range of 0.05 to 0.99 at 77 K using

either an Autosorb-1 automated volumetric adsorption analyzer (UNM) or (at BYU) a volumetric adsorption apparatus [4,5]. Samples were outgassed *in vacuo* at either 383 K for three hours (UNM) or 378 K for 12 hours (BYU). Nitrogen isotherms were analyzed using the BET equation and an area for the nitrogen molecule of either 0.162 nm² (BYU) or 0.170 nm² (UNM) to obtain surface areas.

Pore size distributions for pores in the 1-100 nm range were obtained from extended nitrogen isotherms using the Kelvin equation. Mercury intrusion experiments were obtained (at UNM) for selected samples previously outgassed at 383 K *in vacuo* for one hour in the pressure range of 12 to 33,000 psia. The analysis of the mercury intrusion data was complicated by (i) filling of irregular-shaped voids around particles and (ii) sample compression at higher pressures necessary to fill pores smaller than 3 nm diameter [6].

NMR spin-lattice relaxation measurements of pore volume and pore size distribution were performed (at UNM) at 20 MHz and 303 K on samples saturated with water vapor. Coal and char samples were saturated by placing them in a desiccator, evacuating, backfilling with water or salt solution and allowing the samples to equilibrate with the solution vapor at a given pressure. Samples were weighed into 5 mm NMR tubes and a 180°-t-90° spin-lattice relaxation experiment was performed from which pore size distributions for pores of greater than 0.5 nm were extracted [6,7]. The surface-interaction parameter, β , was determined from measurements at different water contents [8]. Helium or "true" densities were obtained by helium pycnometry at UNM.

RESULTS AND DISCUSSION

Surface areas were measured for six coals and three chars while pore volumes, pore size distributions, and densities were also measured for three coals and three chars (two samples of one of the chars). Data obtained at BYU and the University of New Mexico (UNM) are summarized in Tables 2-4 and in Figure 1.

Table 2 summarizes the results of a repeatability study of CO₂ and nitrogen adsorptions on a Utah Scofield coal using a volumetric system to (i) define pretreatment conditions that would lead to removal of adsorbed CO₂ and allow repeatable measurements on the same sample and (ii) define the precision of CO₂ and N₂ adsorption measurements on the same sample and different samples (of about 1 g). The data (Table 2) indicate that immersing the sample cell in boiling water for five minutes, while evacuating, quantitatively removes adsorbed CO₂ and enables the adsorption measurement to be repeated with a high degree of precision (better than 7%). The data (Table 2) also indicate the precision of both CO₂ and N₂ measurements is within 7% on different samples.

Table 3 summarizes results from a similar repeatability study on high temperature Dietz chars using a flow system. They indicate that different runs on the same sample are repeatable to within 1-2% while the precision of measurements on different samples of the same preparation is 7-14% for samples sizes of 25-35 mg from a poorly-mixed preparation and 2-7% for sample sizes of 75-120 mg from a well-mixed sample. Accordingly, it is clear that the precision of surface area measurements by the flow method is significantly greater for samples larger than 50-75 mg and/or is improved by mixing the sample well. These results emphasize the importance of choosing representative samples and of conducting repeat measurements on different samples of the same preparation rather than repeating measurements on the same sample. Comparison of the data for the Dietz A and B preparations (temperature and residence time were nearly the same) indicates that large variations in surface areas (20% for CO₂ and 300% for N₂) can be obtained with only subtle variations in the preparation conditions. Similar variations are observed for Dietz Chars B and C prepared

under nearly the same conditions (Table 4). This emphasizes the need for careful temperature and residence time control in char preparation. Thus, we are presently computerizing our preparation system to enable better reproduction of gas temperature and particle residence time in our preparations.

Table 4 summarizes our measurements of total surface area, pore volume, pore volume distribution and interaction parameters from NMR measurements for the five coals and 3 chars. Wilc Chars 1 and 2 were prepared separately; the preparation of Wilc Char 2 involved a higher residence time and probably a higher degree of burnout; this is confirmed in part by the larger nitrogen BET surface area of Wilc Char 2 relative to Char 1. Wherever possible, measurements were repeated to obtain a measure of experimental precision; the listed limits of error refer to the the standard deviation for a series of 2-5 measurements.

Several significant trends in the data (Table 4) are evident: (i) CO₂ surface areas of coals are generally 50-300 and of chars 2-5 times larger than the corresponding N₂ surface areas, (ii) CO₂ and N₂ surface areas of chars are higher than those of the corresponding coals, and (iii) the fraction of pores having diameters of less than 0.5 nm is significant for both coals and chars. The first of these trends is explained by the ability of the CO₂ to penetrate micropores (of less than about 1 nm diameter) whereas N₂ is unable to penetrate; accordingly it is clear that most of the internal surface area of coals and much of that of these chars consists of micropores having diameters less than 1 nm. The larger measured surface areas of chars relative to coals is explained by a combination of the following factors: (i) the removal of strongly adsorbed molecules or functional groups from the micropores that would otherwise hinder access of CO₂ and N₂, (ii) creation of new micropores during the restructuring process involved in devolatilization, and (iii) creation of greater macroporosity as volatile materials are removed.

The data in Table 4 and Figure 1 indicate that the net result of these factors is to slightly decrease during char production the fraction of pores in the range of 0.5-1 nm, while significantly increasing the fraction of pores in the range of 1 to 10 nm and to increase pore volume measured by either nitrogen or water adsorptions. The data for the Wilc Char provide an exception to this trend; however in this case, the unexpectedly large pore volume of coal may be due to swelling as water is taken up by the lignite structure. A similar effect may also explain the unexpectedly large fraction of pores less than 0.5 nm for Wilc Char 1.

Table 5 compares surface area and pore volume data available in the literature with those determined in this study. The relatively few surface area data available are in fair to good agreement with the data obtained in this study, while the pore volume data are insufficient to enable comparison. The differences in the results from this and other studies are probably explained by differences in the pretreatments of the samples, e.g., the extent of oxidation and outgassing of the sample and by differences in the conditions of adsorption, e.g. the temperature at which CO₂ was adsorbed and the cross-sectional area used in calculating surface areas. This emphasizes the need for development of standard pretreatment conditions and methods of adsorption. To realize that goal additional studies of pretreatment effects, such as that of Deevi and Suuberg, [10], are needed. It is hoped that this continuing study will contribute to that end.

ACKNOWLEDGEMENTS

This work was sponsored by the Advanced Combustion Engineering Research Center (ACERC) and by DOE/PETC (Grant No. DE-FG22-85PC80529). Funds for ACERC are provided by the National Science Foundation, the State of Utah, 24 industrial participants, and the U. S.

Department of Energy. The authors gratefully acknowledge technical assistance by Mr. R. Merrill, Mr. A. Cook, and Mr. S. Simmerman.

REFERENCES

1. K.L. Smith and L. Douglas Smoot, "Selection and Characteristics of Standard ACERC Coals," Report submitted to ACERC, June 1, 1988.
2. L.D. Smoot, C. H. Bartholomew, and D. W. Pershing, "Research Program," Second Annual Report, Advanced Combustion Engineering Research Center, December 31, 1987, pp. 37-45.
3. R. Merrill, C. H. Bartholomew, and W. C. Hecker, "Char Preparation Facility," Char/ACERC-1, Submitted to ACERC, September 18, 1987.
4. C. H. Bartholomew, Quarterly DOE report, FE-1790-1, Aug. 6, 1975.
5. C. H. Bartholomew and R. B. Parnell, *J. Catal.*, **65**, 390 (1980).
6. D.M. Smith, C. L. Glaves, S. B. Ross, and D. L. Stermer, "Surface Area and Pore Structure of Char," Progress Report submitted to ACERC, December 1987.
7. D.P. Gallegos and D. M. Smith, *J. Colloid Interface Sci.*, **122**,143 (1988).
8. C. L. Glaves, P. J. Davis, D. P. Gallegos, and D. M. Smith, "Pore Structure Analysis of Coals via Low Field Spin-Lattice Relaxation Measurements," *Energy and Fuels*, In press.
9. H. Gan, S. P. Handi, and P. L. Walker, Jr., "Nature of the Porosity in American Coals," *Fuel*, **51**, 272 (1972).
10. S. Deevi and E. M. Suuberg, "Physical Changes Accompanying Drying of Western U. S. Lignites," *Fuel* **66**, 454 (1987).
11. D. P. Gallegos, D. M. Smith and D. L. Stermer, "Pore Structure Analysis of American Coals," in Characterization of Porous Solids, eds. Unger, Rouquerol, Sing, and Kral, Elsevier, 1988.
12. N. Y. Nsakala, R. L. Patel, and T. C. Lao, "Combustion Characterization of Coals for Industrial Applications , Final Technical Report, DOE/PC/40267-5 [DE-AC22-81PC40267], March, 1985.

Table 2: Repeatability Data for CO₂^a and N₂^b Adsorptions on a Utah Bituminous Coal (Scofield Mine; Deseret Coal Co.) Obtained in a Static System

Run No.	Procedure	S.A. (m ² /g)	
		CO ₂	N ₂
1.1	Outgassed; CO ₂ adsorption	129.8	
1.2	Cell immersed in boiling water for 5 min.; pumped 2 hr. to <10 ⁻⁴ torr; CO ₂ adsorption	129.3	0
1.3	Same as run #1.2	132.4	
2.1	Same as run #1.1	156.8	
2.2	Same as run #1.2	140.9	
2.3	Same as run #1.2	147.4	0
3.2	Same as run #1.2	150.8	0
3.3	Same as run #1.2	153.8	
3.4	Same as run #1.2	152.7	
4.1 & 4.2	Pumped to <10 ⁻⁴ Torr		1.72, 1.94
4.3	Same as 4.2		1.95
4.4	Same as 4.2		1.96
4.5	Same as 4.2		1.73

^a CO₂ area = 0.201 nm²; P_{CO₂} = Polynomial Fit

^b N₂ area = 0.162 nm²

Table 3: Repeatability Study in a Flow System of CO₂ and N₂ Adsorptions on Dietz Chars^a

Sample ^b	Run No. ^c	CO ₂ SA (m ² /g)	N ₂ SA (m ² /g)
A-1	1		333
	2		325
	4		327
	5		331
	6		<u>324</u>
	ave 5 runs		328 ± 3.9
B-5	5	289	
	6	296	
	7	289	
	8	293	
	9	<u>298</u>	
	ave 5 runs	293 ± 4.1	
A-1		394	328
A-2		381	322
A-3		<u>304</u>	<u>288</u>
	ave of A samples	360 ± 49	313 ± 22
B-4		301	106
B-5		293	89
B-6		293	93
B-7		307	99
B-8		<u>285</u>	<u>99</u>
	ave of B samples	296 ± 7.6	96.0 ± 5.9

a. Prepared in methane flame (gas temperature of 2000 K; residence time of about 10 ms).

b. A and B are different repeat preparations of char; A-1 to A-3 are different samples of Preparation A. A samples were 25-35 mg and not well mixed; B samples were 75-120 mg and well mixed

c. Run numbers and averages of runs are provided for samples A-1 and B-5 only

Table 4: Physical and Surface Properties of ANL, PETC & Other U.S. Coals and Chars

Sample	Surface Area (m ² /g)		Pore Volume (m ³ /g)			β^d , ^e (nm/s)	Fraction of PV <0.5nm ^d	Density of g/cm ³
	CO ₂ ^a	N ₂ ^b	Hg	N ₂ ^c	H ₂ O ^d			
Pitt #8 (-200+230) ^f	119±17	1.3±0.1	0.43	0.012	0.031	20.4	0.35	1.39±0.01
Pitt #8 (-200+230) ^h	117±18							
Pitt #8 Char ^g	155	74.6	-	0.056	0.053	67.1	0.28	-
Wilc (-200+230) ^f	144±7	3.3	0.16	0.033	0.282	487	0.31	1.48±0.01
Wilc (-200+230) ^h	154							
Wilc Char 1 ^f	253±30	60.5	0.61	0.128	0.124	36.3	0.88	2.03±0.09
Wilc Char 1 ^h	242±35	47						
Wilc Char 2 ^g	252	124	-	0.164	0.153	226	0.22	-
Dietz (-200+230) ^g	218	3.0	-	0.012	0.257	260	0.44	-
Dietz Char A	360±49	313±22						
Dietz Char B	298±6.8	97±7.4						
Dietz Char C ^{g,j}	526±20	131	-	0.107	0.110	123	0.27	
Wyodak (-200+230) ⁱ	206	5.0±0.4						
Wyodak (-325+400) ⁱ	208	5.0±0.1						
B-Zap (-200+230) ⁱ	229±50	0.5±0.2						
B-Zap (-325+400) ⁱ	255±62	1.0±0.6						
Ut Scof (-200+230) ⁱ	153±10	1.6±0.05						
Ut Scof (-325+400) ⁱ	144±11	1.9±0.1						

^a Measured at 0° C at UNM using flow system, 25° C at BYU using static system; Calc. from DP Eqn. using CO₂ area of 0.201 nm²/molec. and P_{CO2} = 26,144.7 mm Hg at 0° C.

^b Measured at -196° C; Calc. from BET Eqn. using N₂ area of 0.170 nm²/molec.

^c From extended BET measurements

^d From NMR analysis of adsorbed water

^e Interaction parameter from NMR

^f Measured by Mr. Wayne White at UNM; SA's by flow measurement

^g Measured by UNM personnel; SA's

^h Measured at BYU by flow method

ⁱ Measured at BYU by volumetric method

^j Char C was prepared under conditions very similar to those of Char B

Table 5: Comparison of Multisource Surface Area & Pore Volume Data for ANL and PETC Coals and Chars

Samples	Surface Area (m ² /g)		Pore Vol (cm ³ /g)		Ref.	
	CO ₂	N ₂	Hg	N ₂		
Coals	Pitt #8	119	1.3	0.43	0.012	This study
		141	<1.0	-	-	9
	Wyodak	207	5.0	-	-	This study
B-Zap		308	2.6	-	-	9
		242	0.5-1.0	-	-	This study
		-	2.2-4.6	0.08-0.14	-	10
		268	<1.0	-	-	9
Chars ^a		115	1.2-2.6	-	-	11
	Wilcox (2,000 K) ^b	252	47-124	-	0.16	This study
	Wilcox (1,700 K) ^c	211	191	0.68	-	12

^a Gas temperatures shown in parenthesis

^b Prepared in a methane flat flame burner

^c Prepared in a drop tube furnace at a residence time of about 0.2 sec.

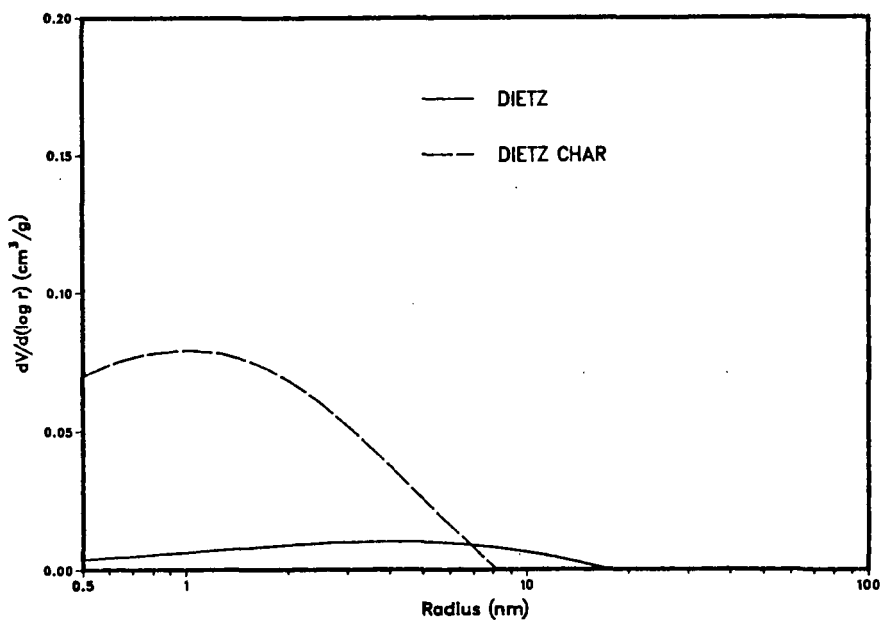
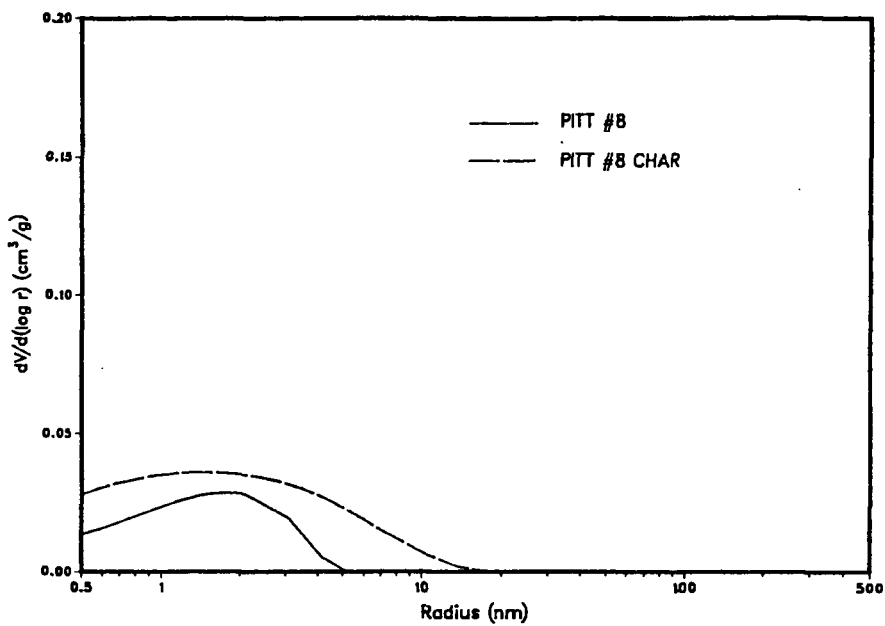


Figure 1. NMR pore volume distributions for two coal/char pairs.

AN EPR STUDY OF PORE ACCESSIBILITY IN ARGONNE PREMIUM COAL SAMPLES

Lalith S. Cooray, Lowell D. Kispert, and Shing K. Wu
Chemistry Department, The University of Alabama
Tuscaloosa, ALabama 35487

INTRODUCTION

We have recently reported (1) an EPR method developed in this lab to determine the pore size and number distribution in high volatile bituminous coal in the presence of a swelling solvent by diffusing nitroxide spin probes of different size, shape and reactivity into the swellable pores of coal samples. The same method has also been shown (2) to be useful in estimating the number distribution of accessible reactive sites containing carboxylic acid, phenol and amine substituents in samples of Mary Lee (A), Black Creek (B), Illinois no. 5 (C) and Illinois no. 6 (D), all high volatile bituminous coal samples by using small size (~0.7 nm radius) spin probes.

It was observed that the distribution of reactive sites varies substantially. For example, the detected acidic and phenolic sites in (B) and (D) (premium coal sample program) exceeded the detected amine site by approximately an order of magnitude. Sample of (B) possessed the greatest number of reactive acidic and phenolic sites of all the coal samples examined. It was also inferred that the ability for the coal pore to hydrogen bond to a spin probe was shown not to be an important process for incorporating spin probes in (A) and (B) and only a slight factor in samples of (C) and (D).

Unfortunately very little independent studies on pore distribution have been reported for coal samples A, B, C and D. Thus it is not possible to verify various conclusions. To remedy this situation, we have expanded our study to include Blind Canyon and Pittsburgh #8 in addition to the Illinois #6 coal samples from the Argonne Premium Coal Sample Program as well as samples from Illinois #6 (PSOC-1354) and New Mexico (PSOC -311) coals wherein comparisons can be made to other studies. For instances, D. Smith and coworkers (3) have studied extensively the pore size distribution for PSOC-311 and PSOC-1354 coals before exposure to solvents by NMR spin-lattice relaxation methods. In addition, small angle neutron scattering studies of Pittsburgh #8 swelled with different solvents have been carried out by Winans and Thiyagarajan (4) while studies by Larsen and Wernett (5) using gas adsorption techniques have permitted some independent measurements of pore accessibility to various solutes in Illinois #6 coal.

This study reports a spin probe - EPR study of pore size distribution, the basic/acidic reactive site distribution, hydrogen bonding site distribution and the effect of a swelling solvent on Blind Canyon, Pittsburgh #8 and Illinois #6 from the Argonne premium coal sample program and Illinois #6 (PSOC-1354) and New Mexico (PSOC-311) from the Penn State Coal Sample Bank at Penn State University.

EXPERIMENTAL

All coal samples were stored and handled under nitrogen or argon. The procedures for preparing (2) the spin probe doped coal samples and analyzing (1,2) the EPR spectra has been described previously. The ash free percentage by weight values for the coal samples obtained from the Argonne Premium Coal Sample Program are as follows: Illinois #6; C(79%), H(5.6%), O(9.7%), and S(5.4%); Pittsburgh #8; C(83%), H(5.8%), O(8%), and S(1.6%); and Blind Canyon; C(79%), H(6.0%), O(13%) and S(0.5%). The proximate and ultimate analysis for PSOC-1354 and PSOC-311 are available from the Penn State Coal Sample Bank at Penn State University. The spin probes (I-IX) were obtained from Molecular Probes, Inc. Junction City, Oregon. The pore size distribution of the coal samples was studied using spin probes I-V while the basic/acid reactive site distribution was examined by using spin probes VI and VII. To differentiate

between hydrogen-bonding to the nitroxyl group and substituents in the swellable pores of the coal, spin probes VIII and IX were used. The effect of a swelling solvent was demonstrated by swelling samples of Pittsburgh #8 coal with toluene, benzene and pyridine. To reduce the sample uncertainty, Professor D. Smith at the University of New Mexico sent his samples of PSOC-311 and PSOC-1354 so that a direct comparison could be made between our results and those he deduced from NMR studies.

RESULTS

Pore Size Distribution

The relative concentration of incorporated spin probes varied among different coal samples and is given in Table I. The relative spin concentration ratio of spin probes I:II:III:IV:V for Illinois #6 (Argonne) and PSOC-1354 (Illinois #6) equals 5.6:15.6:1.3:1.0: 1.9 and 3.5:25.2:1.0:1.0:3:3 respectively. It is clear that both samples have rather similar pore size distribution except that the Illinois #6 (Argonne) coal sample has a greater number of pores with a radius of 0.67-3.4 nm by a factor of 3 to 7. All the coal samples studied show the highest number of cylindrical pores with a diameter of 0.9 nm. However, compared to other samples, Blind Canyon coal has a quite high number of chain-like pore shapes. On the other hand, Pittsburgh #8 coal shows a pore distribution of largely cylindrical type pore shapes. For the coal samples Illinois #6 (Argonne), PSOC-311, and PSOC-1354, the long chain pore (radius = 1.3 nm) occurs the least number of times whereas for Pittsburgh #8 and Blind Canyon coal the long chain pore with a radius of 3.4 nm occurs the least number of times.

The pore structure of PSOC-311 and PSOC-1354 coal samples has been analyzed by Smith et al. (3) using low field NMR spin lattice relaxation measurements. It is known that the spin lattice relaxation time T_1 of H_2O attached to the pore surface differs from the corresponding T_1 for the bulk H_2O . Furthermore, Smith et al. (3) has shown that pore size determination can be deduced from T_1 measurements. Their results show the number of pores in PSOC-1354 with a radius of 0.5-5.0 nm is greater than that found in PSOC-311. In contrast, our studies show just the opposite trend in the presence of a swelling solvent for each spin probe used. This disagreement can be rationalized as follows. The NMR method measures the total volume of pores available in a particular coal sample. However, the spin probe method determines the pore volume that are accessible to a given spin probe upon swelling with a given solvent. On this basis it is possible to deduce that PSOC-1354 coal has more bottleneck pores (unaccessible to spin probes) than the PSOC-311 coal in the presence of toluene.

Recently Small Angle Neutron Scattering (SANS) studies (6) of the pore shapes and sizes of Illinois #6 coal characterize the pore shapes as elongated voids with an average radius of 2.5 nm. Unfortunately the spin probes used in this study are all smaller than this except for V (3.4 nm). Even so the spin probe study indicates a majority of cylindrical and a substantial number of long chain-like pores occur, in reasonable agreement with the SANS data. (6) It has been shown (7) by use of the SANS method that the shape distribution of the micropore and mesopores in unmodified coal do not change when the coal samples in the dry state are suspended in cyclohexane. Toluene, the swelling solvent used in our studies is considered to be a mild swelling solvent and therefore assumed not to significantly change the pore structure. Previous gas adsorption work (5) in Illinois #6 coal samples suggests that coal pores are mostly closed and inaccessible to molecules such as cyclopropane which are not soluble in the coal.

Reactive Site Distribution

The relative acidic/basic reactive site distributions in various samples of coal were determined using spin probes VI and VII. The results are given in Table 2 where the data is normalized to spin probe VI in Pittsburgh #8. The molecular volume of each spin probe is shown within the parenthesis.

The number ratio of pores containing amine groups to those containing acid or phenolic groups is 1:1.2; 1:3.7; 1:5.4; 4.6:1; 1:2.4 for coal samples PSOC-311, PSOC-1354, Illinois #6 (Argonne), Blind Canyon, and Pittsburgh #8 respectively. It is interesting to note that among the data listed in Table 2, only Blind Canyon coal (a low sulfur coal) has more basic sites than acidic acids within the pores defined by spin labels VI and VII. The presence of acidic sites in Illinois #6 has been confirmed by a small angle neutron scattering study (6).

Degree of Hydrogen Bonding in Swellable Pores

The relative spin concentration obtained for spin probes VIII and IX are depicted in Table 3. The volume of each spin probe is given within the parenthesis. It is apparent from the data given in Table 3, that the presence of an additional site for hydrogen bonding slightly benefits the incorporation of spin probes in PSOC-311 and Blind Canyon coal samples. On the contrary, for coal sample PSOC-1354, the presence of additional site for hydrogen bonding is a significant hindrance for spin probe incorporation. Values for Pittsburgh #8 could not be obtained because the EPR spectrum exhibited very poor resolution. Even though the exact reason for this is not understood, it could be due to the failure to collapse sufficient number of pores around the spin probes before being washed away with ethanol.

Pore Distribution Dependence on Swelling Solvent

In Table 4 are presented the changes in the concentration of spin probes I, II and V as Pittsburgh #8 is swelled with toluene, benzene and pyridine. It is to be noted that as the solvent is changed from benzene to pyridine, the number of spherical pores decreases (i.e. spin probe I) while the number of elongated pores increase (spin probe II). Generally, toluene is considered a poor swelling solvent relative to pyridine. Thus the accessible pore volume for those solvents which do not disrupt the original coal structure is significantly reduced over that when a solvent like pyridine is used. These results are in agreement with Winans and Thiyagarajan study (4) using small angle neutron scattering techniques to examine the effect of swelling solvent on pore structure. The results of a mild swelling solvent like benzene was compared to an aggressive swelling solvent (pyridine). The pore structure of Pittsburgh #8 in the presence of benzene was found to be roughly spherical whereas in the presence of pyridine, it was found to be elongated. This very nice agreement with an independent measurement suggests that the spin probe EPR measurements are useful indicators of the behavior of coal pores in the presence of various solvents and measure the relative difference in accessible pores on the molecular level.

CONCLUSION

The spin probe - EPR method showed that as the swelling solvent was changed from benzene to pyridine, the number of spherical pores in Pittsburgh #8 decreased while the number of elongated pores of distinct size increased sharply in agreement with previously reported SANS studies (4). Reasonable agreement was found with independent studies (6) on the average size distribution and the presence of acid character in the accessible pores of Illinois #6. Comparison between NMR data and the pore distribution pattern deduced by the spin-probe EPR method indicates that toluene swelled PSOC-1354 has more bottleneck pores with a radius of less than 5 nm which are not accessible to toluene than PSOC-311.

ACKNOWLEDGMENTS

The authors gratefully acknowledge the U. S. Department of Energy, Pittsburgh Energy Technology Center, University Coal Research Program for support of this research under Grant no. DE-FG22-86PC90502. We wish to thank Professor D. Smith at the University of New Mexico for samples of PSOC-1354 and PSOC - 311 and for numerous discussions.

REFERENCES

1. S. K. Wu and L. D. Kispert, *Fuel*, **64**, 1681 (1985).
2. L. D. Kispert, L. S. Cooray, and S. K. Wu, *Preprints. Div. Fuel Chem., ACS*, **32(4)**, 286 (1987).
3. C. L. Glaves, P. J. Davis, D. P. Gallegos and D. M. Smith, *Energy and Fuel*, in press, 1988.
4. R. E. Winans and P. Thiyagarajan, *Preprints, Div. Fuel Chem., ACS*, **32(4)**, 227 (1987).
5. J. W. Larson and P. C. Wernett, *Preprints. Div. Fuel Chem., ACS*, **32(4)**, 232 (1987).
6. J. S. Gethner, *J. Appl. Phys.*, **59**, 1068 (1986).
7. J. S. Gethner, *Preprints, Div. Fuel Chem., ACS*, **32(1)**, 239 (1987).

Table 1. The relative pore size distribution for spin probes I, II, III, IV, and V (toluene swelling solvent).

Radius ^a Molecular Vol. Sample	I 0.67 nm 143.9 Å ³ Spherical	II 0.90 nm 230.7 Å ³ Cylindrical	III 1.07 308.7 Å ³ Chain	IV 1.3 nm 335.3 Å ³ Long Chain	V 3.4 nm 459.1 Å ³ Long Chain
PSOC-311	48.6	202.6	48.6	7.7	37.7
PSOC-1354	10.2	73.7	2.9	3.0	9.7
ILLINOIS #6	72.3	201.1	17.0	12.8	25.3
BLIND CANYON	15.4	133.0	116.9	70.9	10.3
PITTSBURGH #8	4.0	133.4	1.9	9.3	1.0

(a) Effective radius including Van der Waals nearest approach distance.

Table 2. The relative basic/acid reactive site distributions for spin probes VI and VII (toluene swelling solvent).

Coal Sample	VI (143.6 Å ³) Basic sites	VII (131.5 Å ³) Acid sites
PSOC 311	16.9	21.2
PSOC 1354	1.6	6.1
Illinois #6	3.1	16.9
Blind Canyon	8.8	1.8
Pittsburgh #8	1.0	2.4

Table 3: Relative sites distribution for spin probes VIII and IX (hydrogen-bonding-differences).

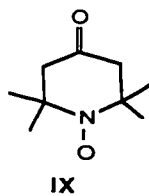
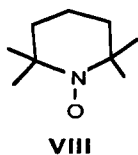
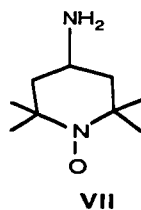
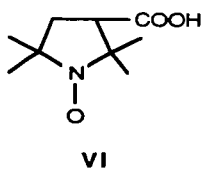
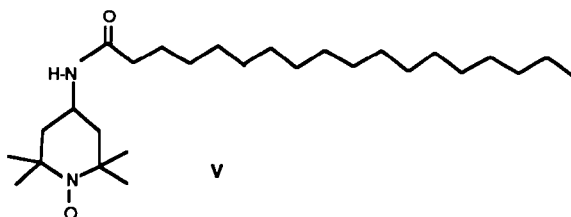
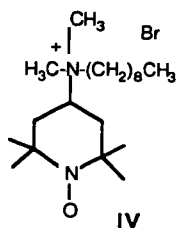
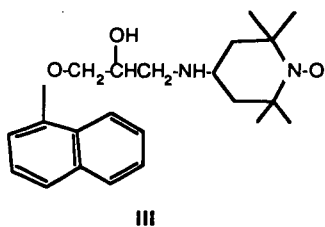
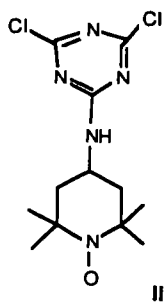
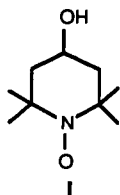
Coal Sample	VIII (138.3 Å ³) (1-H bond site)	IX (138.2 Å ³) (2-H bond sites)
PSOC-311	21.3	37.1
PSOC-1354	25.7	1.0
Illinois #6	3.5	3.7
Blind Canyon	5.7	11.0
Pittsburgh #8	--	---

Table 4. The relative spin probe concentration for probes I, II, III as a function of swelling solvent for Pittsburgh #8 coal.

Spin Probe	Solvent	Spin Probe Concentration Ratio ^a
I (Spherical)	Toluene	4.2
	Benzene	18.8
	Pyridine	1.0
II (Cylindrical)	Toluene	205
	Benzene	348
	Pyridine	2860
V (Long Chain)	Toluene	2.0
	Benzene	5.1
	Pyridine	6.1

(a) normalized to spin probe I in pyridine.

SPIN PROBES I-IX



ANALYSIS OF ARGONNE PREMIUM COAL SAMPLES BY THERMAL METHODS

Fawzy S. Sadek and Sara A. DeBot,
Chemistry Department, Winston-Salem State University,
Martin L. King Blvd., Winston-Salem, N.C. 27110

Thermal methods are used to determine the chemical characteristics of coal as well as its reactivity. Coal grading or ranking is generally based on fixed carbon and volatiles. Percentages of moisture, volatiles, fixed carbon and ash are reported in what is referred to as proximate analysis of coal, coke or fuel materials. ASTM methods can be used to determine each of these values, however, the procedures are time consuming, results are very subjective and the most important value, fixed carbon, is not measured directly. A more reliable and faster method for conducting proximate analysis is thermogravimetry (TG) (1,2). The sample's mass is continuously measured as a function of temperature in a controlled atmosphere and fixed carbon is measured directly as well as the range of medium volatiles and ash.

Coals are further characterized according to heat values, considered by some to be one of their most important properties, especially from a commercial or industrial aspect. Gross calorific value is traditionally determined by ASTM methods which employ various bomb calorimeters (3,4). Although these methods can generate acceptable results, they are also time-consuming, can be dangerous and give only total heat values. Thermogravimetry is an equally accurate technique compared to ASTM procedures, much faster and gives more information about the sample. The calorific value of bituminous coals containing 5-40% volatile matter on dry ash free (DAF) basis can be calculated from proximate analysis data using the Goutal equation (5). Earnest and Fyans (6) developed a modified form of this equation to obtain heat values of anthracitic coals and cokes while Ferguson and Rowe (7) have presented an equation relating calorific values of lignites to their proximate analyses.

A method for calculating heat values from ultimate analysis data has been described by Culmo (8). Percents carbon, hydrogen, nitrogen and sulfur determined by elemental analysis along with TG values of moisture and ash, were used to calculate calorific values from the Dulong equation. Results were reported to be in agreement within $\pm 3\%$ of the ASTM values. Giuzzi and Colombo introduced a modification of this equation for calculating gross and net heat values (9).

An alternative method for the direct determination of calorific values of coals by Differential Scanning Calorimetry (DSC) was introduced by Fyans in 1977 (10). This technique measures heat flow as a function of programmable temperature with the total area under the curve being proportional to the heat of combustion. A typical thermocurve for coal shows a two step decomposition with the first peak being the combustion of volatiles and the second relates to fixed carbon. Fyans and

Earnest have reported surprisingly good agreement between the area of the DSC peaks and the ASTM calorific values (10-12).

In recent years the goals of thermal analysis investigations have become more and more quantitative. Unresolved problems associated with DSC, however, have brought results by this method under question. Varhegyi, et.al. (13), showed that DSC curves reveal considerably less energy release than the true reaction heats of oxidation of organic materials and the measured heat is strongly affected by the experimental conditions. To correctly characterize calorific values for volatiles produced in various steps of thermal decomposition as well as the heat of oxidation of the resulting char, they proposed the use of catalysts as aids to combustion at the low temperatures of DSC. In an effort to improve the DSC technique for coal analysis, we have focused on the use of metal oxides as well as the effects of variables related to sample characteristics. Heat values determined by DSC and bomb calorimeters are compared with calculated values from proximate and ultimate analysis.

EXPERIMENTAL SECTION

Apparatus:

Ultimate Analysis of coals by the determination of C/H/N/S was made on the left channel (O/S) of a Carlo Erba Elemental Analyzer Model 1106. A model C-31 Cahn Co. microbalance and IBM computer were interfaced with the instrument. Eager 100 software of Carlo Erba was used for operating the system and data analysis.

The Mettler system used for proximate analysis and drying of coal samples was composed of a TG-50 thermogravimetric unit, M3 microbalance, TC-10A controller TA processor equipped with TA 3000 version 3.1 software attached to an IBM/PC computer for data storage, TA-70 for data processing, RO-80 Swiss printer/plotter for actual time thermocurve printing and Epson HI-80 for printing processed data. A Mettler DSC 20 with measuring cells containing medium sensitivity sensors was used to determine heat values of coal samples directly. Nitrogen used for pyrolysis was purified with a Supelco High Capacity Heated Carrier Gas Purifier, cat.# 2-3802.

Samples and Materials:

The 100 mesh Premium Coal Samples used in this study were supplied by Argonne National Laboratory (ANL). All chemicals used for filling reactors, and consumables for Elemental Analysis were purchased from Carlo Erba Co.. Platinum crucibles with fine platinum mesh lids were used for proximate analysis of coal. Standard 40 μ l aluminum or gold crucibles were utilized in the determination of heat values by DSC. Two equal weight crucibles with lids were selected and a hole of approximately 0.5mm was made in the center of each lid. A 1:1 mole ratio mixture of

magnesium oxide and silver oxide was finely ground in a mortar and stored in a vial shell in a vacuum dessicator until use. Approximately 0.3 to 0.6 mg dried coal was spread evenly in the center of the crucible and from 8 to 12 mg of the additive mixture was placed over the sample. The heat capacity was counterbalanced by putting an amount of the spent additive in the reference crucible equal to 93% of the freshly prepared mixture.

Ultra high purity (99.99% or better) oxygen, nitrogen, helium and argon were purchased from National Specialty Gases, a division of National Welders Supply. Magnesium oxide, lead chromate (Analytical Reagent, Mallinckrodt), silver oxide (Baker and Adamson), praeaseodymium oxide (Alpha Inorganics), calcium oxide, copper oxide (certified ACS, Fisher), and lead dioxide (Fisher) were used as received.

Procedures:

Remixing of coal samples was done according to recommendations of the supplier before the ampoules were opened in a glove box filled with argon gas. Approximately 25 mg of the as received coal was placed in a platinum crucible in the TGA furnace in dry, oxygen free nitrogen for moisture analysis. The temperature was brought to 112°C at a heating rate of 100 °C/min and then held isothermally for 2 min. The evaporation of moisture from each of the seven samples is graphically presented in Fig. 1.

Proximate and ultimate analyses were made on the dried coal samples. Percent moisture and ash were used for calculating results on dry basis as well as moisture and ash free basis (14). Heat values were calculated from proximate analysis data applying the Goutal equation and using in house software. The software calculates the Heat Value (ΔH) as follows: ΔH (cal/gram) = $82C + aV$, where C is % fixed carbon, V is % volatiles and "a" is the Goutal coefficient. The value of "a" is a function of V and is obtained by interpolating known values of "a" at various values of V as derived by Goutal. Elemental analysis percentages were used in the calculation of heat values from the modified Dulong equation (8). Gross and net heat values are printed at the end of each analysis in calorie/gram units. These are changed to BTU/lb for comparison with ASTM bomb calorimeter values.

A procedure for determining heat values by DSC was stored on the TC-10A processor. This included 10°C/min heating rate from room temperature to 600°C. An oxygen flowrate of 20 ml/min was used. Integration of the heat flow during the dynamic experiment gives the heat change in coal directly. The two peak curve was integrated over a baseline starting at 105°C to the end of the run.

RESULTS AND DISCUSSION

Proximate and ultimate analyses of seven bituminous Premium Coal Samples are shown in Table 1. The calculated percentages are

comparable with those reported by ANL. Proximate analysis data made by TG were calculated by the instrument while data listed for ANL/ASTM were derived indirectly from the values of volatiles and ash provided with the samples. ASTM criteria for proximate analysis precision in reproducibility of data between two laboratories or by different methods are met with minor exceptions found in volatile matter of the Illinois #6 sample and percent ash of the Wyodak sample.

In ultimate analysis (14) the four major elements of coal were determined simultaneously on 1.0 to 3.0 milligram samples (Fig.3). The ANL data were made on different aliquot portions. Results are comparable with the exception of Illinois #6 and Blind Canyon carbon percentages and Upper Freeport hydrogen values. The sulfur values show a distinct difference for Illinois #6. In both proximate and ultimate analysis three or four values are compared with each other or with their counterpart made by a standard method. The logical way to compare sample data is to simplify to one numerical value. Mathematical equations to combine each group of data have existed for several decades. Goutal introduced his equation to give the heat value of bituminous coals as a function of percent volatiles and fixed carbon. By applying this equation to calculate heat values of TG data as well as ANL data we arrived at the values shown in Table 1. The average error of the TG heat values relative to ANL data calculated with the same equation is 3.9%. The difference between TG data and bomb calorimeter values is 3.5%. It is worth mentioning that most TG calculated heat values are slightly higher than those determined by the ASTM/bomb calorimeter method. This phenomenon repeats itself with calculated heat values from elemental analysis results. Work with elemental analysis confirmed that a catalyst is needed to insure the complete combustion of carbon in organic compounds regardless of the use of large amounts of oxygen and high temperatures. Oxides of copper, chromium, tungsten, vanadium and others (14) have been used at temperatures up to 1050°C to accomplish the complete oxidation of carbon to carbon dioxide. A comparison of elemental analysis results with those obtained with bomb calorimeters shows an average error of about 1.5% higher which may indicate a more complete combustion of the sample.

Direct determination of heat values by DSC traditionally has produced results 20 to 40 percent lower than those determined by bomb calorimeters. Varhegyi, et. al., proved by mass spectrometry that these low results are due to the formation of carbon monoxide (13). A mixture of cupric oxide and lead chromate was used as a catalyst but the true heat of combustion of the coal samples was not achieved even though the instruments maximum temperature reaches 750 °C. Many commercially available DSC instruments have a maximum of only 600°C and some manufacturers recommend pressurized containers made of either glass or stainless steel and/or pressurized DSC cells, further complicating the situation. It was found that the effects of factors such as heating rate, sample mass and particle size, type and amount of additive, hole size in container lid as well as

oxygen flowrate, are dependent on each other.

Heating metal oxides in an oxygen atmosphere using TG proved that most of the oxides are stable and usually contain the metals in the highest oxidation state (16). Contrary to this statement the TG curves of calcium, magnesium, lead, praseodymium and silver oxides in Fig. 4 show a mass loss. The curves were obtained in an atmosphere of oxygen and at a heating rate of 40 C/min. Dissociation of these oxides with the release of active oxygen appears to be definite. Magnesium oxide and silver oxide release oxygen and dissociate without phase transitions while calcium oxide and praseodymium oxide dissociate with phase transitions. Lead dioxide loses oxygen as shown in Fig. 4 in two steps below 650°C and a third step above 650°C which disturbs the DSC curve in that region.

Magnesium oxide (Fig. 5) was selected as a combustion aid due to its release of oxygen in the region of coal volatile matter to assist in its complete oxidation. In addition, it has been reported that magnesium oxide catalyses the oxidation of carbon monoxide to carbon dioxide (17). Formation of carbon dioxide releases approximately four times the amount of heat as the formation of carbon monoxide from the same amount of carbon. This is basically the reason for the lower heat values measured in unpressurized low temperature DSC. Silver oxide (Fig.5) releases its oxygen relative to the fixed carbon combustion region as shown in Fig. 6. Heat value results determined using the magnesium-silver oxide mixture are listed in Table 1. DSC results are comparable with ASTM values.

CONCLUSIONS

Thermogravimetric and elemental analysis data have been used to derive heat values of Argonne Bituminous Premium Coal Samples. The average error between heat values calculated from proximate analysis data by the classical Goutal Equation and ASTM/bomb calorimeter values was less than 4%. It was found to be less than 2.0% between Ultimate Analysis values calculated by the Dulong Equation. A comparison of heat values obtained directly by conventional low temperature DSC using metal oxide additives shows an average error of 0.5%.

ACKNOWLEDGMENT

We are grateful to Dr. Karl S. Vorres for providing the Argonne National Laboratory Premium Coal Samples. We also acknowledge G. Paul and D. McMorran of Mettler Co. for valuable information concerning the Mettler DSC 20.

LITERATURE CITED

- (1) Sadek, F.S.; Herrell, A.Y. *Thermochimica Acta*, 81 (1984) 297.
- (2) Ottaway, M., *Fuel* 61 (1982) 713.
- (3) "ASTM Designation D2015-85, Annual Book of ASTM Standards, 05.21 (1985).
- (4) "ASTM Designation D3286-85, Annual Book of ASTM Standards, 05.21 (1985).
- (5) Goutal, M. *Compt. Rend.*, 135 (1902) 477.
- (6) Earnest, C.M.; Fyans, R.L. *Thermal Analysis Applications Study #21*, Perkin-Elmer Corp., Norwalk, CT (1977).
- (7) Ferguson, J.A.; Rowe, M.W. *Thermochimica Acta*, 107 (1986) 291.
- (8) Culmo, R.F., *Elemental analysis Application Study #2*, Perkin-Elmer Corp., Norwalk, CT (1977).
- (9) Giazzi, G.; Colombo, B. *The Journal of Coal Quality*, 2 (1982) 26.
- (10) Fyans, R.L., *Thermal Analysis Application Study #21*, Perkin-Elmer Corp., Norwalk, CT, (1977).
- (11) Earnest, C.M., "Analytical Calorimetry" (Johnson, J.F.; Gill, P.S. Eds.) Vol. 5, Plenum Press, New York, (1984), 343.
- (12) Earnest, C.M. *Int. Instrum. Res.*, (1985), 57.
- (13) Varhegyi, G; Szabo, P.; Till, F. *Thermochimica Acta*, 106 (1986) 191.
- (14) Sadek, F.S.; deBot, S.A. "Rapid Automated Methods For Coal Ultimate Analysis" *Proceedings of the 6th International Coal Testing Conference*, (1987) 97.
- (15) "ASTM Designation D3180, Annual Book of ASTM Standards, Vol. 05.05 (1984).
- (16) Wendlandt, W.W. "Thermal Analysis" 3rd Edition John Wiley & Sons, New York (1986) 179.
- (17) Lundsford, J.H.; Jayne, J.P. *Journal of Chemical Physics*, 44 (1966) 1492.

Table 1. COMPARISON OF ARGONNE PREMIUM COAL SAMPLE DATA OBTAINED BY DIFFERENT THERMAL METHODS.

PROXIMATE ANALYSIS*

	TGA (%)			ANL/ASTM (%)		
	Ash	VM	FC	Ash	VM	FC
1. Upper Freeport	13.2	27.6	59.2	13.2	27.5	59.3
2. Wyodak	7.5	45.2	47.3	8.8	44.7	46.5
3. Illinois #6	15.4	36.6	48.0	15.5	40.1	44.4
4. Pittsburgh #8	9.2	36.7	54.1	9.3	37.8	52.9
5. Pocahontas #3	4.3	19.0	76.7	4.8	18.6	76.6
6. Blind Canyon	4.6	45.2	50.2	4.7	45.8	49.5
7. Lewis Stockton	20.0	30.2	49.8	19.8	30.2	50.0

ULTIMATE ANALYSIS*

	ELEMENTAL ANALYSIS (%)				ANL/ASTM (%)			
	C	H	N	S	C	H	N	S
1. Upper Freeport	75.1	4.6	1.5	2.3	74.2	4.1	1.4	2.3
2. Wyodak	67.9	4.9	1.0	0.8	68.4	4.9	1.0	0.6
3. Illinois #6	64.6	4.5	1.2	4.5	65.7	4.2	1.2	4.8
4. Pittsburgh #8	75.0	5.0	1.5	2.4	75.5	4.8	1.5	2.2
5. Pocahontas #3	85.7	4.4	1.2	0.7	86.7	4.2	1.3	0.7
6. Blind Canyon	74.9	5.6	1.5	0.8	76.9	5.5	1.3	0.6
7. Lewis Stockton	66.3	4.3	1.2	0.8	66.2	4.2	1.3	0.7

HEAT VALUES* (BTU/lb)

	CALC. GOUTAL		CALC. DULONG		DIRECT	
	TGA	ANL	E. A.	ANL	DSC	ANL/ASTM
1. Upper Freeport	13535	13537	13701	12874	13611	13467
2. Wyodak	11687	11487	11578	11641	11800	11717
3. Illinois #6	11817	10982	11664	11363	11951	11951
4. Pittsburgh #8	13200	14356	13684	13415	13740	13629
5. Pocahontas #3	16090	14867	15141	15102	15029	15024
6. Blind Canyon	12417	12240	13633	13743	13896	13925
7. Lewis Stockton	12005	12057	11869	11626	11857	11810

* As received, on dry basis.

Figure 1. Drying of ANL Premium Coal Samples by TGA.

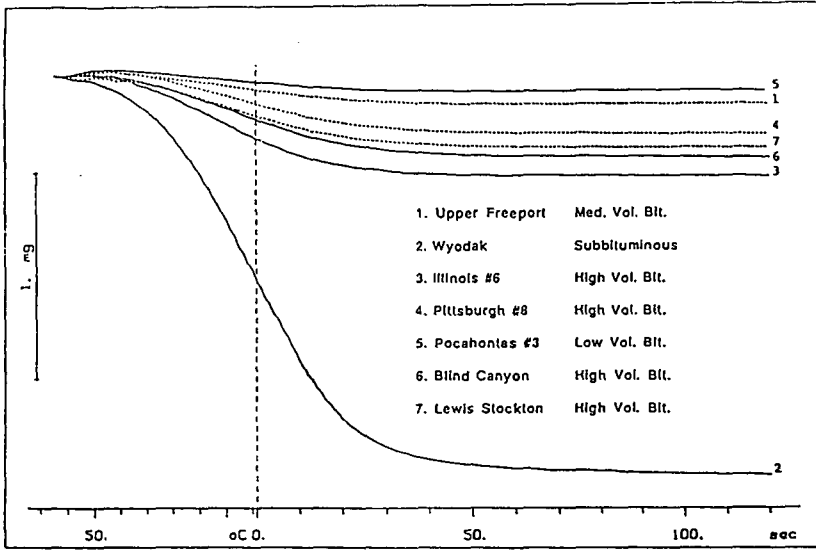


Figure 2. Proximate Analysis of ANL Bituminous Coal on Dry Basis.

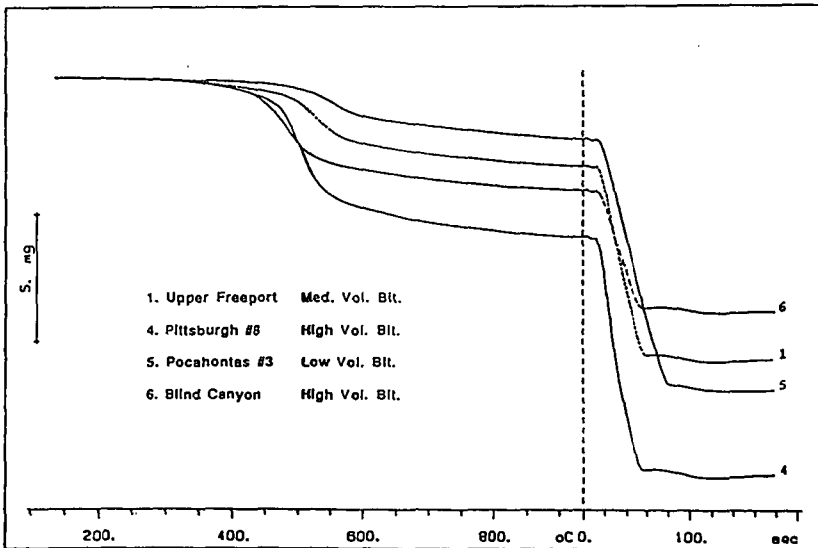
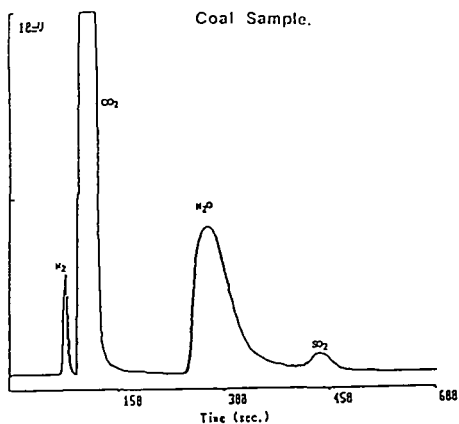


Figure 3. Elemental Analysis of Upper Freeport Coal Sample.



Date : 02-13-1990 Time : 09:32:15 Company name : WSSU
 Sample : 168 COAL 11 AS 15 600 H Type : Unknown
 Sample Weight : 1.8972 Base Line drift (10%) : 12
 Operator : GSK

Ret. T.	Area (10 ⁶ %)	Area 1	Comp. 1	Peak area	
1	77	11390	1.405	1.725122	Nitrogen
2	97	1267850	82.552	21.67212	Carbon
3	274	238704	15.345	4.764939	Hydrogen
4	454	14091	1.031	1.971164	Sulphur

Carb./Hyd. Area = 5.372648 Carb./Sulph. Area = 78.37535
 Carb./Sulph. Area = 89.03542
 G. M. V. = 7871.641 H. M. V. = 7127.518

Figure 4. Thermocurves of Five Metal Oxides.

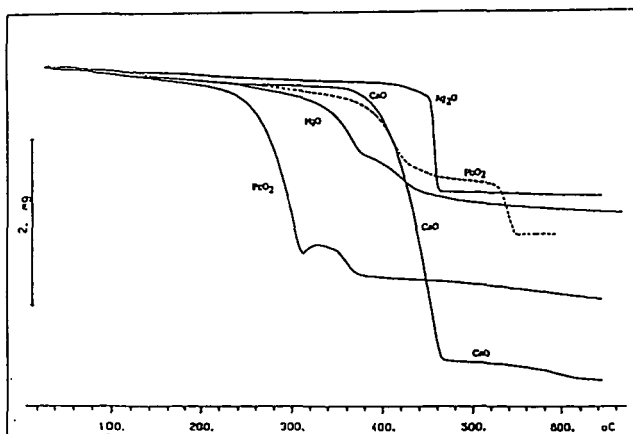


Figure 5. DSC of Magnesium Oxide and Silver Oxide.

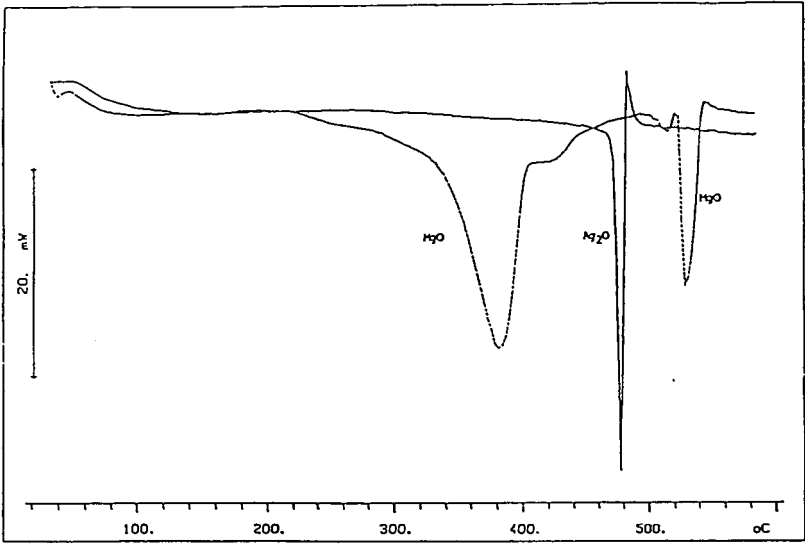
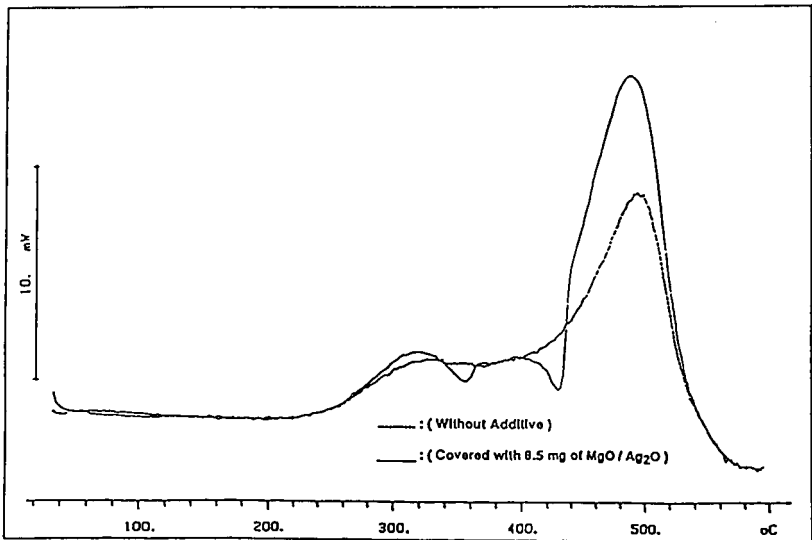


Figure 6. DSC Curves of Pittsburgh #8 Coal Sample at 10° C / min.

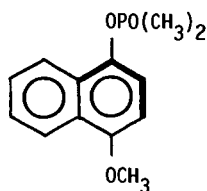


THE DOUBLE CROSS POLARIZATION ^{13}C -NMR EXPERIMENT IN
SOLID FOSSIL FUEL STRUCTURE ANALYSIS

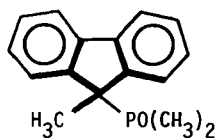
Edward W. Hagaman and Madge C. Woody
Chemistry Division
Oak Ridge National Laboratory
Oak Ridge, Tennessee 37831-6201

The Double Cross Polarization ^{13}C -MAS/NMR experiment has been used to derive a new operational classification of solid fossil fuels based on chemical reactivity^{1,2}. The method requires labeling reactive sites in the organic matrix with a magnetically active isotope not present in the precursor material, and using the local, isolated dipole-dipole interaction between this nucleus and nearby ^{13}C nuclei to detect via cross polarization the carbon centers in the vicinity of the label. The technique is a marriage of chemistry and spectroscopy and the information content of the DCP spectra is defined by both partners.

^1H - ^{13}C - ^{31}P DCP/MAS ^{13}C -NMR spectroscopy has been used to statistically describe phenolic ortho-substitution patterns of coals via their aryl phosphinate or phosphate derivatives, as per model 1. The identification of specific functional group types as the activation source for acidic C-H bonds in these materials has also been effected via the tertiary phosphine oxide derivatives generated from coal carbonions as in model 2. The bold line in these structures indicates the carbon bonding network that is detected by this technique, with signal intensities nominally proportional to the inverse sixth power of the ^{31}P - ^{13}C internuclear distance. The sensitive volume element centered on ^{31}P in which DCP signals are observed is determined by the rate at which the ^{31}P - ^{13}C cross polarization signal accrues, primarily determined by the depolar interaction strength, and the rate at which this signal decays, the ^{13}C rotating frame T_1 . For the ^{31}P - ^{13}C pair, DCP signals are confined to a spherical volume element with a ca. 4 Å radius.



1



2

In these applications of DCP NMR the new, detailed structure and/or reactivity information is realized by detection of carbon resonances one or more bonds removed from the reaction center, but in a volume element of intramolecular dimensions. To the extent that intermolecular contributions to the spectrum are detected, and not recognized as such, the structure/reactivity correlation is weakened.

Direct substitution of phosphorus on the aromatic rings in the organic matrix of the coal is not readily accomplished. This environment potentially can be labeled with fluorine in a selective fashion using newly developed reagents³. The possibility of determining the changes in average ring substitution patterns as a function of chemical treatment or coal diagenesis emerges. Recent developments in the field of DCP ¹³C NMR will be presented.

References

1. Local Structure Evaluation in Solid Organophosphorus Compounds by Double Cross Polarization Carbon-13 Nuclear Magnetic Resonance Spectroscopy. Edward W. Hagaman, submitted for publication.
2. Solid State Nuclear Magnetic Resonance Detection of Reaction Sites in Amorphous, Heterogeneous Organic Matrices. Edward W. Hagaman, submitted for publication.
3. Singh, S., DesMarteau, D. D., Zuberi, S. S., Witz, M., Huang, H.-N. J. Am. Chem. Soc., 1987, 109, 7194-7196.

Acknowledgement

Research sponsored by the Division of Chemical Sciences/Office of Basic Energy Sciences, US Department of Energy under contract DE-AC05-84OR21400 with the Martin Marietta Energy Systems, Inc.

SOLID STATE ^{13}C RELAXATION STUDIES OF COALS

R. E. Botto* and David E. Axelson**

*Chemistry Division, Argonne National Laboratory,
9700 South Cass Avenue, Argonne, IL 60439

**Energy, Mines & Resources Canada, CANMET,
P.O. Box 1280, Devon, Alberta, Canada T0C 1E0

INTRODUCTION

Despite many studies of coal and related fossil fuels, no attempts have been made to systematically correlate changes in the solid state ^{13}C -NMR parameters as a function of static field strength. In particular, questions arise regarding differences in spectral resolution and relaxation parameters. While discrimination among the complex structural components of fossil fuels can be based on relaxation time differences (1), this also necessitates a more intensive study of static field-strength effects if a more complete understanding of coal structure is to be gained.

Carbon-13 spin-lattice relaxation was chosen as the parameter of interest for this study because it represents a "dilute" nuclear spin system, which therefore minimizes spin diffusion interaction among phases. Furthermore, it is not as complicated to interpret as $T_{1\rho}$ measurements, and exhibits a field dependence in the slow motion regime (Figure 1). These studies also comprise part of a more comprehensive on-going evaluation of the Argonne Premium Coal Samples.

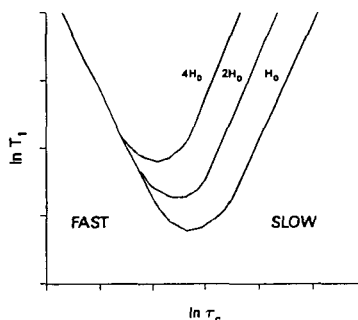


Figure 1. Motional dependence of T_1 with magnetic field.

EXPERIMENTAL

All NMR spectra taken at higher field were obtained on a Bruker CXP-200 spectrometer. Parameters used to acquire data were as follows: spectrometer frequency 50.306 MHz, 3 kHz magic-angle spinning in a boron nitride rotor containing a deuterated polymethylmethacrylate base (exhibiting no ^{13}C background from residual non-deuterated material), dipolar decoupling of 50-60 kHz, 90° pulse width of 4-5 ms, spin temperature alternation of the H-1 pulse, 20 kHz spectral width, 4K data points, 50-75 Hz line broadening, 500-3000 scans/spectrum, ambient temperature, 12 bit digitizer resolution, quadrature detection, both normal and spinning-sideband suppressed spectra (TOSS), recycle delay 3-5 s, contact time 1 ms and 50-80 ms decoupling time. All chemical shifts were reference to TMS via adamantane as a secondary reference.

Spectra taken at lower field at Argonne were obtained at 25.18 MHz using a Bruker CXP-100 spectrometer in the pulse Fourier transform mode with quadrature phase detection. The sample spinners were made of ceramic with an internal volume of 250 μ L and were spun at approximately 4 kHz. Operating parameters in CP experiments included a spectra width of 10 kHz, a 90° proton pulse width of 3.75 μ s (67-kHz proton-decoupling field), an acquisition time of 20 ms, a pulse repetition time of 2s, a contact time of 1.5 ms, and a total accumulation of 1000 transients. In a typical experiment, words of memory were allocated for data acquisition and then increased to 4K (2K real data) by zero filling. Before Fourier transformation of the data, the interferogram was multiplied by a decreasing trapezoidal window function after the first 40 data points. Carbon aromaticities were derived from integrated signal intensities for sp^2 -hybridized (δ 110-160) and sp^3 -hybridized (δ 0-60) carbon absorption bands. For the aromatic carbons, signal intensities of the spinning sidebands were added to the intensity of the centerband. Chemical shifts were referenced to TMS using tetrakis(trimethylsilyl)silane [TKS] as a secondary reference (2).

American coals were obtained from the Argonne Premium Coal Sample Program. For the Canadian coals, homogenized bulk samples representative of the coal deposits from their respective regions were obtained by a bucket auger drill rig. Samples were stored in sealed barrels at low temperatures to minimize long term deterioration. The same samples were used for the NMR measurements on the two instruments to eliminate sample heterogeneity problems for the purposes of this comparison.

RESULTS AND DISCUSSION

Proximate and ultimate analysis of the coals are summarized in Table 1. Apparent aromaticities are given in Table 2 and carbon-13 spin-lattice relaxation measurements are shown in Table 3.

Related studies on proton relaxation at different fields have been reported by Packer et al. (3), Pembleton (4), and Sullivan et al. (5). Dudley and Fyfe (6) discussed carbon relaxation times for a pitch and three Canadian coals. Emphasis was placed on the effects of paramagnetics (including oxygen) in rationalizing the results. Palmer and Maciel (7) reported relaxation parameters for a kerogen concentrate of a Colorado oil shale and Powhatan #5 coal. Aliphatic and aromatic regions exhibited bi-exponential relaxation decay curves for both T_1 and T_2 measurements for the kerogen concentrate. The coal sample was characterized by T_{1C} of 5.8 s for all carbons ($B_0 = 1.4$ T, 21°C). For the kerogen concentrate the effect of the static field strength on the T_{1B} value was also determined. On increasing B_0 from 1.4 T to 4.7 T the proton T_1 increased from about 100 ms to 184 ms. Changing the temperature from ambient to -141C resulted in only a marginal increase in T_1 to 124 ms, whereas the optimum contact time did not change at all.

Figure 2 illustrates the nature of the spectra obtained on a low rank coal (lignite) at the two different field strengths. The 50-MHz CP/MAS spectrum was obtained using sideband suppression (TOSS). No apparent differences in resolution exist under these conditions.

Apparent aromaticities are summarized in Table 2. The average deviation for the ten coals at the two fields is about ± 0.02 units, about equal to the precision

TABLE 1. Ultimate Analysis of Coals.^a

Sample	C	H	N	O	S	A
Beulah-Zap lignite (APCS #8)	72.9	4.83	1.15	20.30	0.70	9.7
Wyodak-Anderson subB (APCS #2)	75.0	5.35	1.12	18.00	0.47	8.8
Herrin hvCB (APCS #3)	77.7	5.00	1.37	13.50	2.38	15.5
Upper Freeport mvB (APCS #1)	85.5	4.70	1.55	13.20	0.74	13.2
Pocahontas lvB (APCS #5)	91.0	4.44	1.33	2.47	0.50	4.2
Ontario lignite	66.9	4.65	0.9	27.23	0.32	4.8
Ardley subB	75.7	4.1	1.2	18.5	0.50	20.0
Smokey Tower subB	75.8	5.1	1.7	16.9	0.50	20.0
Dunvegan hvAB	84.4	5.6	2.1	5.4	2.50	4.4
Gates lvB	93.2	4.63	1.5	0.17	0.50	11.0

^aColumn headings defined as follows: C = % carbon; H = % hydrogen, N = % nitrogen; O = % oxygen; S = % sulfur; A = ash.

TABLE 2. Apparent Carbon Aromaticities of Coals.

Coal	Aromaticity	
	2.3 Tesla CP/MAS	4.7 Tesla TOSS
Beulah-Zap lignite	0.66	0.69
Ontario lignite	0.62	0.61
Wyodak-Anderson subbituminous	0.67	0.63
Ardley subbituminous B	0.74	0.75
Smokey Tower subbituminous A	0.66	0.67
Herrin hvC bituminous	0.72	0.71
Dunvegan hvA bituminous	0.76	0.71
Upper Freeport mv bituminous	0.82	0.81
Pocahontas lv bituminous	0.85	0.86
Gates lv bituminous	0.82	0.82

TABLE 3. Carbon T₁(s) Relaxation in Coals.

Coal	2.3 Tesla		4.7 Tesla	
	Aliphatic	Aromatic	Aliphatic	Aromatic
Beulah-Zap lignite (APCS #8)	0.3 (34%)	0.3 (46%)	0.1 (54%)	0.1 (57%)
	1.7 (66%)	2.4 (54%)	1.9 (46%)	2.0 (43%)
Ontario lignite	0.6 (68%)	0.8 (58%)	0.2 (41%)	0.2 (46%)
	6.7 (32%)	4.7 (42%)	3.3 (59%)	5.0 (54%)
Wyodak-Anderson subbituminous (APCS #2)	0.8 (38%)	0.9 (36%)	0.4 (67%)	0.2 (63%)
	2.1 (62%)	2.2 (64%)	7.5 (33%)	6.0 (37%)
Ardley subbituminous B	---	---	0.6 (45%)	0.7 (46%)
	1.2	1.4	3.0 (55%)	5.2 (54%)
Smokey Tower subbituminous A	0.6 (41%)	0.5 (35%)	0.3 (72%)	0.3 (65%)
	1.2 (59%)	1.6 (65%)	6.1 (28%)	4.5 (35%)
Illinois No. 6 hv bituminous (APCS #3)	1.4 (38%)	3.0 (34%)	0.1 (39%)	0.1 (24%)
	5.5 (62%)	9.9 (65%)	9.2 (61%)	14.7 (76%)
Dunvegan hvA bituminous	3.0 (37%)	6.2 (25%)	0.9 (48%)	---
	5.8 (63%)	13.9 (75%)	22.3 (52%)	25.3
Upper Freeport mv bituminous (APCS #1)	1.2 (60%)	9.0 (9%)	1.5 (38%)	---
	6.9 (40%)	10.2 (91%)	14.8 (62%)	20.6
Pocahontas lv bituminous (APCS #5)	---	4.7 (17%)	0.3 (18%)	0.1 (6%)
	5.6	9.1 (83%)	10.7 (82%)	15.7 (94%)
Gates lv bituminous	---	---	0.4 (38%)	---
	3.5	5.9	9.3 (62%)	15.5

of the aromaticity measurements. The effects of sideband suppression and magic-angle spinning itself on aromaticity measurements of fossil fuels have been discussed previously (8,9). Agreement is reasonably good between aromaticities derived from both normal and sideband suppressed spectra for this series.

More significant deviations in measured aromaticities arise from comparison of values derived from spinning and non-spinning samples (9-12). Line narrowing is found in the strong collision limit ($\omega t \gg 1$) due to effective coherent spatial averaging from magic-angle spinning, as well as in the weak collision limit ($\omega t \ll 1$) due to incoherent averaging from the random molecular motion. In the intermediate regime ($\omega t \approx 1$), where the MAS frequencies are similar to the frequencies associated with the molecular motion of either some or all components of the sample, destructive interference gives rise to severely broadening lines. This phenomenon occurs over a relatively narrow range of spinning frequencies (10,11). A similar destructive interference effect has also been noted between dipolar decoupling frequencies and molecular motion (12). Subject to these considerations, the present data indicate that good agreement can be attained in independent measurements of apparent aromaticities of spinning samples.

The ^{13}C spin-lattice relaxation times (in seconds) and corresponding mass fractions (percentages in brackets) for all samples studied are given in Table 3. Aliphatic and aromatic regions at both field strengths were analyzed separately. Most coals exhibited two-component exponential decays for each region. Differences in relaxation times of these components vary widely (from a factor of about 2 to over 30). Separation of the decays for the more similar relaxation rates gives rise to greater uncertainty in the mass fractions reported, although trends are still discernible as a function of rank.

Figure 3 illustrates one such trend between rank (as denoted by %C) and the ^{13}C T_1 of the long component of the aromatic decay. For the low-rank coals the relaxation time for this fraction is of the order of 2-6 seconds, with the longer relaxation times usually associated with the higher field. Above the 80%C the T_1 difference at the two static field strengths increase significantly for the same sample. In addition, the relaxation times appear to reach a maximum value

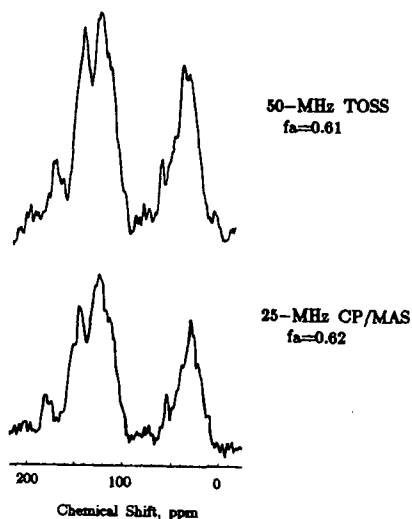


Figure 2. 25- and 50- MHz CP/MAS spectra of Ontario lignite.

at about 85°C. The phenomenon occurs at both fields. A similar trend is observed for the long relaxing component of the aliphatic carbon.

The trends in Figure 3 arise from differences in coal structure that also vary systematically with rank. These compositional variations are reflected in both the field dependence of the measurements and the observation of the maximum. We propose that these data can be related to two general factors: an underlying difference in coal structure as rank increases and the presence of paramagnetic species (oxygen, heavy metal minerals, organic free radicals). In the former case, changes in molecular motion (overall rotational diffusion, local segmental and librational motions) would be manifest as T_1 differences. In the latter instance, paramagnetic species in sufficient quantity could dramatically reduce the T_1 values measured.

A plot of the mass fraction of the long relaxing aromatic component versus %C is shown in Figure 4. At both fields there is a systematic increase in the fraction of species relaxing slowly. This trend may be attributed, in part, to a decrease in the oxygen-rich humic portion of the coals studied with increasing rank. Scatter in mass fraction measurements reflects the relative difficulty of deconvoluting overlapping decays of varying degrees of similarity (and with different signal-to-noise ratios) at the two fields.

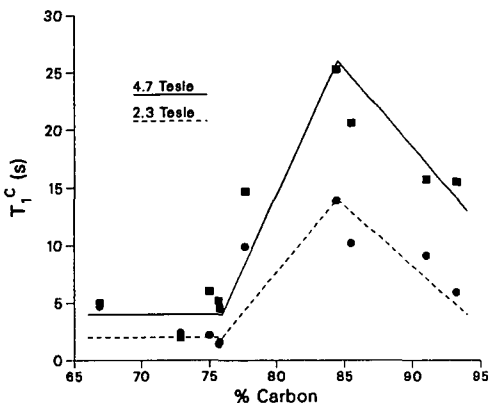


Figure 3. Variation in aromatic carbon relaxation (long) with carbon content of coal.

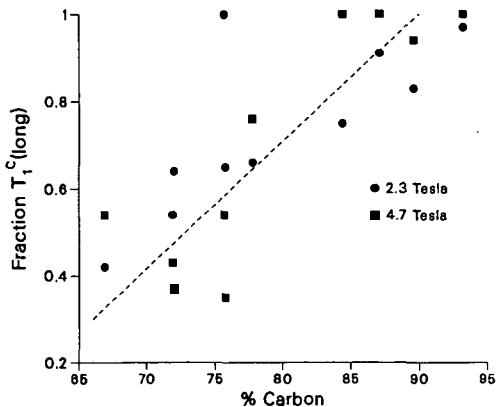


Figure 4. Variation in fraction aromatic T_1^C (long) with carbon content of coal.

As confirmation of the effect of paramagnetic species on our measurements, the Beulah-Zap lignite was treated with a dilute HCl solution to remove iron. The relaxation decay changed significantly as shown in Figure 5. The original two-component decay became a single-exponential decay after treatment, with a concomitant increase in the relaxation time occurring. Atomic absorption data on the HCl washings indicate a significant level of extractable iron in this lignite sample: 1,951 $\mu\text{g Fe/g coal}$. Relaxation discrimination experiments allow the analysis of short and long relaxing components and will be presented.

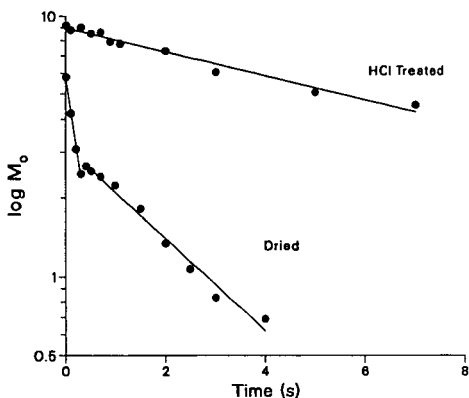


Figure 5. Changes in aromatic carbon T_1 of APCS #8 with acid treatment.

CONCLUSIONS

Spectral resolution is virtually invariant with rank over the static frequency range of 25 to 50 MHz. Although correlations between relaxation times and rank-related parameters are clearly observed at both field strengths, they probably arise from both fundamental changes in coal structure (with increasing degree of coalification) and systematic variations in the nature and extent of paramagnetic species present. The paramagnetic species themselves may represent a combination of stable organic free radicals present in large aromatic ring systems and a distribution of inorganic species, presumably which are chelated to oxygen-rich organic structures (particularly in the low-rank coals). The presence of a maximum in the spin-lattice relaxation time at both fields at 85%C probably reflects these competing interactions.

For the raw, untreated coals there are systematic differences in relaxation times with rank that may be of use in relaxation discrimination experiments.

It remains to be determined how the concentration and exact distribution of paramagnetic species can be quantitatively related to the relaxation rates observed. The rank dependence of these variables is also of ultimate concern for the rationalization of these data.

REFERENCES

1. D. E. Axelson, "Solid State NMR of Fossil Fuels", Multiscience, Montreal, 1985.
2. J. V. Muntean, L. M. Stock, R. E. Botto, J. Magn. Reson., 48, 35 (1988).
3. K. J. Packer, R. K. Harris, A. M. Kenwright, C. E. Snape, Fuel, 62, 999 (1983).
4. R. G. Pembleton, Ph.D. Thesis, Iowa State University, 1978.
5. M. J. Sullivan, N. M. Szeverenyi, G. E. Maciel, "Magnetic Resonance Introduction, Advanced Topics and Applications to Fossil Energy", L. Petrakis, J. P. Fraissard (Eds.), pp. 607-616, D. Reidel Publishing Company, 1984.
6. R. L. Dudley and C. A. Fyfe, Fuel, 61, 651 (1982).
7. A. J. Plamer and G. E. Maciel, Anal. Chem., 54, 2194 (1982).
8. R. E. Botto and R. E. Winans, Fuel, 62, 271 (1983).
9. D. E. Axelson, Fuel, 66, 195-199 (1987).
10. D. Suwelack, W. P. Rothwell, and J. S. Waugh, J. Chem. Phys., 73, 2559 (1980).
11. P. Ollivier and B. C. Gerstein, Carbon, 22, 409 (1984).
12. W. P. Rothwell and J. S. Waugh, J. Chem. Phys., 74, 2721 (1981).

ACKNOWLEDGMENT

This work was performed under the auspices of the Office of Basic Energy Sciences, Division of Chemical Sciences, U.S. Department of Energy, under contract number W-31-109-ENG-38.

THE DETERMINATION OF THE HYDROXYL AND CARBOXYLIC ACID CONTENT OF COAL MACERALS USING COMBINED CHEMICAL AND SPECTROSCOPIC TECHNIQUES

Chol-yoo Choi, John V. Muntean, and Arthur R. Thompson

Chemistry Division, Argonne National Laboratory,
9700 South Cass Avenue, Argonne, IL 60439 and
Department of Chemistry, The University of Chicago,
Chicago, IL 60637

ABSTRACT

Macerals were separated from two high volatile bituminous coals obtained from the Argonne Premium Coal Sample Program and one high volatile bituminous coal from the Pennsylvania State University Coal Sample Bank. A preliminary survey of the nature of these macerals using chemical and spectroscopic techniques are reported. Alkylation using ^{13}C enriched methyl iodide followed by solid ^{13}C NMR analysis were used to determine the concentrations of acidic OH and CH sites in these macerals. The relative quantities of various types of methyl ethers and methyl esters were also estimated from the NMR spectra.

INTRODUCTION

The combined use of alkylation using ^{13}C enriched reagents and solid ^{13}C NMR spectroscopy has been shown to be an effective procedure for the determination of the different types of acidic sites in coals (1-7). Alkylation using tetra-butylammonium hydroxide as base catalyst alkylates the acidic oxygen functional groups in coal such as phenols and carboxylic acids to produce ethers and esters (8). Certain acidic carbon sites in structures such as fluorene, indene, and benzanthrene can also be alkylated under these reaction conditions (3,5). The distinct chemical shift differences of methyls on carbon and oxygen allows the estimation of the relative degree of methylation on oxygen versus carbon. Furthermore, the O-methyl region of the ^{13}C spectra can be resolved into three distinct regions corresponding to the methyl carboxylates, unhindered aryl methyl esters and hindered aryl methyl ethers.

Macerals were separated from three high volatile bituminous coals by density gradient centrifugation (9). The concentration of the various types of hydroxyl and carboxylic acid groups in these macerals as estimated by ^{13}C enriched methylation and solid ^{13}C NMR spectroscopy are reported.

RESULTS AND DISCUSSION

Preliminary Survey. The coals used in this study were obtained from the Pennsylvania State University Coal Sample Bank and the Argonne Premium Coal Sample Program. These were the West Virginia Upper Kittanning seam hvA bituminous coal (PSOC-732), the Utah Blind Canyon seam hvB bituminous coal (APCS-6), and the West Virginia Lewiston-Stockton seam hvA bituminous coal (APCS-7). Maceral groups were separated from these coals using density gradient centrifugation (9). The elemental data for the coals and macerals, which can conveniently be discussed in terms of mole ratios, are shown in Table I. The

H/C values for the macerals follow the order: liptinite > vitrinite > inertinite for the West Virginia Upper Kittanning and the West Virginia Lewiston-Stockton macerals, and resinite > sporinite > vitrinite for the Utah Blind Canyon macerals. Nitrogen is more concentrated in the vitrinites than in the other macerals. The nitrogen content is substantially lower in the Utah Blind Canyon resinite than in the other macerals from this coal, and this finding is in accord with previous reports of other Utah resinites (10,11). The O/C values follow the order: vitrinite - inertinite > liptinite for all the macerals. It should be noted that the oxygen content was calculated by difference from the C, H, N microanalyses. The contributions from sulfur and mineral matter were not taken into consideration even though significant differences in the sulfur content of different maceral types in the same coal have been reported (12-14).

The solid ^{13}C -CP/MAS spectra of the macerals are shown in Figures 1-3. The NMR spectra are scaled to the intensity of the largest signal. The fraction of carbon aromaticity (f_a) in CP/MAS experiments are shown in Table II. Quantitative interpretations of CP/MAS experiments must be made with caution. Recent experiments suggest that f_a values determined by CP/MAS techniques may underestimate the aromatic carbon content of coals and macerals (15).

Hydroxyl and Carboxylic Acid Concentration. The macerals were alkylated with ^{13}C enriched methyl iodide (98% ^{13}C) using tetrabutylammonium hydroxide as the basic catalyst in tetrahydrofuran following Liotta's procedure (8). The degree of alkylation estimated from the elemental data as methyl groups that had been added to each 100 carbon atoms of the maceral group is shown in Table III.

Methylation on carbon occurs to the extent of 10 to 25 percent of the total methyls added to the macerals of the West Virginia Upper Kittanning and Lewiston-Stockton coals. Methylation occurs on carbon to a lesser degree for the macerals of the Utah Blind Canyon coal, as expected for a less mature coal. The observation that less methyls were added on the whole coals rather than the individual macerals of the Utah Blind Canyon and West Virginia Lewiston-Stockton coals may be due to the larger particle size of the whole coals relative to the macerals. Thus, reagent accessibility may be a factor for these alkylations. However, the relative O- vs. C-methylation ratio for the whole coal is similar to that of the vitrinite, which suggests that the alkylatable oxygen and carbon sites are randomly dispersed.

The CP/MAS spectra of the Utah Blind Canyon macerals alkylated with ^{13}C enriched methyl iodide is shown in Figure 4. The O-methylation region of the ^{13}C NMR spectra appear in three distinct regions. The relative contributions of the three regions based on their relative intensities are summarized in Table IV. The most plausible structural elements in methylated coal that give rise to resonances centered at 50 ppm are the methyl carboxylates; centered at 55 ppm are the unhindered aryl ethers; and at 60 ppm are the hindered aryl ethers (16).

Methyl carboxylates represent a major proportion of the O-methylated products of the liptinites from all three coals while little or no methyl carboxylates are detected in the methylated vitrinites or inertinites. The higher concentration of carboxylic acid in liptinites relative to vitrinites have been noted by others using infrared spectroscopy (17-19), but the comparative estimates of the carboxylic acid concentration have not been previously reported for macerals.

The relative intensities of the two resonances centered at 55 ppm and 60 ppm that can be assigned to unhindered methyl ethers and hindered methyl ethers vary between the maceral types. The ratio of hindered methyl ethers to unhindered methyl ethers follow the order: liptinites > vitrinites > inertinites. This is consistent with the notion that this reflects the degree of alkyl substituents on the aromatic structures in these macerals.

ACKNOWLEDGMENTS

We gratefully acknowledge the support of this work by the Office of Basic Energy Sciences, Division of Chemical Sciences, U.S. Department of Energy, under contract number W-31-109-ENG-38. The elemental microanalyses were performed by Steve Newnam of the Analytical Chemistry Laboratory at Argonne National Laboratory. We thank C.A.A. Bloomquist, R.E. Botto, and G.R. Dyrkacz for helpful discussions. This paper is dedicated to the memory of Prof. Peter H. Given.

REFERENCES

1. Liotta, R.; Brons, G. J. Am. Chem. Soc., 1981, 103, 1735-1742.
2. Hagaman, E.W.; Woody, M.C. Fuel, 1982, 61, 53-57.
3. Chambers, R.R., Jr.; Hagaman, E.W.; Woody, M.C.; Smith, K.E.; McKamey, D.R. Fuel, 1985, 64, 1349-1354.
4. Hagaman, E.W.; Chambers, R.R., Jr.; Woody, M.C. Anal. Chem., 1986, 58, 387-394.
5. Botto, R.E.; Choi, C.Y.; Muntean, J.V.; Stock, L.M. Energy Fuels, 1987, 1, 270-360.
6. Hagaman, E.W.; Chambers, R.R., Jr.; Woody, M.C. Energy Fuels, 1987, 1, 352-360.
7. Chambers, R.R., Jr.; Hagaman, E.W.; Woody, M.C. In "Polynuclear Aromatic Compounds"; Ebert, L.B., Ed.; Advances in Chemistry Series 217, American Chemical Society; Washington, D.C. 1988.
8. Liotta, R. Fuel, 1979, 58, 724-728.
9. Dyrkacz, G.R.; Horwitz, E.P. 1982, 61, 3-12.
10. Winans, R.E.; Hayatsu, R.; Scott, R.G.; McBeth, R.L. In "Chemistry and Characterization of Coal Macerals", Winans, R.E.; Crelling, J.C., Eds.; ACS Symposium Series 252, American Chemical Society, Washington, D.C., 1984.
11. Bodily, D.M.; Kopp, V. Prepr. Pap.-Am. Chem. Soc., Div. Fuel Chem. 1987, 32(1), 554-7.
12. Raymond, R., Jr. Proc.-Int. Kohlenwiss. Tag., 1981, 857-862.
13. Dyrkacz, G.R.; Bloomquist, C.A.A.; Ruscic, L. Fuel, 1984, 63, 1367-1373.
14. Tseng, B.H.; Buckentin, M.; Hsieh, K.C.; Wert, C.A.; Dyrkacz, G.R. Fuel, 1986, 65, 385-389.
15. Botto, R.E.; Wilson, R.; Winans, R.E. Energy Fuels, 1987, 1, 173-181.
16. Stock, L.M.; Willis, R.S.; J. Org. Chem., 1985, 50, 3566-3573.
17. Bent, R.; Brown, J.K. Fuel, 1961, 40, 47-56.
18. Allan, J., Ph.D. Dissertation, University of Newcastle upon Tyne, Great Britain, 1975.
19. Dyrkacz, G.R.; Bloomquist, C.A.A.; Solomon, P.R. Fuel, 1984, 63, 536-542.

TABLE I. The Elemental Data of the Macerals Expressed as Molar Ratios.

Maceral Group	H/C	N/C	O/C ^a
<u>West Virginia Upper Kittanning (PSOC-732)</u>			
Whole Coal	0.67	0.015	0.11
Liptinite	0.88	0.012	0.05
Vitrinite	0.71	0.017	0.10
Inertinite	0.56	0.014	0.11
<u>Utah Blind Canyon (APCS-6)</u>			
Whole Coal	0.90	0.016	0.19
Resinite	1.41	0.005	0.05
Sporinite	1.07	0.013	0.13
Vitrinite	0.92	0.016	0.19
<u>West Virginia Lewiston-Stockton (APCS-7)</u>			
Whole Coal	0.75	0.016	0.12
Liptinite	0.97	0.012	0.10
Vitrinite	0.70	0.016	0.13
Inertinite	0.49	0.011	0.12

^aThe oxygen content was determined by difference from the C,H,N microanalyses.

TABLE II. Carbon Aromaticities Estimated by Cross-Polarization NMR.

Maceral Group	f ^a (CP)*
<u>West Virginia Upper Kittanning (PSOC-732)</u>	
Whole Coal	0.78
Liptinite	0.59
Vitrinite	0.79
Inertinite	0.87
<u>Utah Blind Canyon (APCS-6)</u>	
Whole Coal	0.60
Resinite	0.16
Sporinite	0.46
Vitrinite	0.63
<u>West Virginia Lewiston-Stockton (APCS-7)</u>	
Whole Coal	0.74
Liptinite	0.54
Vitrinite	0.76
Inertinite	0.87

*CP Experiments: 2 ms. mix time.

TABLE III. Distribution of Added Methyl Groups as Estimated by Solid ¹³C NMR Spectra.

Maceral Group	Methyl Groups/100°C		
	Total	On Oxygen	On Carbon
<u>West Virginia Upper Kittanning (PSOC-732)</u>			
Whole Coal	4.8	3.8	1.0
Liptinite	6.0	5.0	1.0
Vitrinite	5.2	4.4	0.8
Inertinite	1.6	1.3	0.3
<u>Utah Blind Canyon (APCS-6)</u>			
Whole Coal	1.9	1.8	0.1
Resinite	0.9	0.9	<0.1
Sporinite	2.1	2.0	0.1
Vitrinite	3.1	2.8	0.3
<u>West Virginia Lewiston-Stockton (APCS-7)</u>			
Whole Coal	1.3	1.2	0.1
Liptinite	4.2	3.2	1.0
Vitrinite	3.1	2.8	0.3
Inertinite	2.5	2.0	0.5

TABLE IV. Relative Quantities of Methyl Ethers and Methyl Esters.

Maceral Group	60 ppm	55 ppm	50 ppm
<u>West Virginia Upper Kittanning (PSOC-732)</u>			
Whole Coal	1.1	2.7	0
Liptinite	1.2	2.4	1.4
Vitrinite	1.2	3.2	0
Inertinite	0.2	1.1	0
<u>Utah Blind Canyon (APCS-6)</u>			
Whole Coal	0.7	1.1	0
Resinite	0.3	0.2	0.4
Sporinite	0.9	0.9	0.2
Vitrinite	1.0	1.8	0
<u>West Virginia Lewiston-Stockton (APCS-7)</u>			
Whole Coal	0.4	0.8	0.1
Liptinite	1.5	1.2	0.5
Vitrinite	0.8	1.9	0.1
Inertinite	0.2	1.8	0

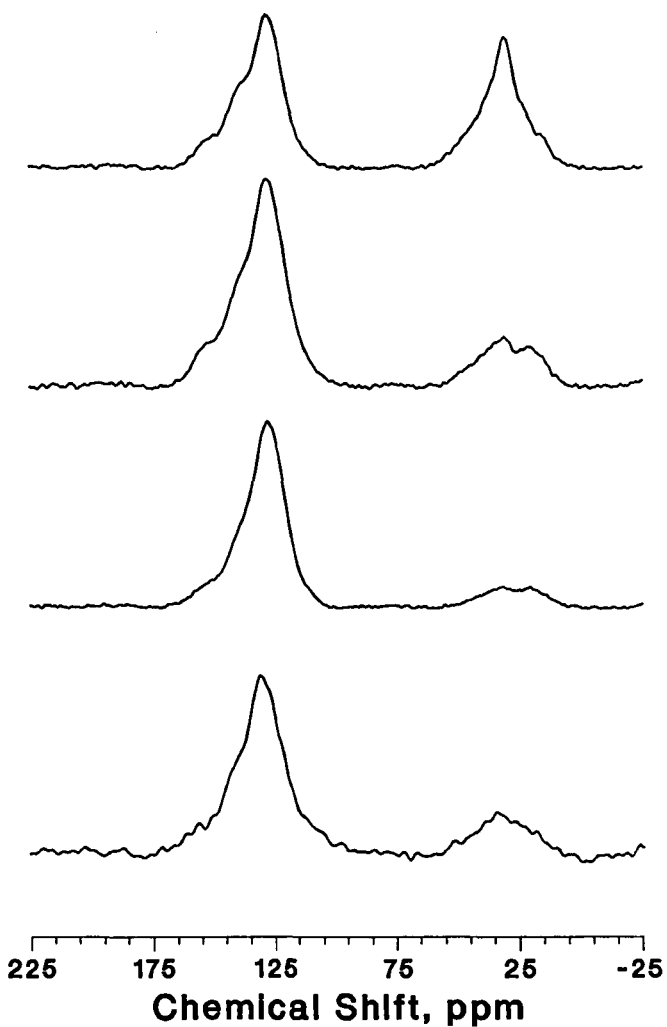


Figure 1. Solid ^{13}C CPMAS spectra of West Virginia Upper Kittanning Coal (PSOC 732). (A) Liptinite; (B) Vitrinite; (C) Inertinite; (D) Whole Coal.

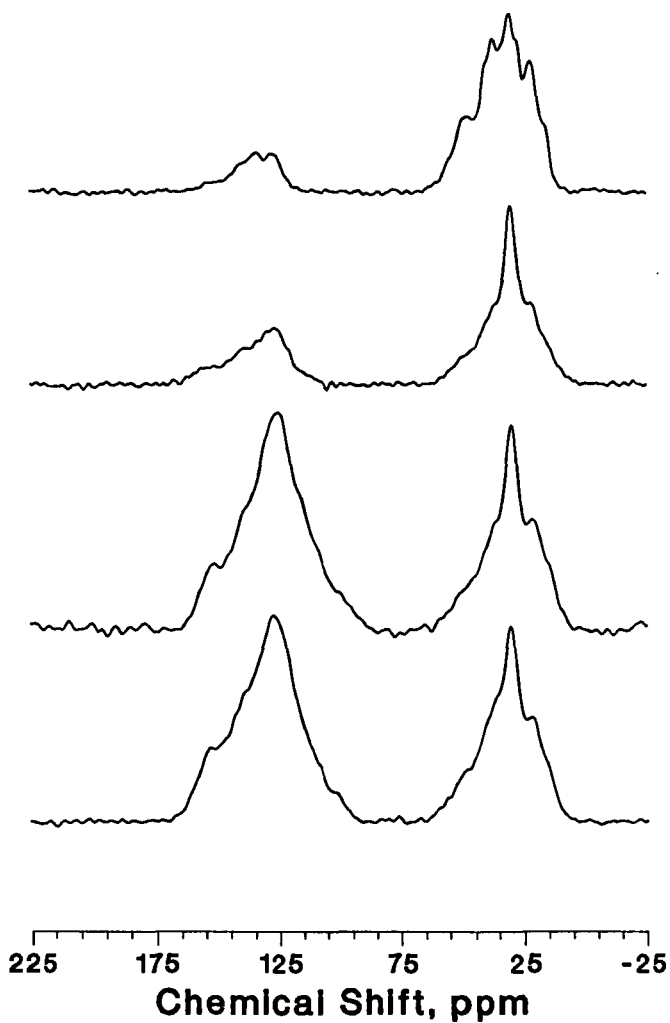


Figure 2. Solid ^{13}C CPMAS spectra of Utah Blind Canyon Coal (APCS #6). (A) Resinite; (B) Sporinite; (C) Vitrinite; (D) Whole Coal.

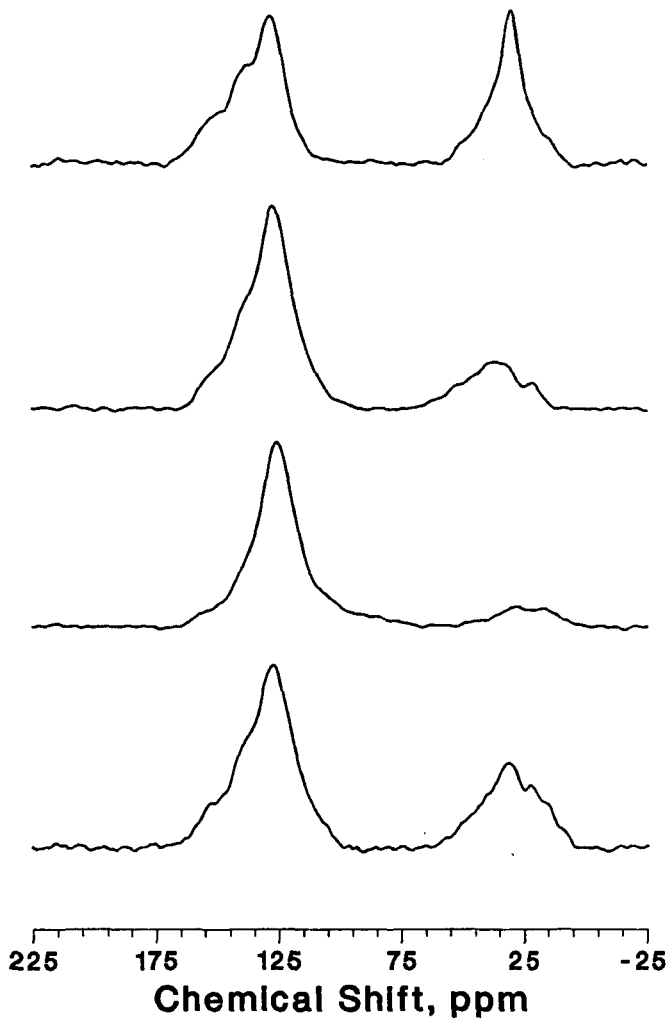


Figure 3. Solid ^{13}C CPMAS spectra of West Virginia Lewiston-Stockton Coal (APCS #7). (A) Liptinite; (B) Vitrinite; (C) Inertinite; (D) Whole Coal.

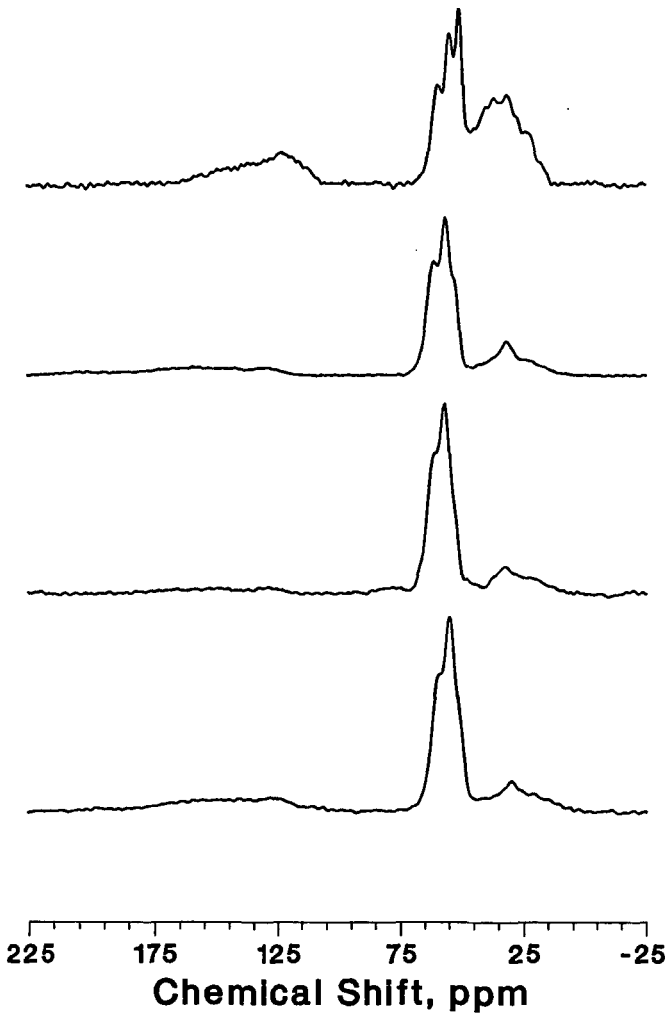


Figure 4. Solid ^{13}C CPMAS spectra of Utah Blind Canyon Coal (APCS #6) methylated with ^{13}C enriched methyl iodide. (A) Resinite; (B) Sporinite; (C) Vitrinite; (D) Whole Coal.

AN INVESTIGATION OF HEATING RATE AND PRESSURE EFFECTS IN COAL PYROLYSIS AND HYDROPYROLYSIS

Jon Gibbins-Matham and Rafael Kandiyoti
Chemical Engineering Department
Imperial College, London SW7 2AZ

INTRODUCTION

The high-pressure wire-mesh apparatus (perhaps best known from work by Anthony^{1,2} and Suuberg^{2,3} at MIT) allows a well-dispersed coal sample to be used, which minimises secondary effects and enables a wide range of heating rates to be applied. Generally, however, the heating rates that have been employed in high-pressure wire-mesh experiments have been limited to about 50 K/s and above by the relatively simple one- or two-stage, fixed-level heating systems that have been used, while the absence of any cooling to prevent reactor components overheating has limited maximum run times to about 30 seconds. In this study it has been possible to extend the investigation of the effects of pressure to heating rates as low as 5 K/s in a wire-mesh apparatus with a computerised feedback temperature control system. Water cooling has also been provided for the parts of the apparatus in contact with the heated sample holder, allowing holding times as long as 200 seconds at 600°C. Preliminary data from the apparatus is presented, showing the effect of heating rate on pyrolysis yields under inert gas pressure and the role of heating rate and holding time at temperature in hydroxyolysis reactions.

SAMPLE PREPARATION

The principal coal used in this study is Pittsburgh No. 8 from the Argonne Premium Coal Sample Program. A single 10 gram sample of -20 mesh coal was used for all experiments. All the sample was ground by hand in air, within about 30 minutes, to pass through a 150 micron sieve and then screened to +100 microns. Some supplementary data is also given for a UK bituminous coal, Linby. This was obtained as washed singles (25 mm sized coal) and was first crushed to approximately 6 mm by hand in air and then ground in a small hammer-mill and sieved to 100-150 microns in a glove-box under nitrogen. The sample used was sealed in a screw-top jar in the glove-box and stored for approximately 18 months in a domestic freezer before use; this had no detectable effect on the pyrolysis yields. Both coal samples were dried overnight under nitrogen at 105°C and stored under flowing nitrogen until required. The analysis of the Linby coal is given in Table I.

EXPERIMENTAL APPARATUS AND METHOD

The high pressure wire-mesh apparatus used in this study is shown in Fig. 1. The wire-mesh sample holder (1) is folded to contain the coal sample between two single layers of 65 micron AISI 304 stainless steel mesh. The sample holder, which also serves as an electrical resistance heater, is held between two electrode/clamps (2 and 3), one of which (3) is sprung to keep the sample holder taut when thermal expansion takes place. Beneath the sample holder is a water-cooled brass plate (4) with a 30 mm diameter hole in it below the working section where the coal sample is spread. A layer of amber mica (5), approximately 0.25 mm thick, electrically insulates the sample holder from the brass plate, while still allowing heat conduction. Another layer of mica (6)

is used to isolate the live electrode (2) which is connected to an insulated terminal (7). Cooling water travels through two hollow support pillars (8) connected to longitudinal holes in the brass plate (4) which communicate in turn with the hollow earthed electrode (3) through two 3.5 mm diameter stainless steel tubes (9), which also act as springs. The base of the pressure vessel (10), the top (11) and the clamping collar (12) are made from 316 stainless steel. The apparatus, with the electrode assembly in position, has been hydraulically tested to 300 bars, giving a 50% safety margin at the maximum pressurising gas cylinder pressure of 200 bars. The gas inlet (13) for helium or hydrogen is a compression fitting sealed with a taper thread in the base. A diffuser (14), consisting of approximately twenty layers of wire-mesh in a brass frame, is provided to break up the jet from the small-bore inlet. Other compression fittings are used for the gas outlet (15) at the top and a pressure tapping (16) in the base.

The regulator on the appropriate gas cylinder is used to set the internal gas pressure in the apparatus. This can be held within about ± 1.5 bars of the desired value, over a range of 20 to 170 bars. The gas flow rate is set by a pressure letdown/flow control valve on the outlet line from the reactor and measured, at atmospheric pressure, by a dry gas meter with an opto-electronic shaft encoder added in-house. By counting the encoder's output pulses on a microcomputer the average flow rate is calculated over ten second intervals.

A sample of 100-150 micron coal is placed in a pre-weighed sample holder which is then stretched between the electrodes. A suction nozzle is used to distribute the coal evenly in an approximately 12 mm diameter circle at the centre of the working section; the suction also serves to remove any particles which can pass through the mesh. The sample holder is then re-weighed to determine the sample size. After the sample holder is replaced in the apparatus two thermocouples are formed, at the edge and centre of the sample respectively, by inserting the thermocouple wires through holes in the mesh. This arrangement avoids distortion of the mesh by welding and, since the short length of mesh between the thermocouple wires is itself part of the thermocouple circuit, unambiguously locates the measuring junction on the surface of the sample holder. Before heating, the system is filled to 100 bars with the working gas and then emptied three times to remove air. The apparatus is then pressurised to the desired value and the flow control valve opened to set the required flow rate of 1 litre/min for every bar of internal pressure. After heating is completed the gas supply is shut off and the internal pressure allowed to come to atmospheric. If hydrogen has been used the apparatus is repressurised to 100 bars with helium and emptied again to avoid the risk of ignition when it is opened. Finally, after the thermocouple wires have been withdrawn, the sample holder is removed and weighed to establish the total volatile yield. Further details of the equipment and experimental methods are given elsewhere for this apparatus⁴ and a very similar wire-mesh reactor for atmospheric pressure and vacuum pyrolysis studies^{5,6}.

When the apparatus was conceived it was hoped to provide a forced sweep of gas through the sample holder, a technique that has been demonstrated successfully in this laboratory for atmospheric pressure operation^{5,6}. This would have given positive removal of the volatiles from the hot zone around the sample holder and allowed tars to be collected in an external trap. Unfortunately, even at 20 bars the cooling effect of gas flowing at only a few cm/s through the sample holder was found to be so intense that uniform temperatures could not be maintained and, because very high power inputs therefore had to be applied, even slight deviations in the local cooling effect could cause severe

overheating and melting of the sample holder material. After extensive trials with various gas flow arrangements the best that could be achieved was to provide a diffuse flow of gas upwards from the base of the vessel at a volumetric flow rate (at the internal pressure) of 1 litre/min. This provides some entrainment of the products and also relieves expansion on heating.

In order to observe the flow patterns and to see whether yields differed from other atmospheric pressure results with a forced sweep gas flow, Linby coal was pyrolysed in helium at atmospheric pressure with the diffuse flow. The high-pressure apparatus was used, but with the steel top replaced by a glass top of similar dimensions. As Fig. 2 shows, the absence of the forced sweep caused only a small reduction in total volatile yields and, since tars could be seen to be recirculated back onto the sample holder by natural convection currents, this reduction was probably due more to secondary re-deposition of the volatiles rather than to a significant increase in the surface mass transfer resistance. Some discolouration of the working section of the sample holder was also observed, which tends to confirm this, but when high pressure hydrogen is used no visible deposit is formed on the sample holder. Any tars which touch the surface apparently crack to form lighter volatiles rather than char. As discussed later, however, a direct test of the effect of sweep velocity at pressure would be desirable.

Even with the diffuse flow regime, heat losses by convection from the sample holder are very large: at 70 bars the power input must be increased approximately five-fold compared to atmospheric pressure operation to hold the temperature steady at the same value and the ratio between convective and other heat losses, which is roughly 1:1 at atmospheric pressure, then rises to about 9:1. With convection so dominant, only slight variations in the gas flow are needed to cause significant (up to about ± 50 K) fluctuations in the local temperature of the sample holder. Although the computer feedback control system can usually hold the average of the readings from the two thermocouples within 20 K or less of the desired value, the instantaneous difference between the individual readings is determined solely by the unsteady physical conditions inside the reactor. Similar fluctuations in temperature at high pressures (measured with a single thermocouple) are reported by Anthony¹, despite the use of an insulated baffle below his sample holder to reduce circulation currents. The temperature fluctuations have a time-scale of the order of 0.2 seconds, so to give reasonably representative time-averages for the peak temperature (rather than a possibly misleading instantaneous value) a significantly longer holding period at peak temperature is generally used. The fluctuations do, however, limit the precision with which the effective transition between a slow-heating stage and a rapid-heating stage can be located, since the control system must be set to start rapid heating when the instantaneous control temperature (i.e., the average of the two thermocouple readings) reaches a specified value.

RESULTS AND DISCUSSION

In order to give the effect of hydrogen pressure on primary coal pyrolysis reactions the greatest possible weighting compared to char hydrogasification reactions a peak temperature of 600°C is used in most of the results presented here. Atmospheric-pressure data obtained in this laboratory for Pittsburgh No. 8^{3,6} and Linby⁴ coals suggest that, for holding times in excess of about 5 seconds, this temperature is high enough for the bulk of the thermally-induced primary breakdown reactions to run to completion. A longer hold time,

10 seconds, was chosen to allow for a possible increase in resistance to volatile transport at elevated pressure, and as Fig. 3 for Linby coal shows, even at 100 bars this appears to give an adequate margin for thermally initiated breakdown reactions. As data presented below (Fig. 7) shows, the hydrogasification reactions carry on for a much longer period. With the standard conditions selected, the effect of heating rate on pyrolysis yields for Pittsburgh No. 8 in hydrogen and helium at 70 bars (1000 psig) was investigated. The results (presented in Fig. 4) showed that at 70 bars the yields in helium appear to be unchanged or to decrease slightly, while yields in hydrogen show a very pronounced fall, from about 52% of the daf sample at 5 K/s to around 47% at 1000 K/s.

Although more data over a range of temperatures and pressures, as well as at lower heating rates, is required to allow firm conclusions to be drawn, the level or slight downward trend with increased heating rate in helium at 70 bars is of interest because previous studies in this laboratory^{5,6} have shown an opposite effect of heating rate in helium at atmospheric pressure, with tar being the main product affected. It was suspected at the time (partly because vacuum pyrolysis showed an even greater sensitivity to heating rate) that tar transport was being enhanced due to the greater sample plasticity and more rapid outward flow of volatiles at high heating rates. While observations suggest that plasticity, if anything, increases with pressure, the volume of the volatile products and hence the rapidity of their outward flow must be reduced by the applied pressure, which may account for the observed equality between fast and slow heating at 70 bars in inert gas.

In addition, the helium results can be regarded as a base-line for the hydrolysis data, showing the purely physical effect of the applied gas pressure. The yield at 5 K/s must then reflect a greater degree of chemical interaction between the hydrogen and the coal, but it cannot be deduced from Fig. 4 whether this is due to hydrogen promoting yields during the initial, rapid volatile release stage of pyrolysis or simply more char gasification occurring in the longer time available (ie. during heating, since hold times are identical) at the slower heating rate.

To investigate the temperature range over which hydrogen was enhancing yields at 5 K/s, two-stage heating was used. The sample holder was heated at 5 K/s to the required intermediate temperature and then immediately heated at 1000 K/s to 600°C and held there for 10 seconds. The results, shown in Fig. 5, suggest that varying the heating rate between 5 K/s and 1000 K/s will have no effect below about 500°C. As discussed earlier, precise resolution of the intermediate temperature is difficult, but it appears likely that there is a gradual transition to the higher yield above 500°C. If the effect had been observed at lower temperatures, before significant amounts of volatiles were evolved, it might have been possible to rule out hydrogasification reactions, but Fig. 6 shows that appreciable amounts of devolatilisation will have taken place by 500°C even at 1000 K/s and differentiation between enhanced primary pyrolysis and hydrogasification is therefore not feasible.

To attempt to distinguish between a possible beneficial effect of a lower heating rate in the later stages of the initial, rapid pyrolysis reactions and more extensive char gasification in the extra 20 seconds available between 500°C and 600°C, the total volatile yields as a function of holding time after 5 K/s and 1000 K/s heating were measured. If it was simply that extra time for hydrogasification is available at 5 K/s then presumably this difference would become less significant at longer holding times and the two sets of data would

converge to the same asymptotic value. In fact, as Fig. 7 shows, while the differences do become less significant at longer hold times, even when yields superficially seem to have reached an asymptotic value at 200 seconds there is still an offset of about 2% of the daf sample.

It is tempting to ascribe the additional 2% of material that apparently can be volatilised by reducing the heating rate from 1000 K/s to 5 K/s to increased interaction between hydrogen and the pyrolysing mass; stabilisation of the heavy tar precursors remaining as the melt start to coke could be a feasible mechanism. The magnitude of the difference is, however, well within the likely experimental scatter and a more detailed study would be needed to allow such a definite conclusion. It would also be possible to explain the apparent trends if slower heating produced a more reactive char, unless the extra products could be analysed and shown not to be able to come from char gasification reactions; more detailed product distribution data, including tar/liquid yields, would be needed for this.

Finally, in all the experiments some coked residue from fluid material that had been evolved from the coal particles could be seen. This was much more noticeable for runs in helium, when globules of charred liquid residue covered large areas of the outer faces of the mesh adjacent to the sample. Hydrogen appears to be giving a higher volatile yield as a result of chemical removal of some of this material, probably before charring takes place. While a sweep flow has been shown to be relatively unimportant at atmospheric pressure and flow rates up to 0.3 m/s, the visible availability of un-removed liquid material suggests that a gas sweep, perhaps at a higher flow, might be able to increase volatile yields by promoting evaporation and possibly entrainment.

ACKNOWLEDGEMENTS

The authors are grateful to many colleagues in the Chemical Engineering Department for assistance with this project, particularly to Dr. G. Saville, Mr. R. King and Mr. T. Meredith for their contributions to the mechanical design and construction of the apparatus and to Mr. R. Wood for the electrical components. The sample of Linby coal was supplied by British Coal, Coal Research Establishment. Financial support was provided by the UK Science and Engineering Research Council under grants GR/B/58962 and GR/D/06582.

REFERENCES

1. Anthony, D. B., Sc.D thesis, MIT, 1974.
2. Howard, J. B., Ch.12 in Chemistry of Coal Utilization, 2nd Supp., (Ed. Elliott, M. A.), Wiley, NY, 1981.
3. Suuberg, E. M., Sc.D thesis, MIT, 1977.
4. Gibbins-Matham, J. R., Ph.D thesis, Imperial College, 1988 (in preparation).
5. Gibbins-Matham, J. R. & Kandiyoti, R., ACS DFC Prepr. 32(4), 1987, 318-323.
6. Gibbins-Matham, J. R. & Kandiyoti, R., Energy & Fuels (accepted for publication).

TABLE I Linby Coal: Proximate and Ultimate Analyses

----- % dry basis -----							
VM	FC	Ash	C	H	O	N	S
36	60	4.0	77.8	5.1	10.1	1.6	1.4

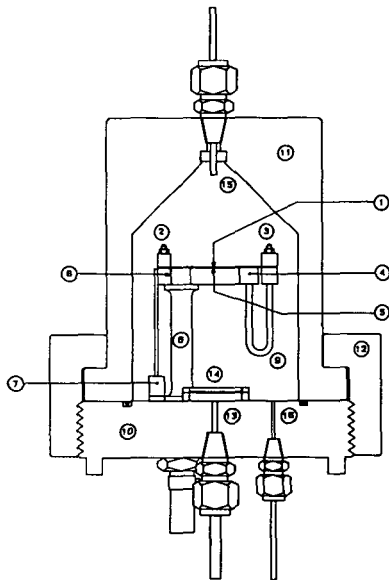


Fig. 1 High pressure wire-mesh apparatus.

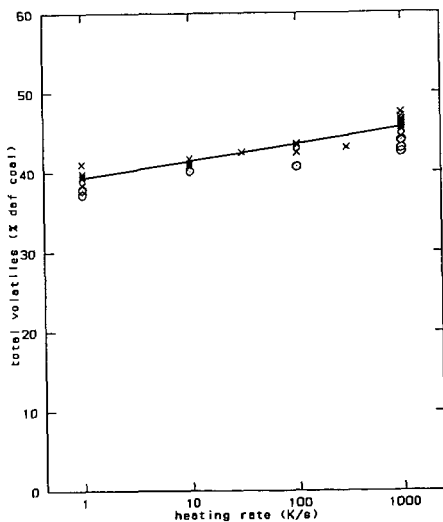


Fig. 2 Effect of 'diffuse flow' regime on total volatile yields from Linby coal heated to 700 deg.C with 30 seconds hold, in helium at 1.2 bars.
x, D.1-0.3 m/s sweep.
o, diffuse flow.

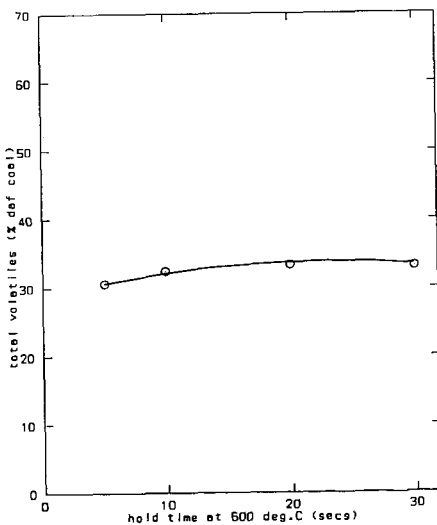


Fig. 3 Effect of hold time at 600 deg.C on volatile yields from Linby coal heated at 625 K/s in helium at 100 bars, diffuse flow.

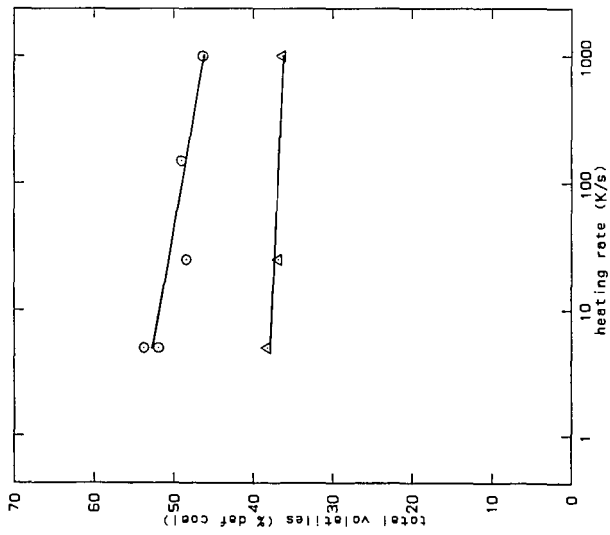


Fig. 4 Effect of heating rate on total volatile yields from Pittsburgh #8 at 70 bars with diffuse flow.
 O, 600 deg.C, 10 s hold, hydrogen.
 Δ, 600 deg.C, 10 s hold, helium.

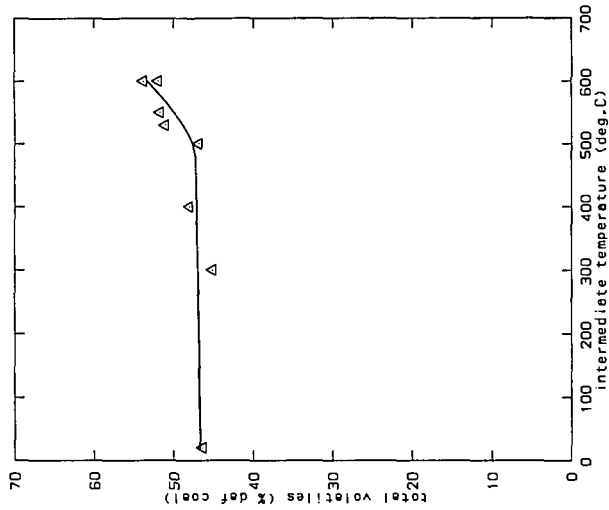


Fig. 5 Effect of intermediate temperature between 5 K/s and 1000 K/s heating on total volatile yields from Pittsburgh #8 in hydrogen at 70 bars.
 Final temperature 600 deg.C, hold time 10 s.

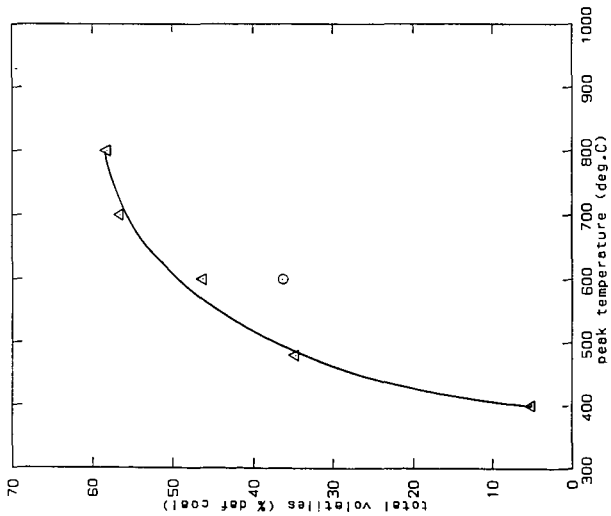


Fig. 5 Effect of peak temperature on total volatile yields from Pittsburgh #8 at 70 bars.
 Δ , 1000 K/s, 10 s hold, hydrogen, diffuse flow.
 \circ , 1000 K/s, 10 s hold, helium, diffuse flow.

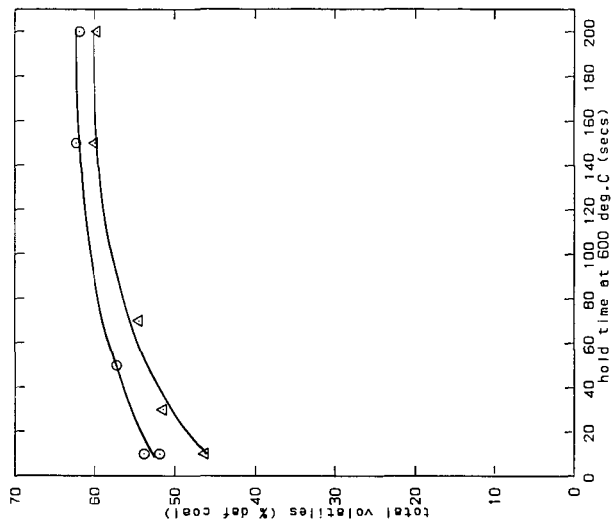


Fig. 7 Effect of hold time at 600 deg.C on total volatile yields from Pittsburgh #8 in hydrogen at 70 bars with diffuse flow.
 Δ , 1000 K/s heating; \circ , 5 K/s heating.

SIMULTANEOUS THERMOGRAVIMETRIC AND MASS SPECTROMETRIC OBSERVATIONS ON VACUUM PYROLYSIS OF ARGONNE PCSP COALS

Yongseung Yun and Henk L.C. Meuzelaar
Center for Micro Analysis & Reaction Chemistry, University of Utah
Salt Lake City, Utah 84112

ABSTRACT

The most serious limitations of many coal gasification and liquefaction models are due to the lack of reliable char and total volatiles yield data, of accurate kinetic parameters, and of reliable data on the composition of the total volatiles in the initial devolatilization step. Consequently, a vacuum thermogravimetry/mass spectrometry (TG/MS) system consisting of a Mettler TA1 Thermoanalyzer and a Finnigan MAT 3200 quadrupole mass filter was built to obtain accurate quantitative and qualitative data on coal devolatilization processes at heating rates in the 10^{-2} - 10^0 K/s range. Hundreds of mass spectra can be obtained during a single TG run, thereby providing detailed information about the concentration of various devolatilization products as a function of temperature while continuously recording the sample weight loss. Moreover, factor analysis-based methods enable deconvolution of overlapping trends and numerical extraction of chemical component spectra. TG/MS results on four Argonne PCSP coals are discussed.

INTRODUCTION

Previous mass spectrometric studies of coal devolatilization phenomena in our laboratory [1, 2, 3] have focussed on the use of Curie-point pyrolysis mass spectrometry (Py-MS) techniques using heating rates in the 10^2 - 10^4 K/s range. This enabled Chakravarty *et al.* [1] to identify at least four structural components with distinct kinetic profiles in an ANL-PCSP Pittsburgh #8 coal: (1) a relatively minor vacuum distillate fraction consisting primarily of alkylsubstituted one- and two-ring aromatic hydrocarbons; (2) a sporinite-like fraction consisting of branched and/or alicyclic hydrocarbon components; (3) a cutinite- or alginite-like polymethylenic component; and (4) a vitrinite-like component consisting primarily of alkylsubstituted hydroxyaromatic and aromatic moieties. Attention was drawn to the fact that only the two aliphatic components appeared to exhibit a simple depolymerization behavior consistent with the idea of a first-order unimolecular decomposition reaction. The vacuum distillate component was thought to be more appropriately described by a reaction order between 0 and 1, whereas the vitrinite-like component appeared to behave like a char-forming thermoset, and thus, should be described by a reaction order considerably greater than 1. Attempts to obtain more accurate kinetic parameters, however, were only partially successful due to the very short reaction times involved (approx. 8 s) and the significant broadening of the product evolution profiles by diffusion processes between the pyrolysis zone and the ionization region.

In order to overcome this problem we decided to build a vacuum thermogravimetry/mass spectrometry (TG/MS) system capable of precisely controlling heating rates in the 10^{-2} - 10^0 K/s range while providing accurate temperature and weight loss information and simultaneously recording the evolution profiles of gas and tar products.

Vacuum TG/MS experiments with coals have been reported previously by Ohrback *et al.* [4, 5]. However, in the experiments reported here we were especially interested in using the set of eight standard coals available from the Argonne National Laboratory Premium Coal Sample Program (ANL-PCSP) in order to enable direct comparison with TG/FTIR experiments performed by Serio *et al.* [6], as well as to enable reproduction of our experiments by other researchers. Moreover, since most of our extensive Py-MS data on U.S. coals [7, 8, 9] has been obtained under low voltage (approx. 12-14 eV) electron ionization conditions, we wanted to perform the TG/MS analyses under comparable ionization conditions.

Finally, an important goal of the experiments reported here was to use sophisticated multivariate analysis techniques, as developed by Windig *et al.* [10], in order to deconvolute overlapping trends in the TG/MS data and to identify the underlying chemical components.

At the time of writing, only 4 of the 8 ANL-PCSP coals have been analyzed and a full report of the results on all 8 coals will be published elsewhere.

EXPERIMENTAL

Four ANL ampule samples (Pittsburgh #8 (-100 mesh), Illinois #6 (-100 mesh), Wyodak (-20 mesh), Beulah-Zap (-100 mesh)) were employed in vacuum TG/MS runs and the ultimate analysis data of the samples were described elsewhere [11]. The TG/MS system (Figure 1) consists of a Mettler TA1 Thermoanalyzer directly interfaced to a small Finnigan MAT 3200 quadupole mass filter. Pyrolysis was performed directly in front of the ion source of the mass spectrometer in order to prevent recombination reactions and/or secondary decomposition of reactive compounds as well as to minimize the loss of polar compounds through condensation. A turbomolecular pump (Balzers TPU 050) was used for evacuating the MS chamber up to 4×10^{-7} torr in 7-8 minutes. In addition, two diffusion pumps were employed to maintain a pressure of less than 1×10^{-4} torr in the TG balance chamber. Moreover, the LN₂ cold trap in Figure 1 was used to guarantee a low background signal level in the mass spectra. A detailed description of time-resolved Curie-point pyrolysis MS (TR Py-MS) can be found elsewhere [2].

Sample aliquots of approximately 4-5 mg were heated under vacuum ($3-6 \times 10^{-7}$ torr) while the temperature was increased from ambient to 700°C at 25°C/min. MS conditions were as follows: electron impact energy 14 eV, mass range scanned m/z 33 to 193 (m/z 48-193 for Pittsburgh #8 seam coal), total number of scans 80, and total scan time 27 minutes. Each spectrum scanned was stored separately in the memory of an IBM 9000 computer.

Factor analysis was employed to deconvolute overlapping time trends and to numerically extract the chemical component spectra. In order to give all the variables an equal contribution, factor analysis was done on the correlation around the origin matrix. Deconvolution was performed by using a combination of pure mass [12, 13] and variance diagram (VARDIA) [10, 14] techniques.

RESULTS AND DISCUSSION

The time-integrated low voltage mass spectra of Pittsburgh coal obtained by TG/MS and by TR Py-MS are highly similar with regard to type and relative abundance of the pyrolysis products (as shown in Figure 2) in spite of a

factor 3×10^2 difference in heating rate and a factor 2×10^2 difference in sample size, as well as differences in pyrolysis technique, ion source, quadrupole, etc. In fact, since Curie-point Py-MS patterns obtained at heating rates of 6×10^4 K/s and 1×10^2 K/s are highly similar too (not shown here), we can conclude that the mechanisms of primary coal devolatilization reactions appear to be independent of heating rate over at least five orders of magnitude (10^{-1} - 10^4 K/s range).

The main differences between the TG/MS and TR Py-MS data on Pittsburgh #8 coal in Figure 1 appear to be the much larger SO_2^+ and HSSH^+ signals (due to the higher end temperature of the TG/MS system; similar SO_2 increases can be seen when using higher temperature Curie-point wires), and the somewhat increased dihydroxybenzene. The dihydroxybenzene intensities in the TR Py-MS spectrum can be increased by preheating the pyrolysis chamber. Hydroaromatics (e.g. tetralins) tend to form relatively late during the devolatilization process, therefore the higher end temperatures explain their increased abundance in the TG/MS spectrum.

The sharp evolution profile and the constant evolution temperature of SO_2 , as illustrated in Figure 3, offer exciting possibilities for controlling the final distribution of sulfur between the char and the gas phase (e.g., in low temperature gasification and/or liquefaction processes). However, we do not see the very early SO_2 components shown by Serio *et al.* [6] in TG/FTIR. Possibly, the FTIR signal shows interference from a different compound.

Four factors were employed to deconvolute overlapping trends in total ion count profiles from TG/MS. The eigenvalues and variances explained by the first six factors are illustrated in Table 1, showing that the first four factors can explain approx. 98% of total variance for each coal. Our deconvoluted data provide a strong indication for the presence of two kinetically distinct pyrolysis regimes (under our TG conditions at approx. 370-380°C and at 420-440°C, respectively). Whereas each of these regimes may indeed be relatively independent of rank as suggested by Serio *et al.* [6], the "vitrinitic component" (m/z 124/138) appears to shift from the lower to the higher temperature regime with increasing rank. The aliphatic hydrocarbon component always pyrolyzes in the higher regime. The following hypothesis for these observations would be possible: the two temperature regimes represent ether bridges (or other weak bonds) and methylenic bridges, respectively. In liptinites such as alginites or cutinites methylenic bridges are present from the beginning (and thus already in low rank coals). In vitrinitic macerals derived from lignin-like structures the initial bridges are primarily ether type. With increasing rank these are "replaced" by methylenic bridges (or perhaps lost through CO elimination with consequent formation of new methylenic cross-links).

The rank dependent shift in the ratio of aromatic vs. terpenoid (isoprenoid) structure reported by Blazso *et al.* [15] was also confirmed by our findings (disappearance of m/z 191 component, appearance of m/z 156 component).

The rank dependent appearance of the "oil formation" window in high volatile A and B bituminous coal [1] is evident in Pittsburgh #8 coal. Perhaps this could be called "geothermal pyrolysis". However, the relatively aromatic oil formed does not appear to contain many polymethylenic moieties (contrary to the suggestion by Serio *et al.* [6]). Also the term "guest molecules" is an obvious misnomer. These are not "guests" but "offspring" (sons or

daughters). The TG/DTG curves (only shown DTG curve in this preprint) show only very small quantities of these vacuum distillable components. This can be explained as follows: assume that the total amount is only a few percent of dry coal weight and that the total tar yield is approx. 20%, then (e.g., 30% gas, 40% char, 10% ash) the vacuum distillable "bitumen" could still be as much as approx. 10% of the tar.

Although SO₂ evolution appears to coincide with the end of the main tar formation phase (and/or onset of the char formation process) neither the origin nor the mechanistic significance of the SO₂ evolution are entirely clear at present.

It should be pointed out here that the charring stage is strongly underrepresented in our study due to the limited lower mass range ($\geq m/z$ 34) and the low voltage EI conditions (low MW pyrolysis products tend to have higher ionization potentials). Further TG/MS runs are planned to investigate low MW pyrolysis products.

ACKNOWLEDGEMENTS

This work was sponsored by the Advanced Combustion Engineering Research Center. Funds for this Center are received from the National Science Foundation, the State of Utah, 23 participants and the U.S. Department of Energy.

REFERENCES

1. Chakravarty, T., H.L.C. Meuzelaar, W. Windig and G.R. Hill, ACS Preprints (Div. of Fuel Chem.), 32(3) 1988, 211-216.
2. Jakab, E., W. Windig, and H.L.C. Meuzelaar, Energy and Fuels, 1(2), 1987, 161-167.
3. Jakab, R., B. Hoesterey, W. Windig, G.R. Hill and H.L.C. Meuzelaar, Fuel, 67, 1988, 73-79.
4. Ohrback, K.H. and A. Kettrup, ACS Preprints (Div. of Fuel Chem.), 29(2), 1984, 12-19.
5. Ohrback, K.H., A. Kettrup and G. Radhoff, J. of Analytical and Applied Pyrolysis, 8, 1985, 195-199.
6. Serio, M.A., P.R. Solomon and R.M. Carangelo, ACS Preprints (Div. of Fuel Chem.), 33(2), 1988, 295-309.
7. Meuzelaar, H.L.C., A.M. Harper, G.R. Hill and P.H. Given, Fuel, 63, 1984, 640-652.
8. Harper, A.M., H.L.C. Meuzelaar and P.H. Given, Fuel, 63, 1984, 793-802.
9. Metcalf, G.S., W. Windig, G.R. Hill and H.L.C. Meuzelaar, Int. J. of Coal Geology, 7, 1987, 245-268.
10. Windig, W. and H.L.C. Meuzelaar, Anal. Chem., 56, 1984, 2297-2303.
11. Vorres, K.S., ACS Preprints (Div. of Fuel Chem.), 32(4), 1987, 221-226.
12. Knorr, F.J. and J.H. Futrell, Anal. Chem., 51, 1979, 1236-1241.
13. Malinowski, E.R. and D.G. Howery, Factor Analysis in Chemistry, John Wiley & Sons, 1980, New York.
14. Windig, W., E. Jakab, J.M. Richards, and H.L.C. Meuzelaar, Anal. Chem., 59, 1987, 317-323.
15. Balzso, M., T. Szekely, F. Till, G. Varhegyi, E. Jakab and P. Szabo, J. of Analytical & Applied Pyrolysis, 8, 1985, 255-269.

TABLE 1
 VARIANCE EXPLAINED BY THE FIRST SIX FACTORS OBTAINED BY PRINCIPAL COMPONENT
 ANALYSIS OF THE CORRELATION AROUND-THE-ORIGIN MATRIX FOR EACH TG/MS DATA SET

Factor Number	Pittsburgh #8		Illinois #6		Wyodak		Beulah-Zap	
	Eigen-value	% variance	Eigen-value	% variance	Eigen-value	% variance	Eigen-value	% variance
1	119.99	87.27	138.07	88.29	135.92	87.39	129.53	84.32
2	7.02	5.11	8.33	5.33	8.92	5.74	12.46	8.11
3	5.07	3.68	4.43	2.83	5.29	3.40	6.66	4.33
4	2.43	1.77	3.47	2.22	2.99	1.90	2.83	1.85
5	1.74	1.27	1.38	0.88	1.48	0.95	1.31	0.85
6	1.23	0.90	0.71	0.46	0.92	0.59	0.83	0.54

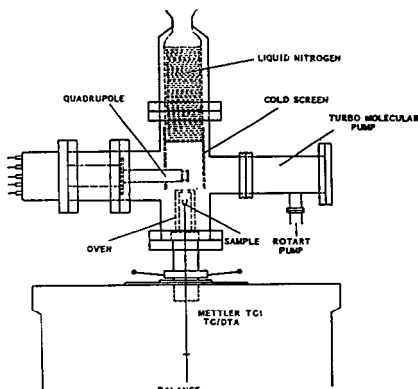


Figure 1. Schematic diagram of vacuum TG/MS system, based on the combination of a Mettler TA1 TG/DTA system and a Finnigan MAT 3200 mass spectrometer with specifically designed vacuum housing.

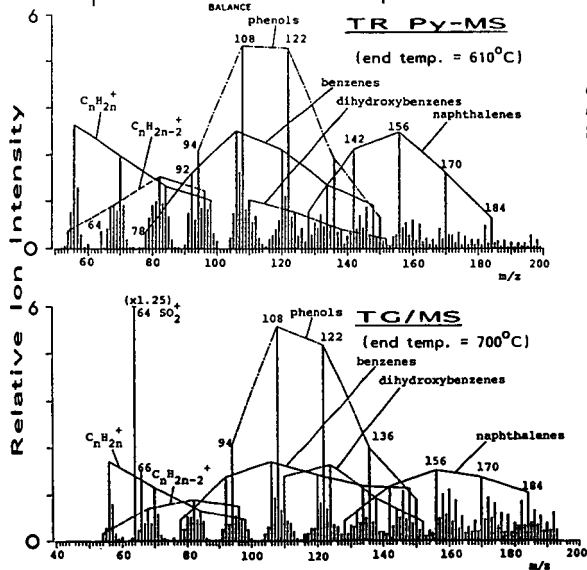


Figure 2. Time-integrated spectrum obtained by summing all 41 (TR Py-MS), 80 (TG/MS) spectra scanned on Pittsburgh #8.

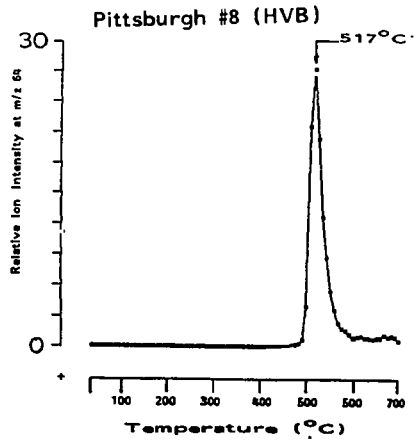
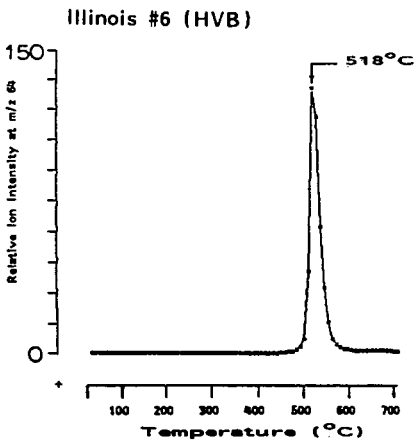
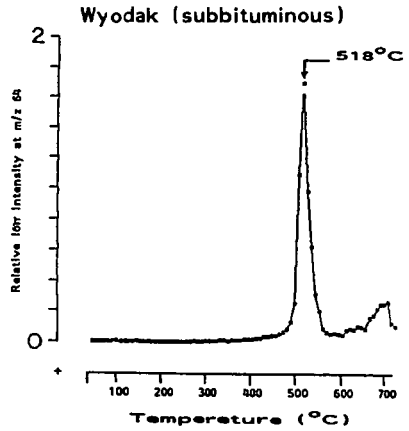
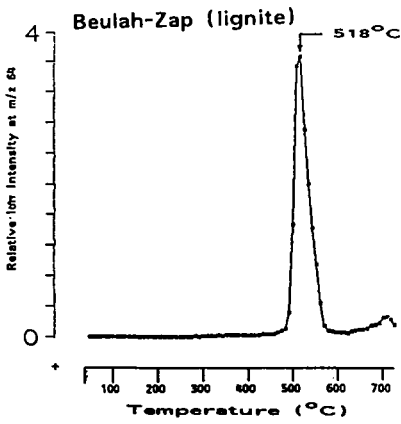


Figure 3. Evolution profiles of m/z 64 (SO_2^+) for four ANL-PCSP coals. Note the similar evolution profile and maximum evolution temperature independent of rank.

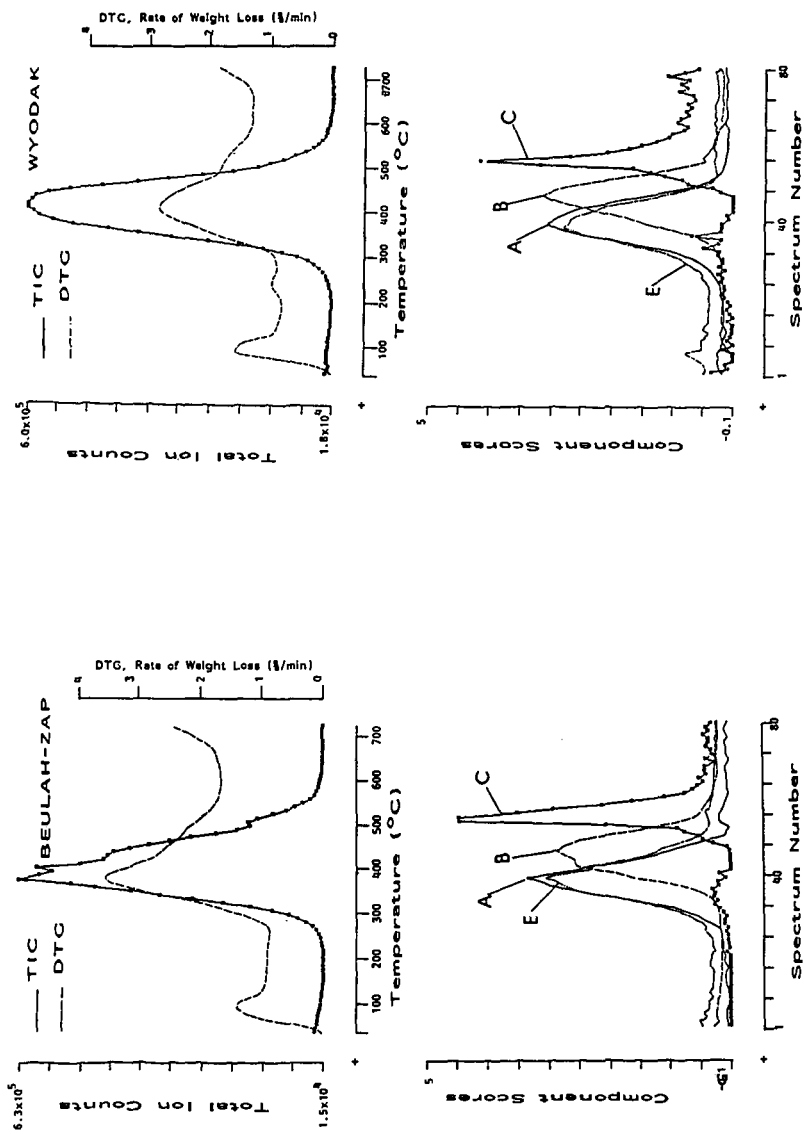


Figure 4. TIC, DTG profiles with temperature and the corresponding deconvoluted components (A,B,C,E) for Wyodak, Beulah-Zap coals. The numerically extracted ("deconvoluted") spectra of each component are shown in Figure 6. Mainly component A consists of dihydroxybenzenes, component B aliphatics + phenols, component C SO₂, component E terpenoid fragments.

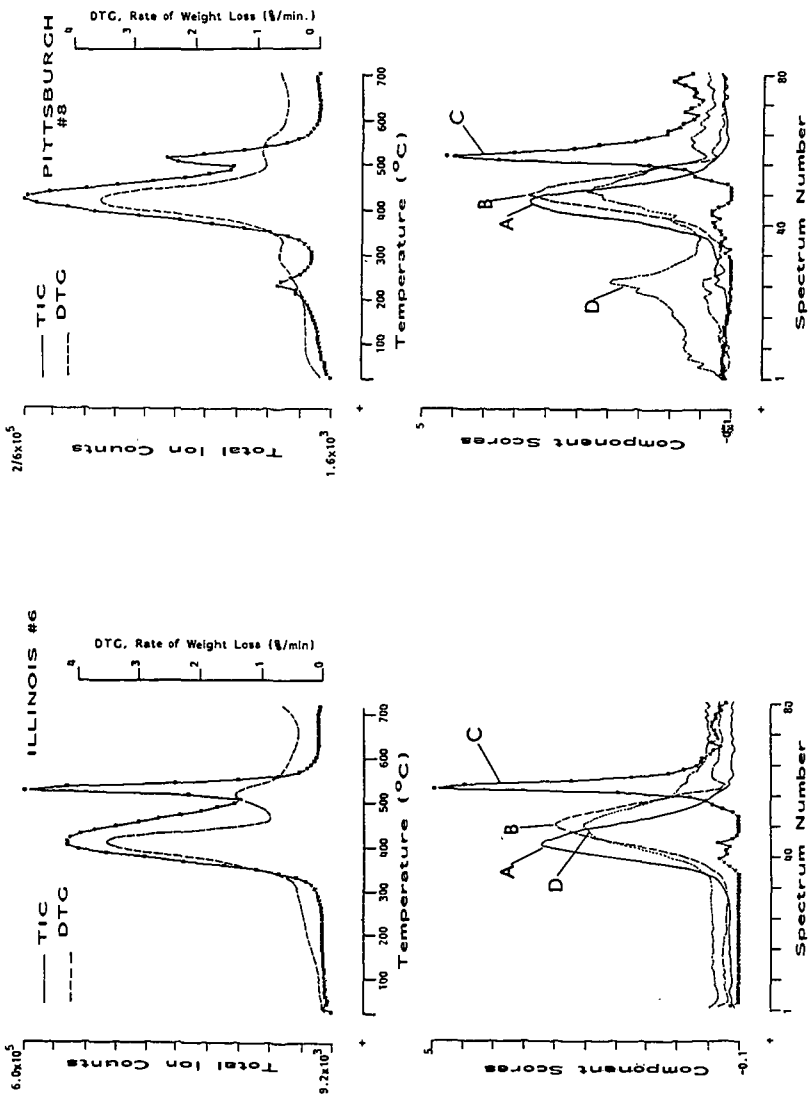


Figure 5. TIC, DTC profiles with temperature and the corresponding deconvoluted components (A, B, C, D) for Illinois #6, Pittsburgh #8 coals. The numerically extracted ("deconvoluted") spectra of each component are shown in Figure 7. Mainly component A consists of dihydroxybenzenes, component B aliphatics + phenols, component C SO_2 , component D bitumen (benzenes + naphthalenes).

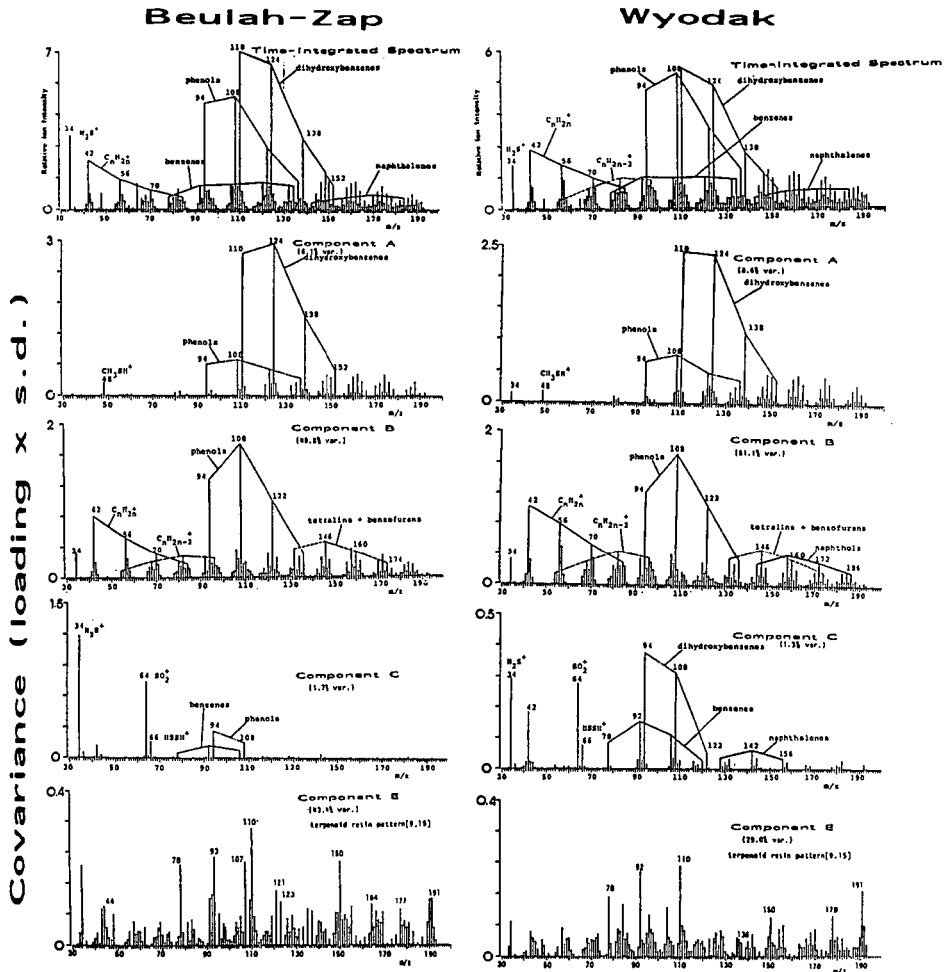


Figure 6. Time-integrated spectra obtained by summing all 80 spectra scanned during TG/MS runs and numerically extracted ("deconvoluted") spectra of the four components shown in Figure 4 for Beulah-Zap and Wyodak coals.

Illinois #6

Pittsburgh #8

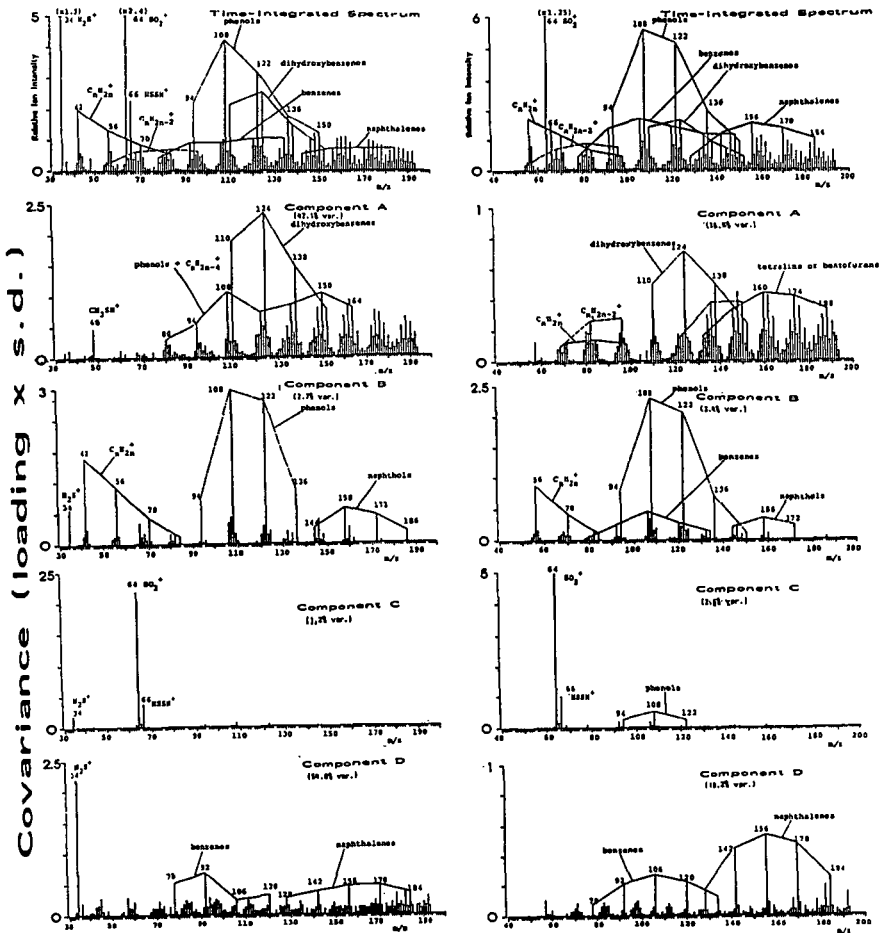


Figure 7. Time-integrated spectra obtained by summing all 80 spectra scanned during TG/MS runs and numerically extracted ("deconvoluted") spectra of the four components shown in Figure 5 for Illinois #6 and Pittsburgh #8 coals.

CHARACTERIZATION OF THE ARGONNE PREMIUM COAL SAMPLES BY PYROLYSIS HIGH RESOLUTION MASS SPECTROMETRY

Randall E. Winans, Robert L. McBeth and Paul H. Neill
Chemistry Division, Argonne National Laboratory, Argonne, IL 60439

INTRODUCTION

The complete set of Argonne Premium Coal Samples have been characterized using Pyrolysis High Resolution Mass Spectrometry (PyHRMS). A major objective in the study is to examine differences in the heteroatom (oxygen, sulfur and nitrogen) containing molecules as a function of rank of the coals. Operating in the high resolution mode makes it possible to directly separate these species from each other and from the hydrocarbon molecules. In addition, many molecules, which can not be observed with gas chromatography by virtue of their size or polarity, can be observed with this method.

We have applied PyHRMS to characterization of separated coal macerals and coal degradation products.¹⁻³ There are many papers on low resolution PyMS applied to coals^{4,5} and one applied to these premium coals.⁶ The PyMS approach can provide very detailed information on the molecules which are released in vacuum pyrolysis, however the probability of secondary reactions is a consideration and all interpretation must be made with this fact in mind. This approach yields more specific molecular data than any other method. A problem with low resolution PyMS is that in many if not most cases there may be several ions present with the same nominal mass but with different chemical compositions. This problem is eliminated by using an high resolution spectrometer which may scan more slowly, but will resolve peaks which overlapped at lower resolution and yield more information.

EXPERIMENTAL

The samples have been obtained from the Argonne Premium Coal Sample Program and the preparation of the samples has been described.⁷ The appropriate elemental analysis for the samples is presented in Table 1. A second set of samples was obtained by extracting the original coals in refluxing pyridine under a nitrogen atmosphere. The residue was washed with dilute aqueous HCl and with methanol and dried *in vacuo* at 60°C.

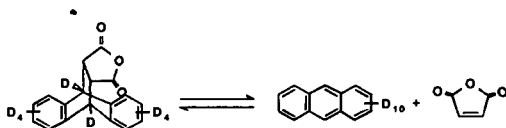
TABLE 1. Elemental Analysis for the Fresh Coal Samples.

Sample	Name	%C(maf)	Per 100 Carbons				Ash
			H	N	S	O	
1	Upper Freeport mvB	85.5	66.0	1.55	0.32	6.59	13.20
2	Wyodak-Anderson SubB	75.0	85.6	1.28	0.23	18.00	8.77
3	Herrin hvCB	77.7	77.2	1.51	1.15	13.03	15.50
4	Pittsburgh hvAB	83.2	76.7	1.69	0.40	7.96	9.25
5	Pocahontas lvB	91.0	58.5	1.25	0.21	2.04	4.23
6	Blind Canyon hvBB	80.7	85.7	1.67	0.17	10.78	4.71
7	Stockton-Lewiston hvAB	82.6	76.3	1.62	0.30	8.93	19.80
8	Beulah-Zap Lignite	72.9	79.5	1.35	0.36	20.88	9.72

Both sets of samples, fresh coal and extract residue, were pyrolysed under the same conditions, in an all glass heated inlet system (AGHS), rapidly to 600°C. The inlet system was designed in this laboratory to use a quartz pyrolysis probe fitted with a platinum grid which was heated by a computer controlled DC power supply. The inlet system was thermostated at 300°C and a silicon-carbide leak metered the sample into the mass spectrometer. An internal standard has been used which was the Diels-Alder adduct of D¹⁰-anthracene and maleic anhydride prepared from the two reactants in refluxing p-xylene. The spectrometer, a Kratos MS-50, was operated at 40,000 dynamic resolving power scanning at 100 sec/decade, with an EI source set at 70 eV. The resulting data (10 scans) were averaged and sorted according to heteroatom content and hydrogen deficiency (Z number = number of double bonds + rings).

RESULTS AND DISCUSSION

The internal standard is very important for comparing the results of the PyMS between the different rank coals. It allows a more quantitative comparison, while ideally not participating in any secondary reactions. Our standard appears to function very well. The Diels-Alder product shown below undergoes a thermally induced retro-reaction very cleanly at approximately 300°C to yield D¹⁰-anthracene quantitatively. In the precise mass measurement mode it is easy to separate this ion from the coal pyrolysis products. All of the data presented in this paper have been normalized to this standard. Since this standard is



released at a lower temperature than the coal pyrolysis there is no evidence for deuterium scrambling. The peaks resulting from the standard are excluded from the final averaged spectra and from the Z number and heteroatom analysis. In the analysis the following heteroatoms or combination of heteroatoms were searched for: none, oxygen, two oxygens, three oxygens, sulfur, two sulfurs, sulfur-oxygen, sulfur-nitrogen, and nitrogen. Typically, peaks accounting for greater than 90% of the total ion current can be assigned reasonable formula. This approach has been used to characterize petroleum and coal liquids and has recently been described in detail.⁸

A typical averaged spectra is shown in Figure 1 for the fresh Illinois Herrin Seam coal (APCS #3). Note that there are a significant number of peaks at m/z ratios greater than 200, which is characteristic for all the high volatile bituminous coals. Hydrocarbons are usually found in the 400 region which can be attributed to molecules derived from pentacyclic triterpenoids. This is especially true in the Utah coal (APCS #6) which is rich in liptinites. Most of these types of molecules are extractable, which is seen in the loss of these high mass peaks in the pyridine extracted Utah coal.

The effect of pyridine extraction on the distribution of pyrolysis products is very rank dependent. There is very little difference between raw and extracted coals for those of higher rank such as the low volatile bituminous coal, while

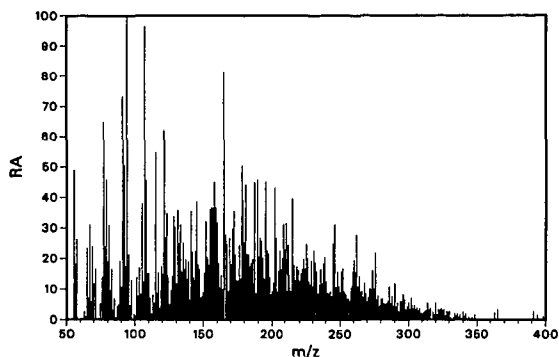


Figure 1. Averaged mass spectra for the fresh Herrin Seam coal (APCS #3), [RA = relative abundance].

an increased yield of pyrolysis products and a greater variety of molecules is found for the lower rank coals which have been extracted. The results for the subbituminous coal are shown in Figure 2. Also, note that the higher mass peaks (>200) are more abundant in the extracted sample. This effect may be simply due to the fact that the low rank coals contain a significant amount of water.

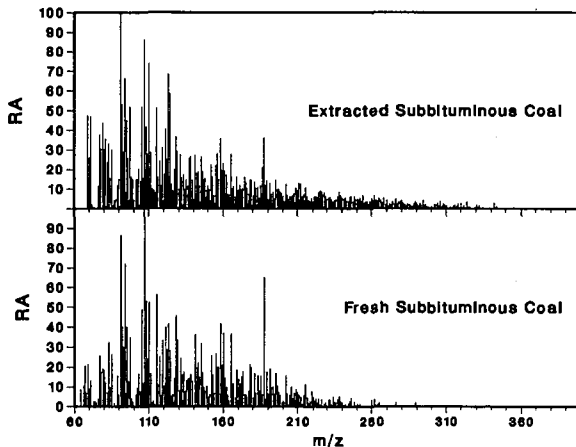


Figure 2. Comparison between averaged mass spectra for fresh and extracted subbituminous coal (APCS #2).

The analysis of the as received sample indicated 28% moisture for the subbituminous coal. The pyridine extraction will effectively remove this water and the sample was vacuum dried. The effect of vacuum drying on the fresh samples is being explored.

The oxygen content of these coals greatly varies from 20% in the lignite down to 2.5% in the lv bituminous. However, the relative yields of oxygen containing species in the pyrolysis product does not change as much as one would

expect based on this variation in oxygen content. There is a decrease with rank which can be seen in the adjacent Figure 3. Also, species with two oxygens are almost absent in the higher rank coals, the mv and lv bituminous ranks. It is known that for lignite and subbituminous coals significant amounts of the oxygen is lost as CO and CO₂.⁹ However, it may be possible that in the higher rank coals the pyrolysis products are enriched in the oxygen containing molecules while the residue is depleted compared to the original oxygen content. These coals have not been exposed to atmospheric oxygen making it unlikely that these oxygen containing aromatics were formed from surface oxidation.

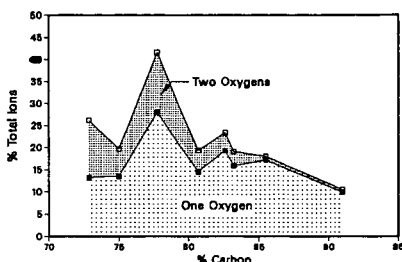


Figure 3. Variation in the oxygen containing products as a function of carbon content presented in a stacked plot.

Although the total amount of oxygen-containing species in the products does not change dramatically with rank, the types of molecules that are seen do change with rank. As can be seen in the adjacent Figure 4, the amount of ions in single ring aromatics (Z=4) decreases with increasing rank while the larger heteroaromatics such as dibenzofuran (Z=9) and naphthobenzofuran (Z=12) are more prevalent in the higher rank coals. These compounds are likely assignments for a combination of these Z numbers and the carbon number for the first peak seen in the series with one oxygen. For example, while hydroxyfluorene has a Z number of 9, the parent molecule has a carbon count of 13 which is one greater than dibenzofuran. Presently, a method is being used to help to distinguish between hydroxylated aromatics and both aryl ethers and annellated furans by modifying the acidic hydroxyls prior to pyrolysis.² With the Pocahontas low volatile bituminous coal, molecules with a single oxygen were observed at up to Z=19 with significant abundances at up to Z=17. With the lignite coal the maximum hydrogen deficiency observed was 12.

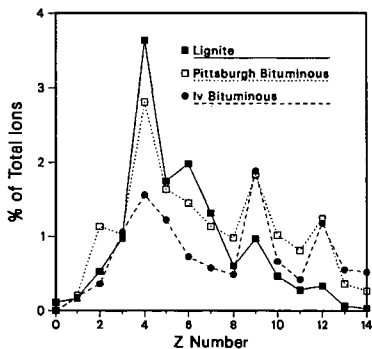


Figure 4. Distribution of molecules which contain one oxygen as a function of hydrogen deficiency for three coals.

Examination of the data from molecules containing a single sulfur yielded two very interesting results for the higher rank coals. Data from the very sulfur-rich Illinois Herrin Seam coal are compared to those from the low volatile bituminous coal in Figure 5. First, the yield of sulfur in the low volatile coal seems to be enhanced in comparison to the original amount of sulfur in the coal. The hv bituminous coal has five times as much, 'organic' sulfur in it as the low volatile coal. The yield of H_2S is probably much larger for the Herrin Seam coal. Second, in the Pocahontas coal small amounts of thiophene (Z=3) and dibenzothiophene (Z=9) are observed. These species along with benzothiophene and naphthobenzothiophene are typical sulfur heterocyclics found in coal liquefaction products^{10,11} and coal extracts.^{11,12} However, in duplicate experiment for both the fresh and extracted sample, the most abundant class of sulfur compounds had a Z number of 10 as is seen in Figure 5 and a carbon number of 14 for the parent molecule in the series. This result was also observed in the Upper Freeport mv bituminous coal. Selected peaks for the Herrin coal and the Pocahontas low volatile coal are shown in

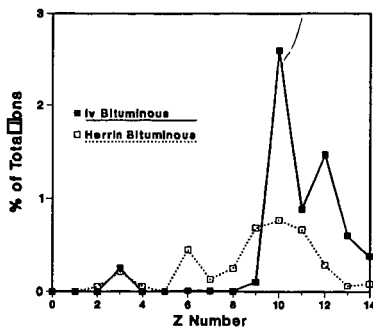


Figure 5. Distribution of species containing a single sulfur atom for two of the fresh coals.

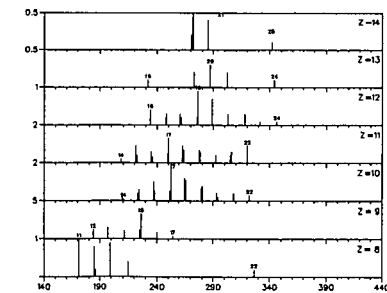


Figure 6. Selected ion peaks containing one sulfur from Z = 8 - 14 for the Herrin seam coal.

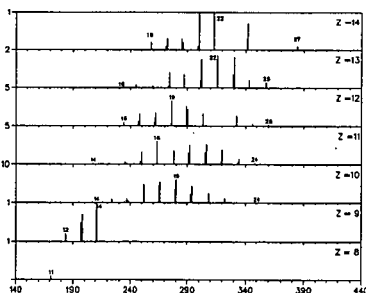


Figure 7. Selected ion peaks with one sulfur for Z = 8 - 14 for the Pocahontas low volatile coal (APCS #5).

Figures 6 and 7. Note that in both these plots the relative abundances for each subplot will vary since they are automatically scaled. The numbers on each plot represent the carbon number for the adjacent peak. In Figure 7 the most abundant peak has 19 carbons and a hydrogen deficiency of 10. A possible structure which would fit this data is alkylated phenylbenzothiophene. Phenylthiophenes have been identified in the extracts of Wyoming coal (PSOC-521).¹¹ The position of the phenyl group would determine if fragmentation would result in benzothiophene fragment peaks which are not seen in the high rank coal. The benzothiophene

fragment is observed if the phenyl were on the thiophene ring.¹³ Another possibility, although it seems less likely, is an addition of a 5-member ring to dibenzothiophene which one would expect to be converted to an indene type structure in the pyrolysis. The results are being investigated further using PyGCMS for these high rank coals.

SUMMARY

Extraction of the coals yielded variable results ranging from enhanced pyrolysis yield from the low rank coals to no difference for the very high rank coal. It was shown that this approach is useful for examining the distribution of heteroatom containing molecules which are produced in the vacuum pyrolysis. It is interesting to note that these species appear to be enriched in the products produced from the higher rank coals.

ACKNOWLEDGMENTS

This work was performed under the auspices of the Office of Basic Energy Sciences, Division of Chemical Sciences, U.S. Department of Energy, under contract number W-31-109-ENG-38. The AGHIS and probe were constructed by J. Gregar in the ANL Chemistry Division.

REFERENCES

1. Winans, R.E.; Hayatsu, R.; Scott, R.G.; McBeth, R.L. In *Chemistry and Characterization of Coal Macerals*; Winans, R.E.; Crelling, J.C., Eds.; ACS Symposium Series No. 252; American Chemical Society: Washington, D.C. 1984; pp. 137-155.
2. Winans, R.E.; Scott, R.G.; Neill, P.H.; Dyrkacz, G.R.; Hayatsu, R. *Fuel Proc. Tech.* 1986 12, 77-88.
3. Winans, R.E.; Hayatsu, R.; McBeth, R.L.; Scott, R.G.; Botto, R.E., *Preprints, Div. Fuel Chem., ACS 1988*, 33(1), 407-414.
4. Melcalf, G.S.; Windig, W.; Hill, G.R.; Meuzelaar, H.L.C. *Int. J. Coal Geol.* 1987, 1, 245-268.
5. van Graas, G.; de Leeuw, J.W.; Schenk, P.A. In *Advances in Organic Geochemistry 1979*; Douglas, A.G.; Maxwell, J.R., Eds.; Pergamon Press: Oxford, 1980; pp. 485-493.
6. Yun, Y.; Hoesterey, B.L.; Meuzelaar, H.L.C.; Hill, G.R., *Preprints, Div. Fuel Chem., ACS 1987*, 32(4), 301-308.
7. Vorres, K.S.; Janikowski, S.K., *Preprints, Div. Fuel Chem., ACS 1987*, 32(1), 492-499.
8. Schmidt, C.E.; Sprecher, R.F.; Batts, B.D. *Anal. Chem.* 1987, 59, 2027.
9. Serio, M.A.; Solomon, P.R.; Yu, Z.Z.; Deshpande, G.V.; Hamblen, D.G., *Preprints, Div. Fuel Chem., ACS 1988*, 33(3), 91-101.
10. Nishioka, M.; Lee, M.L.; Castle, R.N. *Fuel* 1986, 65, 390-396.
11. Nishioka, M. *Energy Fuels* 1988, 2, 214-219.
12. White, C.M.; Douglas, L.J.; Perry, M.B.; Schmidt, C.E. *Energy Fuels* 1987, 1, 222-226.
13. Blatt, H.; Brophy, J.J.; Colman, L.J.; Tairyck, W.T. *Aust. J. Chem.* 1976, 29, 883-890.

PYROLYSIS MODELING OF THE ARGONNE PREMIUM COALS

M.A. Serio, P.R. Solomon, Z.Z. Yu, G.V. Deshpande, and D.G. Hamblen

Advanced Fuel Research, Inc., 87 Church Street, East Hartford, CT 06108 USA

INTRODUCTION

The establishment of the Argonne Premium Sample Bank (1) provides a good opportunity to test a recently developed "general" model of coal devolatilization (2-4). The model, which is called "FG-DVC", combines a functional group model for gas evolution (FG) and a statistical model for tar formation (DVC). It assumes that the kinetics of functional group decomposition are independent of coal type, but that the amounts do vary with coal type (5-7). The rank dependence of the tar yield, tar molecular weight distribution, extract yields, and viscosity are explained by the rank dependence of CO₂ yields according to this model (2,8). The early evolution of CO₂ in low rank coals appears to lead to crosslinking at low temperatures and hence thermosetting behavior, low tar yields, and low extract yields (8).

The validation of the FG-DVC model was previously done for two coals, North Dakota lignite and Pittsburgh Seam bituminous (2). The Argonne Premium Sample set provides six more coals and different samples of these same two coals for comparison. In order to compare with data over a wide range of conditions, pyrolysis experiments were done in three different reactor systems, as described below.

EXPERIMENTAL

Coal Properties - Elemental and ultimate analysis data are given for the eight Argonne coals in Table 1. This information was obtained either from Reference 1 or directly from Karl Vorres. The values were normalized to equal 100%. Note that the coals have been numbered in descending rank order based on carbon content. This is a different numbering system than the Argonne sample designations.

Reactors - The reactors used included a thermogravimetric analyzer (TG) with evolved gas analysis by Fourier Transform Infrared (FT-IR) spectroscopy. The TG-FTIR apparatus is offered commercially by Bomem, Inc. under the name TG/Plus. The TG/Plus couples a Dupont 951 TGA with a Bomem Michelson 100 FT-IR spectrometer. The details of the TG-FTIR apparatus can be found in several publications (6,9,10). Under the present work, approximately 35 mg of the -100 mesh fraction of each coal sample was heated at 30°C/min, first to 150°C for drying, and then to 900°C for pyrolysis.

The entrained flow reactor (EFR) has been described previously in other papers (7,11). The experiments were done at a single injector/collector separation of 24" at three different temperatures (700, 1100, and 1400°C). The heating rate in this system is approximately 5000°C/s and the total residence time is approximately 0.5 s.

The molecular weight distribution of tar evolved during pyrolysis at 0.05°C/s under vacuum to 450 or 500°C was determined by Field Ionization Mass Spectrometry (FIMS) at SRI International. The apparatus has been described by St. John et al. (12). The total weight loss under these conditions was also determined.

A summary of the experimental conditions is given in Table 2. The TG-FTIR and FIMS experiment were done with the -100 mesh ampoules, while the EFR experiments were done with bulk samples supplied by Karl Vorres.

RESULTS AND DISCUSSION

Experimental Data - The experimental results for these coals from the TG-FTIR have been presented in a previous paper (6). These data showed some variations (e.g., 15°C for CH₄, 60°C for tar, 60-90°C for most oxygenates) in the peak temperatures for the maximum evolution rate, particularly in the case of oxygenated volatiles. The variations in the peak temperatures for the various species are consistent with results from an earlier programmed pyrolysis experiment on ten coals (5). However, for each species, the variation in the peak temperature with rank is small relative to a) the width of the peak; b) the variations among species; c) the variations among experiments with significantly different heating rates; d) the typical variations in the data of different investigators for the same species from the same coal. In view of the relative insensitivity of individual species kinetics when compared to these factors, the FG-DVC model assumption of rank independent rates appears sound. The corollary conclusion that the principal variation of pyrolysis behavior with rank is due to variations in the concentration of functional groups and hence, the amount of each pyrolysis product is also unchanged. These conclusions are supported by the ability of the FG-DVC model, which incorporates these assumptions, to fit pyrolysis data for a wide range of coal types over a wide range of conditions, as discussed below.

The complete set of data for the EFR experiments has been given in DOE reports (13). The data for the three temperatures for a high rank (Pocahontas) and low rank (Wyodak) coal are shown in Figs. 1 and 2, respectively. The Wyodak coal shows a significantly higher volatile yield (lower char yield) which can be accounted for by higher yields of oxygenated volatiles. Both coals show the influence of secondary cracking reactions above 700°C and secondary gasification reactions above 1100°C. At 1400°C, the products are close to thermodynamic equilibrium in both cases and consist primarily of char, CO, and H₂. Models have been developed to describe secondary reactions (7), but these have not been included in the version of the model used here, except for the tar cracking which is part of the standard FG model used for reactors where the tar is not quenched (2,7). Consequently, we do not show model predictions for the 1400°C EFR experiments which are dominated by these effects.

Determination of Parameters for the FG-DVC Model - The FG-DVC model contains several parameters, some of which depend on the coal and one which depends on the experiment type. The large number of parameters has been criticized by some. However, it should be pointed out that the model is able to predict a large number of pyrolysis phenomena such as the yields of individual gas species, the yields of tar and char, the tar molecular weight distribution, the crosslink density and the viscosity. The model also accounts for the variation of these quantities with temperature, heating rate, residence time, and pressure in a manner that agrees well with experiment. The details of the model inputs and a sensitivity analysis are included in a recent paper (2).

The first step is to obtain elemental analysis data for C, H, N, O, and S. This is needed to construct a coal composition file. The next step is to determine the amounts of the individual functional group (FG) pools (CO₂-extra loose, CO₂-loose, CO₂-tight, CH₄-loose, etc). This requires data from at least two standard pyrolysis experiments. The first is a slow heating pyrolysis

experiment, like the TG-FTIR experiment, which can provide good quantitative gas yields and differential evolution curves. This type of experiment is best able to resolve the individual loose, tight, etc. pools for a given gas, especially when both the integral and differential curves are compared with the model predictions. The values of the FG pools so determined are checked against a second pyrolysis experiment done at high heating rates, such as the EFR 1100°C data. The pools are adjusted to simultaneously fit the low and high heating rate experiments. This usually involves a series of iterations.

This procedure has been followed for the eight Argonne coals and the results are shown in Fig. 3 for the major FG pools, which are CH₄, CO₂, H₂O, and CO. These values have not yet been fully optimized and may change slightly in the future, but give good agreement with experiment except in the case of H₂O where the data are scattered. The oxygenated species show a systematic increase with decreasing rank. The amount of CH₄ goes through a maximum in the medium rank coals, as do other hydrocarbon species such as tar (see below).

Once the functional group pools have been established to allow a good match between the integral and/or differential yield curves for two pyrolysis experiments, the input parameters for the DVC (tar formation) part of the model are determined. The first step is to adjust the average oligomer length to match the coal extract yield. The next step is to adjust the number of unbreakable bridges ("hard" bonds) between monomer clusters to fit the experimentally observed tar yields for the same low and high heating rate experiments used to calibrate the functional group pools. The relationships between these input quantities and the experimentally measured quantities are shown in Figs. 4 and 5. The extract yield data (which were obtained from Professor Milton Lee at Brigham Young University) and the average oligomer length are inversely correlated. The same is true of the number of hard bonds and the tar yield. Again, these values have not been fully optimized and are subject to change.

Other parameters which go into the tar formation model are the average monomer molecular weight (M_{avg}) and the average molecular weight between crosslinks (M_c). The value of M_c is interpolated from the literature data of Nelson (14). We eventually plan to use literature data for M_{avg} as well. However, the size of the average cluster varies significantly among different research groups and the reported rank variations are not systematic or clearly understood. Currently, we are using a value of 256 for all the coals except the Pocahontas where a value of 506 is used. The significantly higher average cluster size for the Pocahontas compared to the others is supported by the calculations of Gerstein et al. (15) based on NMR, FT-IR and elemental analysis data obtained for a number of coals.

The last important parameter to be selected is the value of ΔP , which is the average pressure difference between the ambient and the particle's interior during pyrolysis. This parameter is used in the internal transport model. The choice of ΔP has a significant effect on tar yield and the tar molecular weight distribution for non-softening coals under most conditions except high pressure. For fluid coals, a value of $\Delta P = 0$ is a good approximation for pressures of one atm or higher. The sensitivity of the model to the choice of ΔP is discussed in a recent paper (2). This is the only parameter in the model which is adjusted for each type of experiment. The original FG model also had a fitting parameter, X_0 , which was used to match the final tar yield to account for differences in particle size, heating rate, bed depth and reactor geometry (2). While it can be said that we have traded one adjustable parameter, X_0 , in the FG model for

another, ΔP , in the FG-DVC model, this is not exactly true as the latter model is much richer in its ability to predict a variety of pyrolysis events. The values of ΔP are more restricted than X_0 and have a more fundamental basis that it is related to the coal's viscosity.

The use of the FG-DVC model involves several constraints: 1) Where experimental data are available on the starting coal, such as for the molecular weight between crosslinks (M_c), the extract yield, or the elemental analysis, they are used as inputs. Additional information will be incorporated as it becomes available. 2) The kinetic parameters for the evolution of the FG group pools are assumed to be invariant with coal type. 3) The amounts of the FG pools are constrained to fit data from experiments at very low (0.5°C/s) and very high (5000°C/s) heating rates. This results in a model which is very robust in its ability to fit pyrolysis data over a wide range of conditions. It is also true that when enough coals have been studied, a detailed calibration of the model may not be needed and perhaps the elemental analysis, the particle size and the reactor conditions will be sufficient.

Comparison of Model with Experimental Data - The model is compared with experimental data from the three reactors in Figs. 6 and 7. Except for H_2O , the agreement of the model is generally quite good over a wide range of extents of pyrolysis and for what is a wide range of coal types. A comparison is made between the tar molecular weight measured by FIMS and the predicted values in Fig. 8. The model predicts rank dependent phenomena, such as the steep drop off in the distribution for the low rank coal due to crosslinking events (2,8).

CONCLUSIONS

The conclusions for this work are as follows:

- The pyrolysis kinetic data for this series of coals support the assumption of relative rank insensitivity, as does the ability of the model to fit the data using rank independent rates.
- There is a systematic variation in the amounts of individual pyrolysis gases with rank. The oxygenates (CO , CO_2 , H_2O) are highest for the low rank coals while the hydrocarbons are highest for the medium rank coals.
- There is a systematic variation in the tar yield and tar molecular weight distribution with rank. The tar yield is highest for medium rank coals. The mean of the tar average molecular weight distribution is highest for the high rank coals. The drop-off in the tar molecular weight distribution is greatest for low rank coals.
- The rank dependent phenomena are well described by the FG-DVC model over a wide range of experimental conditions.

ACKNOWLEDGEMENTS

This work was supported under DOE Contract No. DE-AC21-86MC23075 through the Morgantown Energy Technology Center. Justin L. Beeson is the Project Manager. Karl Vorres supplied bulk samples of the Argonne coals for the EFR experiments.

REFERENCES

1. Vorres, K.S., ACS Fuel Chem Div. Preprints, **32**(4), 221 (1987).
2. Solomon, P.R., Hamblen, D.G., Carangelo, R.M., Serio, M.A. and Deshpande, G.V., "A General Model of Coal Devolatilization", accepted for publication, Energy and Fuel, (1988).
3. Solomon, P.R., Hamblen, D.G., Carangelo, R.M., Serio, M.A. and Deshpande, G.V., ACS Fuel Div. Preprint, **32**(3), 83 (1987).
4. Solomon, P.R., Hamblen, D.G., Carangelo, R.M., Serio, M.A. and Deshpande, G.V., Combustion and Flame, **71**, 137 (1988).
5. Solomon, P.R. and Hamblen, D.G., Prog. Energy Combust. Sci., **9**, 323 (1983).
6. Serio, M.A., Solomon, P.R., and Carangelo, R.M., ACS Div. of Fuel Chem. Preprints, **33**, (2), 295, (1988).
7. Serio, M.A., Hamblen, D.G., Markham, J.R., and Solomon, P.R., Energy and Fuels, **1**, 138, (1987).
8. Deshpande, G.V., Solomon, P.R., and Serio, M.A., ACS Div. of Fuel Chem. Preprints, **33**, (2), 310, (1988).
9. Carangelo, R.M., Solomon, P.R. and Gerson, D.J., Fuel, **66**, 960 (1987).
10. Whelan, J.K., Solomon, P.R., Deshpande, G.V., and Carangelo, R.M., Energy and Fuels, **2**, 65, (1988).
11. Solomon, P.R., Hamblen, D.G., Carangelo, R.M., and Krause, J.L., 19th Symposium (Int) on Combustion, The Combustion Institute, Pittsburgh, PA, 1139, (1982).
12. St. John, G.A., Buttrill, Jr., S.E. and Anbar, M., ACS Symposium Series, **71**, 223 (1978).
13. Solomon, P.R., Hamblen, D.G., Serio, M.A., Smoot, L.D. and Brewster, S., "Measurement and Modeling of Advanced Coal Conversion", First Annual Report DOE/METC Contract #DE-AC21-86MC23075 (1987).
14. Nelson, J.R., Fuel, **62**, 112 (1983).
15. Gerstein, B., Murphy, P.D. and Ryan, L.M., Coal Structure, (R.A. Meyers, Ed.) Chapter 4, Academic Press, New York (1982).

Table 1- Elemental Analysis of Argonne Premium Coal Samples.

	% daf Basis					As-Received	
	C	H	O	N	S	% Dry Basis	Basis
	Ash	Moisture					
1. Pocahontas	90	4.7	3	1.3	1.0	5	0.6
2. Upper Freeport	84	5.0	7	1.5	2.5	13	1.1
3. Pittsburgh #8	82	5.8	8.8	1.6	1.8	9	1.6
4. Lewiston-Stockton	81	5.5	11	1.6	0.8	20	2.4
5. Utah Blind Canyon	79	6.0	13	1.6	0.5	5	4.6
6. Illinois #6	76	5.7	10	1.4	6.4	16	8.0
7. Wyodak	74	5.1	19	1.1	0.4	8	28.1
8. Beulah-Zap	72	5.2	21	1.1	0.8	6	32.2

Table 2 - Experimental Conditions

Reactor	Temperature (°C)	Heating Rate °C/s	Hold Time s	Pressure atm
TG-FTIR	900	0.5	0	1
EFR	700, 1100, 1400	5000	0.5	1
FIMS	500	0.05	0	0

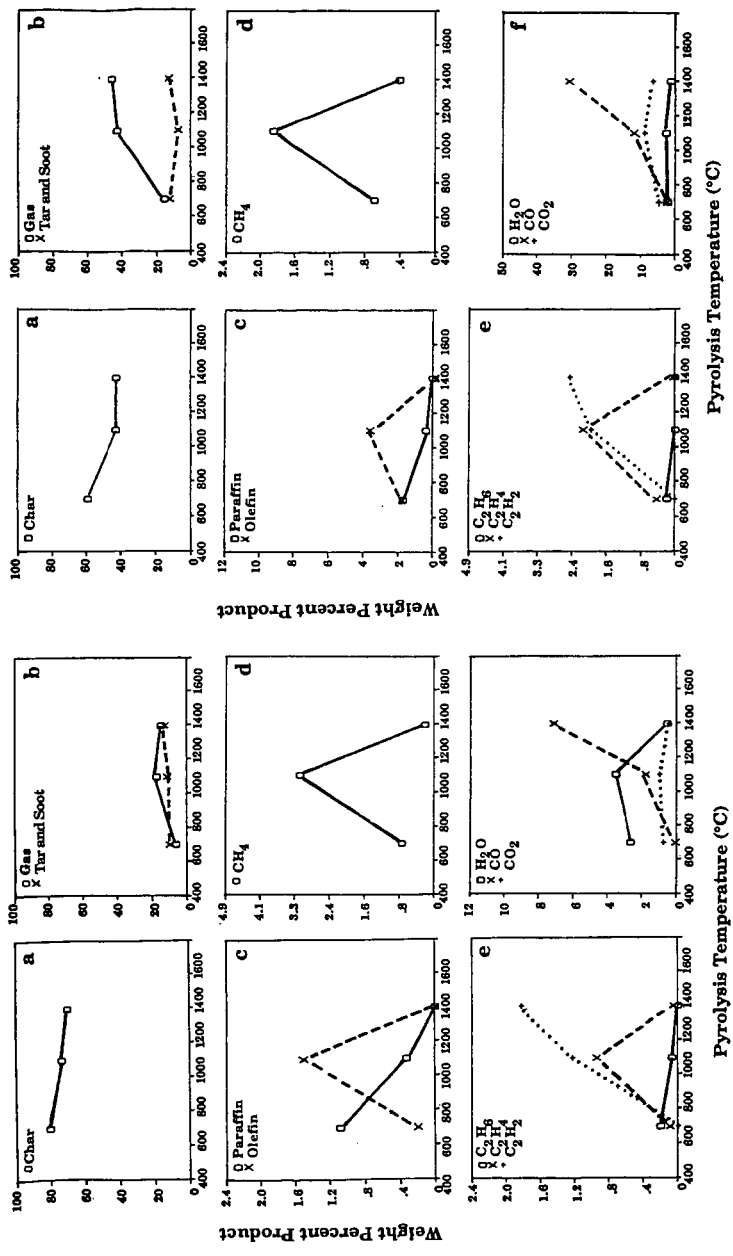


Figure 1. Pyrolysis Results for Pocahontas Bituminous Coal, 200 x 325 mesh, in the Entrained Flow Reactor. The Solid, Dashed and Dotted Lines are used to connect the Data and are not Model Predictions.

Figure 2. Pyrolysis Results for Wyodak Subbituminous Coal, 200 x 325 mesh, in the Entrained Flow Reactor. The Solid, Dashed and Dotted Lines are used to connect the Data and are not Model Predictions.

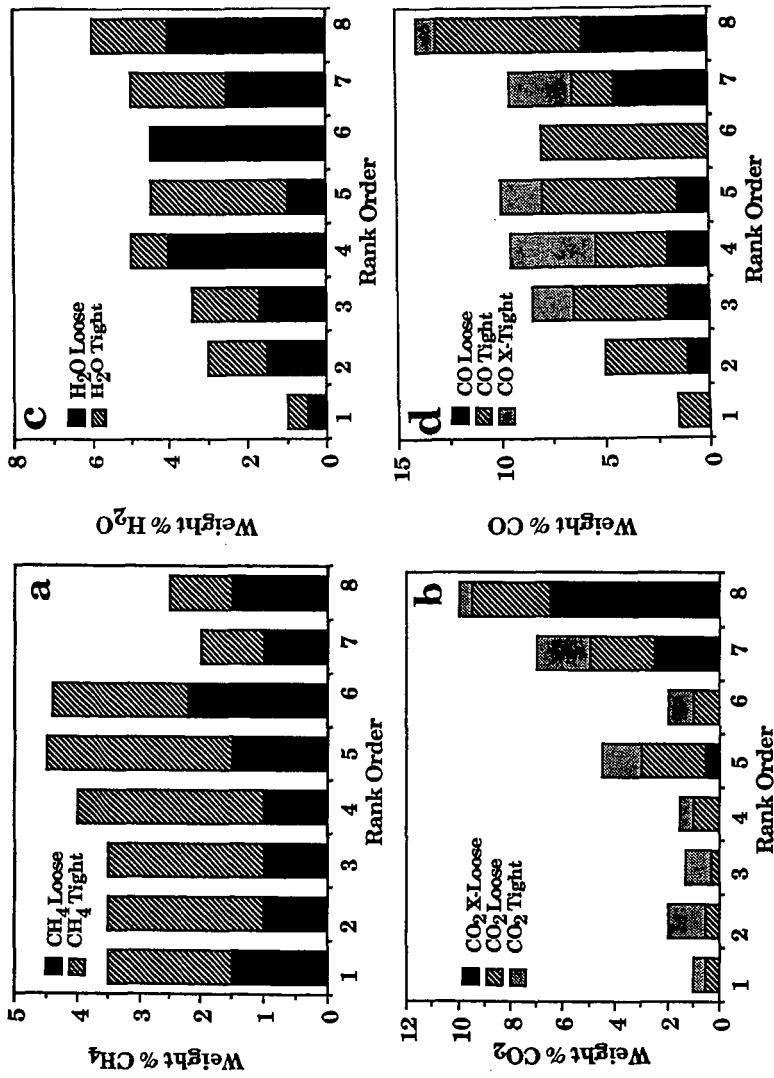


Figure 3. Variation of Functional Group Pools with Rank Order.

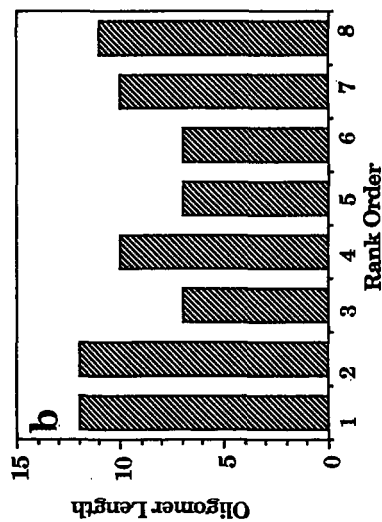
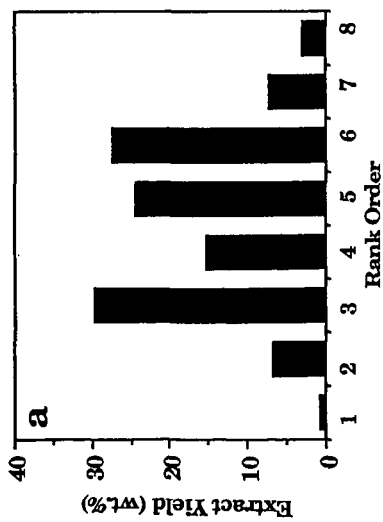


Figure 4. Variation of Extract Yield and Oligomer Length with Rank Order.

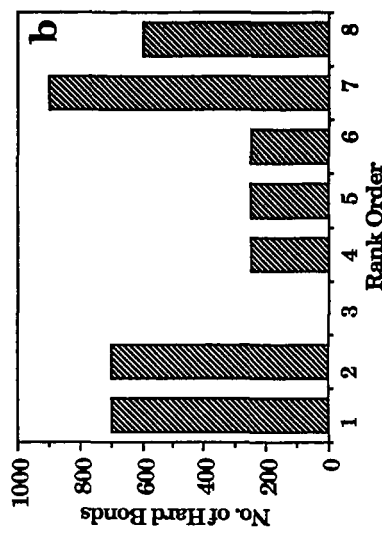
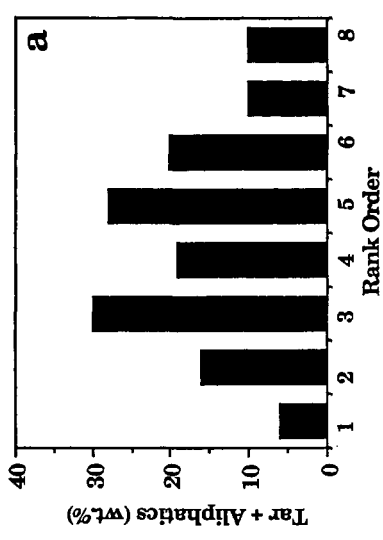


Figure 5. Variation of Tar Yield from TG-FTIR Experiment and Number of Hard Bonds with Rank Order.

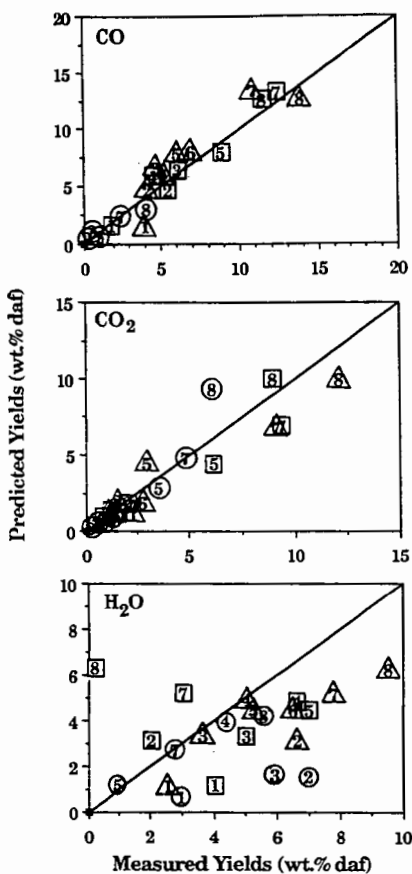


Figure 6. Comparison of Model Predictions with Data for the Yields of Oxygenated Species. The Numbers Refer to the Coal Type. The Symbols Around the Numbers Refer to the Reactor Type. ○ - EFR, 700°C; □ - EFR, 1100°C; △ - TG-FTIR; No Symbol - FIMS.

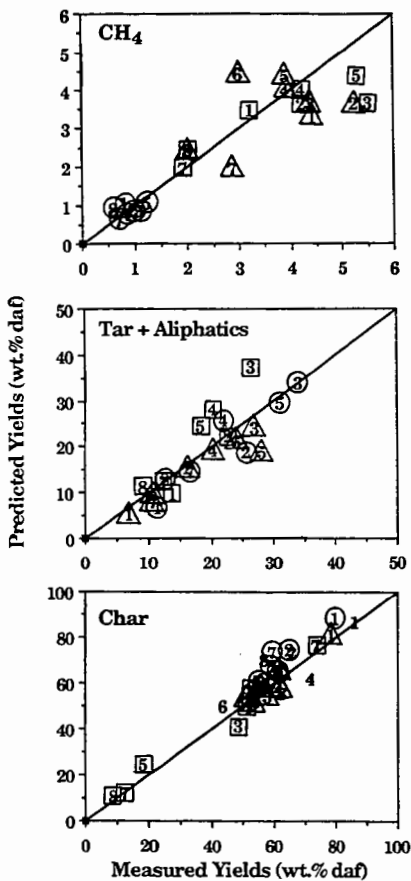


Figure 7. Comparison of Model Predictions with Data for CH₄, Tar Plus Aliphatics, and Char. The Numbers Refer to the Coal Type. The Symbols Around the Numbers Refer to the Reactor Type. ○ - EFR, 700°C; □ - EFR, 1100°C; △ - TG-FTIR; No Symbol - FIMS.

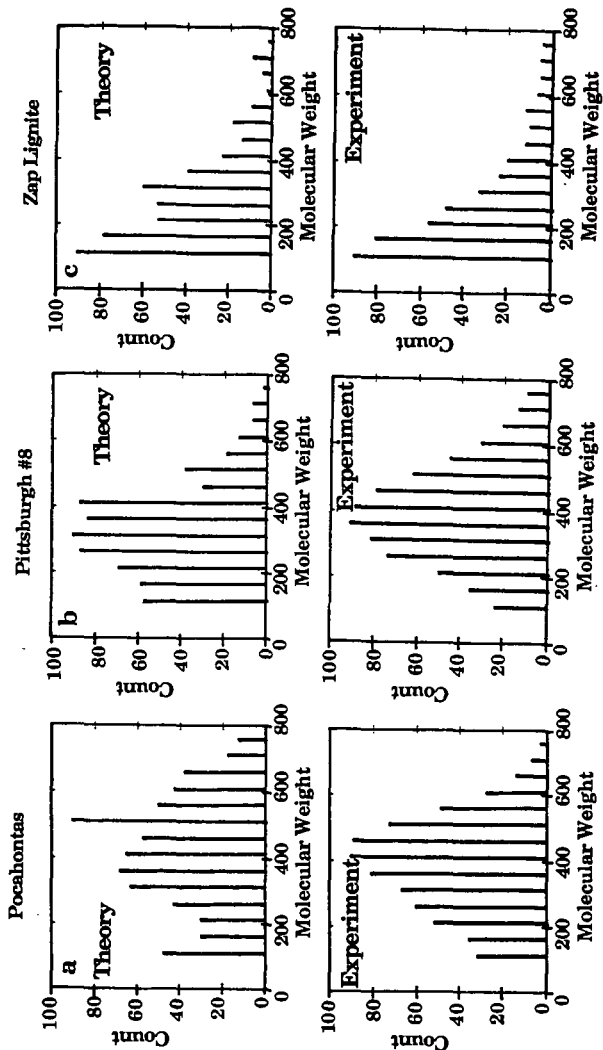


Figure 8. Comparison of Measured and Predicted Tar Molecular Weight Distributions.

THERMOCHEMICAL COMPARISON OF ARGONNE PREMIUM COAL SAMPLES WITH MODEL SOLID ACIDS.

by

Edward M. Arnett*
Brenda J. Hutchinson
Michael Gumkowski
Qitao Liu

Department of Chemistry
Duke University
Durham, North Carolina 27706

Abstract

This presentation will be a summary of results acquired over the last five years using the heats of interaction of a series of bases with various solid acids as a means for classifying them. A sulfonic acid resin provides a solid model for Brønsted acidity. Silica is a model solid for hydrogen bonding interactions and several grades of graphitized carbon black are an excellent model for van der Waals/dispersion force interactions. Heats of interaction of the series of bases with several types of Argonne premium coals will be compared with those for the model solids and will serve as a means for coal classification.

INTRODUCTION

Thermochemical methods based on various types of calorimetry are a powerful tool for comparing acid-base interactions both in homogeneous and heterogeneous systems. Previous reports from this laboratory have described the thermochemical method for comparing solid acids with their homogeneous analogues in response to interactions with a variety of basic liquids. We have attempted to find appropriate solid prototypes for Brønsted acidity (1), hydrogen-bonding acidity (2), and dispersion force interactions (3). These could be used as standards for comparison in classifying more complex solid acids such as coals.

Much of the recent literature on the thermochemistry of adsorption onto coals has focused on their interactions with water or alkanols so that pre-treatment conditions could be examined with respect to their influence on the resulting heat of interaction (4-7). Some studies have examined other types of interacting compounds, such as amines, pyridines, and alkanes (8-12).

The present report compares six carefully classified coals from the Argonne National Laboratory Premium Coal bank by two calorimetric methods (heats of immersion and thermometric titration) using a series of twelve solvents chosen especially to bring out the differences between Brønsted acidity, hydrogen-bonding and dispersion force interactions (13).

RESULTS

Heats of immersion of the six premium coal samples, three coals from a previous study and two prototype solids (Dowex, silica) into twelve carefully chosen solvents at 75° are listed in Table I. Also listed in Table I are the heats of adsorption of the bases with Carboxpack F. The values reported are averages of two or three measurements, along with the standard deviation.

DISCUSSION

An important goal of this project is to see whether acid-base interactions of complex solids such as coals can be characterized thermochemically in the same manner which has been successful for characterizing acid-base interactions of homogeneous systems. A number of years ago, we demonstrated that there was a clear difference between the thermochemical order for interaction of a series of bases with the strong Brønsted acid, fluorosulfuric acid, as compared with the hydrogen-bonding acid, *p*-fluorophenol (14,15). The twelve basic solvents listed in Table I were chosen primarily to discriminate between surface sites which form hydrogen-bonds and those which are capable of Brønsted acid interactions. For example, dimethyl sulfoxide is a strong hydrogen-bond acceptor although it is a relatively weak proton acceptor from Brønsted acids in solution (15).

Comparison of Premium Coals with Each Other. Heats of immersion data for six coals listed in Table I were subjected to linear correlation analysis. By heat of immersion, the greatest similarity is between Illinois #6 and Pittsburgh #8 and between Wyodak and N. Dakota lignite. The biggest difference is between Pittsburgh #8 and Pocahontas #3.

Comparison with Earlier Work. The premium Wyodak coal sample (taken from the Gillette strip-mine) may be compared to the four year old sample of Wyoming Rawhide coal obtained from Exxon and kept dry under nitrogen. Comparison of heats of immersion in ten solvents (see Table I) gives a correlation coefficient of 0.96. A similar correlation for the Exxon sample of Illinois #6 as compared to the Argonne Premium, using only six bases, has an *r* value of 0.97. Finally, with a sample of only five bases, correlation of the old data for Texas Big Brown lignite with the Premium sample of North Dakota lignite gives an *r* value of 0.97.

Comparison with Standard Solid Acids. Heats of immersion of Dowex sulfonic acid resin, the prototype Brønsted acid, and of silica, the prototype solid hydrogen-bonding acid, can be compared with heats of immersion of the five premium coals using data for ten bases: pyridine, dimethyl sulfoxide, 4-methylpyridine, toluene, cyclohexanone, 2,6-dimethylpyridine, 2,4,6-trimethylpyridine, *n*-butylamine, propylene carbonate and *n*-hexylamine as shown by the correlations in Table II.

It is clear that by themselves neither Dowex, silica, or graphitized carbon black provide good models for the interaction of basic liquids with these coals. When two parameter equations are used to include contributions from both Brønsted acidity and hydrogen-bonding, there is considerable improvement. As might be expected, the introduction of yet another correlation parameter for dispersion forces improves things even more. Recent work in this laboratory indicates that Carbo-pack F[®], graphitized carbon black, is a better model than graphite for non-specific physical adsorption. Regression equations using heats of immersion of Dowex, silica and van't Hoff heats of adsorption determined by gas chromatography on Carbo-pack F as parameters to describe the heats of immersion of five premium coals in ten liquids are also shown in Table II.

The percentage contributions of Brønsted acidity (Dowex), hydrogen bonding (Silica), and dispersion force interactions (Carbo-pack) to the heats of immersion for each coal in ten bases were determined by the method of Swain and Lupton. It is interesting to see the variation of these contributions from one type of coal to another and the relatively large role of hydrogen-bonding. This supports the proposal of Larsen (16) for the role of this type of interaction to the swelling and solubilization of coal. This treatment has the advantage of expressing the results of three types of actions that are presumed to affect an interaction (such as that between a solid and liquid) in percentage terms. However, its shortcoming is that the results are assumed to be completely

determined by these actions, that is, they add up to 100%, which in turn implies that a perfect fit should be obtained with three parameters. This is clearly far from the case.

Table II shows that our fundamental strategy of trying to dissect the interactions of a complex solid, such as a coal, with a series of solvents into contributions that are modeled by prototype "simpler" solids has had only modest success.

Finally, it may be asked whether accessibility or acid properties are strongly affected by the surface areas of the coals. These have been determined by BET analysis and when the results are compared with heats of immersion or titrametric heats there is no indication that surface area is a significant factor. This behavior is very different from heats of immersion of silicas in the same bases where surface area plays a key role (2). In all probability the difference lies in the fact that coals are readily swollen and penetrated by the basic solvents so that eventually most acid sites are reached in the open cross-linked gel network. In contrast silica is a relatively undeformable solid.

References

1. Arnett, E.M.; Haaksma, R.A.; Chawla, B.; Healy, M.H., J. Am. Chem. Soc. 1986, 108, 4888.
2. Arnett, E.M.; and Cassidy, K.F., Reviews of Chemical Intermediates, 1988, 9, 27.
3. Arnett, E.M.; Hutchinson, B.J.; Healy, M.H., J. Am. Chem. Soc. (In press.)
4. Fuller, E.L., Jr., J. Coll. Interf. Sci., 1980, 75, 577.
5. Senkan, S.M.; Fuller, E.L., Jr., Fuel, 1979, 58, 729.
6. Glanville, J.O.; Newcomb, K.L.; and Wightman, J.P., Fuel, 1986, 65, 485.
7. Phillips, K.M.; Glanville, J.O.; and Wightman, J.P., Colloids and Surfaces, 1986, 21, 1.
8. Brooks, D.; Finch, A.; Gardner, P.J.; Harington, R., Fuel, 1986, 65, 1750.
9. Larsen, J.W.; and Knemmerle, E.W., Fuel, 1978, 57, 59.
10. Glanville, J.O.; Wightman, J.P., Fuel, 1980, 59, 557.
11. Larsen, J.W.; Kennard, L.; and Kuemmerle, E.W., Fuel, 1978, 57, 309.
12. Chawla, B., Arnett, E.M., J. Org. Chem. 1984, 49, 3054.
13. Gunkowski, M.; Liu, Q.; Arnett, E.M., Energy and Fuels, 1988, 2, 0. (In press)
14. Arnett, E.M.; Quirk, R.P.; Larsen, J.W., J. Am. Chem. Soc., 1970, 92, 3977.
15. Arnett, E.M.; Mitchell, E.J.; Murty, T.S.S.R., J. Am. Chem. Soc. 1974, 96, 3875.
16. Larsen, J.W.; Green, T.K; Kovac, J., J. Org. Chem. 1985, 50 4729.

Table II. Regression of Premium Coal Immersion Values Against Those for Dowex and Silica and Carbopack-F for Ten Bases (see Table I).

(10 Bases as listed in Table I).

$$\Delta H_{\text{Wyodak}} = -10.833 - 0.754\Delta H_{\text{Dowex}} + 4.440\Delta H_{\text{silica}} - 7.218\Delta H_{\text{Carbopack-F}}$$
$$r = 0.962; r_{\text{Dowex}} = -.546; r_{\text{silica}} = 0.886; r_{\text{Carbopack-F}} = 0.468$$

$$\Delta H_{\text{Ill. #6}} = 61.806 - 0.312\Delta H_{\text{Dowex}} + 3.625\Delta H_{\text{silica}} + 1.126\Delta H_{\text{Carbopack-F}}$$
$$r = 0.947; r_{\text{Dowex}} = 0.662; r_{\text{silica}} = 0.942; r_{\text{Carbopack-F}} = 0.078$$

$$\Delta H_{\text{Pitts. #8}} = 29.867 - 0.366\Delta H_{\text{Dowex}} + 2.821\Delta H_{\text{silica}} - 1.197\Delta H_{\text{Carbopack-F}}$$
$$r = 0.946; r_{\text{Dowex}} = 0.618; r_{\text{silica}} = 0.934; r_{\text{Carbopack-F}} = 0.235$$

$$\Delta H_{\text{Pocah. #3}} = -5.084 - 0.085\Delta H_{\text{Dowex}} + 0.202\Delta H_{\text{silica}} - 0.519\Delta H_{\text{Carbopack-F}}$$
$$r = 0.658; r_{\text{Dowex}} = 0.156; r_{\text{silica}} = 0.466; r_{\text{Carbopack-F}} = 0.453$$

$$\Delta H_{\text{N.Dakota}} = -52.691 - 0.905\Delta H_{\text{Dowex}} + 3.481\Delta H_{\text{silica}} - 9.556\Delta H_{\text{Carbopack-F}}$$
$$r = 0.893; r_{\text{Dowex}} = 0.375; r_{\text{silica}} = 0.715; r_{\text{Carbopack-F}} = 0.596$$

DETERMINATION OF PHENOLIC STRUCTURES IN LOW RANK COALS: ELUCIDATION OF TRANSFORMATION PROCESSES OF LIGNIN AT THE EARLY STAGE OF COALIFICATION

R. Hayatsu, R. L. McBeth, R. G. Scott, and R. E. Winans

Chemistry Division, Argonne National Laboratory,
9700 South Cass Avenue, Argonne, IL 60439

INTRODUCTION

Because lignin is considered to be a major precursor of coal vitrinite, chemical alteration studies of lignin structure are important for elucidating coalification processes as well as for understanding the chemical structure of vitrinite. Many investigators have attempted to elucidate the chemical processes in the coalification lignin. For example, Wayman et al. (1) have reported that a 100-million-year-old conifer consists of lignin-like material which is about one-third demethylated. Extensive cleavage of lignin ether linkages was also observed. Recently, based on ^{13}C NMR study, Hatcher (2) has concluded that the defunctionalization reactions of lignin-derived aromatic structures occur sequentially during coalification. A similar pathway has been suggested by Wilson (3). From a comparative NMR study of [$\beta\text{-}^{13}\text{C}$]lignin and its coalified products, Botto (4) has suggested that transformation of lignin is initiated by the heterolytic bond cleavage of labile β -aryl ether groups.

The present study continues our investigation of transformation processes of plant organic material to coal during early stages of coalification. To understand alteration of phenolic structures in lignin, and natural and synthetic coals have been characterized by using two-step depolymerization procedure of alkaline hydrolysis followed by silver oxide oxidation. In parallel experiments, lignin model compounds and a polymer have been transformed using thermal catalytic reaction conditions that mimic natural catagenetic metamorphism.

EXPERIMENTAL

Samples. The elemental compositions are presented in Table 1. Prior to the oxidations, all coal samples were exhaustively extracted with benzene-methanol (3:1) and CHCl_3 under reflux, and these were demineralized with HCl-HF at room temperature. A softwood lignin was isolated from pine.

Alkaline Hydrolysis. Each sample (0.5-1.0 g) was hydrolyzed with 12% NaOH aq. solution in an autoclave at 180°C for 4 hours. The air in the autoclave was replaced by nitrogen. The yields of alkaline hydrolyzed fractions from all samples are shown in Table 1. The soluble hydrolyzed fraction (after acidity) consists of humic acid-like material (soluble in alkali only but not HCl and organic solvents) and small molecules (soluble in organic solvents); dried at 60°C under vacuum.

Oxidation. Each alkaline hydrolyzed fraction was methylated with dimethyl- d_6 sulfate (5) before oxidation. A methylated- d_3 sample (0.3 ~ 0.4 g) was oxidized with alkaline silver oxide (freshly prepared 6 g of Ag_2O and 60 ml of 16% NaOH

TABLE 1. Elemental and Maceral Compositions of Samples.

No.	Sample	Elemental Composition per 100 Carbons	Soluble ^a	Insoluble ^b	Loss (by difference)
1	Victorian Brown Coal (Pale Lithotype)	$C_{100}H_{89}O_{34}N_{0.5}S_{0.2}$	64.3	28.7	7.0
2	Beulah-Zap Lignite (APCS #8)	$C_{100}H_{80}O_{21}N_{1.4}S_{0.4}$	57.5	28.5	14.0
3	Wyodak-Anderson Subbituminous (APCS #2)	$C_{100}H_{86}O_{18}N_{1.3}S_{0.2}$	53.0	31.4	15.6
4	Illinois #6 seam hvC Bituminous (APCS #3)	$C_{100}H_{77}O_{13}N_{1.5}S_1$	12.7	79.9	7.4
5	Blind Canyon hvB Bituminous (APCS #6)	$C_{100}H_{88}O_{11}N_{1.7}S_{0.2}$	32.7	58.8	8.5
6	Upper Freeport mv Bituminous (APCS #1)	$C_{100}H_{66}O_{6.6}N_{1.6}S_{0.3}$	8.6	84.5	6.9
L	Lignin	$C_{100}H_{108}O_{33}$	69.3	22.0	8.7
SY	Synthetic Coal	$C_{100}H_{86}O_{23}N_{1.2}S_{0.3}$	54.4	29.3	16.3

^aThe soluble, in experimental hydrolyzed fraction (after acidity) consists of humic acid-like material (soluble in alkali only but not HCl and organic solvents) and small molecules (soluble in organic solvents); dried at 60°C under vacuum.

^bInsoluble residue was determined after washing with HCl, H₂O and organic solvents, dried at 80°C under vacuum.

aqueous solution) at 80°C for 10 hours. After filtration, the reaction mixture was acidified with 10% HCl, concentrated, and extracted with benzene-methanol (3:1) and ether-methanol (3:1). Finally the solvent extractable material was esterified with diazomethane for GCMS analysis.

Thermal Catalytic Reaction. As shown in Table 2, six lignin model compounds and a polymer were used. Each sample (0.5 g) and montmorillonite K-10 (Aldrich Chemical Co.) were placed in a 25 x 2 cm i.d. glass tube. After evacuation, the tube was sealed and then heated at 150°C for two weeks. After the reaction, the mixture was extracted with refluxing benzene-methanol (3:1) and then CHCl₃.

In general, phenolic groups are strongly adsorbed on the surface of clay minerals. Therefore, it is necessary to treat the reaction mixture with 6N-HCl (reflux for 6 hrs.) before extraction with organic solvent. The solvent insoluble residue was treated with concentrated HCl-HF (1:1) at room temperature to remove the clay. A synthetic coal was prepared by heating a mixture of lignin, amino acids and K-10 at 150°C for two months (6-7).

Characterization and Identification Procedures. The analytical procedures used in this study have been described in detail previously (5,7-8).

RESULTS AND DISCUSSION

We have found that the alkaline hydrolysis effectively solubilizes lignin and low rank coals. The most likely mechanism of solubilization is the cleavage of ether linkages except aryl methyl and diaryl ethers. As expected, high oxygen containing samples (L, No. 1-3 and SY in Table 1) were hydrolyzed appreciably and produced significant amounts of solubilized materials.

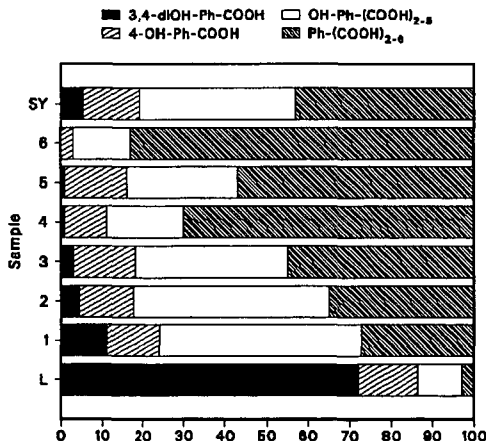
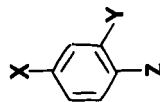


Figure 1. Relative abundances of the phenolic- and benzene-carboxylic acids obtained from silver oxide oxidation of alkaline solubilized materials; determined by GCMS as methyl esters.

TABLE 2. Summary of the Thermal Catalytic Reaction of Lignin Models.

Run	Model			Yield of Product wt%		Soluble Products (GCMS Analysis)	
	X	Y	Z	Soluble	Insoluble Polymers	Major	Minor
1	CH ₂ OH	OME	OH	38	42	C ₁₋₃ alkyl-catechols	dimers
2	O-nBu	H	H	53	10	C ₁₋₇ alkyl-phenols	dimers, trimers
3	OCD ₃	H	{CH-CH ₂ } _n	27	61	C ₁₋₃ alkyl, CD ₃ -phenols	dimers
4	OCH ₂ Ph	H	H	45	41	hydroxyl-diphenylmethanes	dimers
5	H	OH	OCH ₂ Ph	63	16	benzylcatechols	dimers, trimers
6	CH ₂ OCH ₂ Ph	H	H	42	37	C ₁₋₂ alkyl-diphenylmethanes	triphenylalkanes
7	OPh	H	H	79	13	starting material	monomeric and dimeric phenols

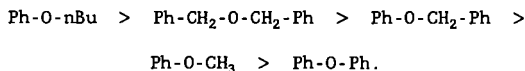


A summary of the silver oxide oxidation products from d_3 -methylated solubilized materials is shown in Fig. 1. The yields are 63-89 wt%. The major product from oxidation of lignin is 3-methoxy-4-methoxy- d_3 -benzoic acid. This result is in excellent agreement with the latest softwood lignin model (9) and other oxidation studies (e.g. 10). On the other hand, the oxidation of coal samples shows much smaller yields of dimethoxybenzoic acid. The GCMS analyses of coal oxidation products indicated that the concentration of 3,4-dimethoxy- d_6 derivative is much higher than that of 3-methoxy-4-methoxy- d_3 compound which is lignin's major product; $(OCD_3)_2/OCD_3OCH_3$ ratios are 0.16 for lignin and 4.7 - 7.5 for coal samples.

Most informative was the identification of large amounts of phenol-polycarboxylic and benzene-polycarboxylic acids in the oxidation products of low rank coals (Nos. 1-3). These acids are found in very little or negligible concentration in the oxidation products of lignin or slightly altered lignin. These observations apparently show that phenolic structures in lignin are considerably changed even at early stages of coalification.

With increasing rank (HV bituminous coals), the yield of phenolic acids decreases; benzenecarboxylic acids become the most abundant products. Polynuclear aromatics such as naphthalene carboxylic acids have also been found as minor products.

As shown by the results of thermal catalytic reactions of lignin models in Table 2, it is apparent that the reactions proceed by intra- and inter-molecular rearrangements of ethers. Aryl methyl and aryl butyl ethers (runs 1-3) rearrange to alkyl phenols; benzyl ethers were found to be converted to diphenylmethane derivatives through cleavage of ether linkages and benzylation. The reactivity of ethers under the reaction conditions used in this study are shown to increase in the following series:



These results imply that ether linkages in lignin structures (benzyl aryl type ethers; β -O-4, α -O-4 and γ -O-4) are labile and readily cleaved with accompanying intra- and inter-molecular rearrangements at early stages of coalification. Botto has observed (4) the occurrence of such rearrangement reactions from ^{13}C NMR studies of [β - ^{13}C] lignin samples coalified by the thermal catalytic reactions.

In this and previous (6-7) studies, we have also found that the oxidation results of synthetic coals obtained from lignin closely resemble those of the oxidation of samples No. 1 and 2 (Fig. 1), and other coals and vitrinites (6-7). Both natural and synthetic coals produce phenolic- and benzene-polycarboxylic acids as major oxidation products.

An important problem has been understanding how phenolic structures in lignin are altered to benzene and other aromatic structures such as naphthalene and tetralin. In our preliminary studies, we have found that phenols and phenyl ethers undergo catalytic hydrogen transfer reactions with terpenoids found in

low rank coals and sedimentary rocks. The terpenoids are apparently acting as hydrogen donors. These reactions are believed to be catalyzed by clay minerals.

One of our experiments indicates that the reaction of p-hydroxy-polystyrene and d-limonene in the presence of montmorillonite K-10 produce alkyl benzenes and p-cymene together with alkyl phenols. Such hydrogen transfer reactions may reveal the processes by which benzene rings are formed at the expense of lignin-phenols. It is considered that somewhat transformed lignin may also contain hydrogen donors such as hydroaromatics. Indeed, Botto has suggested (4) formation of hydroaromatic structures such as dihydrofurans during coalification of lignin. Detailed results for this study will be reported.

SUMMARY

The present study indicates that natural alteration processes from lignin to low rank coal are highly diverse and involve many types of organic reactions. Among them are clay catalyzed intra/inter-molecular rearrangement, hydrogen transfer and transalkylation reactions (11-14) which occur simultaneously rather than sequentially.

ACKNOWLEDGMENT

This work was performed under the auspices of the Office of Basic Energy Sciences, Division of Chemical Sciences, U.S. Department of Energy, under contract number W-31-109-ENG-38.

REFERENCES

1. M. Wayman, M. R. Azhar and Z. Koran, Wood Fiber, **3**, 153 (1971).
2. P. G. Hatcher, Energy & Fuels, **2**, 48 (1988).
3. M. A. Wilson, "NMR Techniques and Applications in Geochemistry and Soil Chemistry", Pergamon Press, p. (1987).
4. R. E. Botto, Energy & Fuels, **1**, 228 (1987).
5. R. Hayatsu, R. G. Scott and R. E. Winans, In "Oxidation in Organic Chemistry" Part D, Academic Press, p. 279 (1982).
6. R. Hayatsu, R. L. McBeth, R. G. Scott, R. E. Botto and R. E. Winans, Org. Geochem., **6**, 463 (1984).
7. R. Hayatsu, R. E. Botto, R. G. Scott, R. L. McBeth and R. E. Winans, Fuel, **65**, 821 (1986).
8. R. Hayatsu, R. E. Botto, R. L. McBeth, R. G. Scott and R. E. Winans, Energy & Fuels, submitted.
9. A. Sakakibara, Wood Sci. Technol. **14**, 89 (1980).
10. N. Morohoshi and W. G. Glasser, Wood Sci. Technol., **13**, 165 (1979).
11. R. M. Roberts and A. A. Khalaf, "Friedel-Crafts Alkylation Chemistry", Marcel Dekker, (1984).
12. P. Laszlo (Ed.), "Preparative Chemistry Using Supported Reagents", Part VIII, Academic Press, (1987).
13. T. P. Goldstein, Am. Assoc. Petrol. Geol. Bull., **67**, 152 (1983).
14. P. Laszlo, Acc. Chem. Res., **19**, 121 (1986); Science, **235**, 1473 (1987).

THE DESULFURIZATION OF COAL AND MODEL COAL COMPOUNDS IN AMBIENT TEMPERATURE MOLTEN SALTS

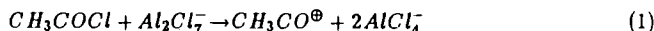
David S. Newman, Ellen M. Kurt, and Denguan Chen
Department of Chemistry
Bowling Green State University
Bowling Green, Ohio 43403

ABSTRACT

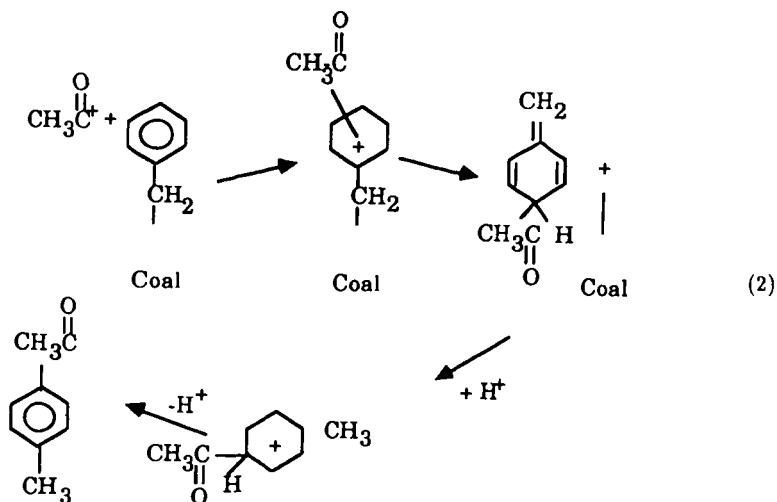
An ambient temperature molten salt, $C_5H_5N^+ \cdot Al_2Cl_7^-$ (pyridinium heptachloroaluminate) containing dissolved $CdCl_2$ was used as the reaction medium and catalyst for the acylation and concomitant desulfurization of IL #6 coal and several model coal compounds. The reactions were done at 40°C and 1 at. pressure and, in the case of the model compounds, products were identified and mechanisms proposed.

INTRODUCTION

Gaseous byproducts of the combustion of coal are the major contributors to acid rain. Since a gradual change from a primarily petroleum-based economy to a coal-based economy is virtually inevitable, cleaning, liquefying, gasifying, and generally modifying coal have become major goals of chemistry and chemical engineering. Ideally, coal should be modified by means of chemical scission reactions which remove designated portions of the coal or break specific chemical bonds via a known mechanism. Moreover, these scission reactions should occur at ambient temperature and atmospheric pressure so that unwanted side reactions occur at a minimal rate. To this end we have developed a series of Friedel-Crafts acylations and alkylations that take place in the ambient temperature molten salt $C_5H_5N^+ Al_2Cl_7^-$ (pyridinium heptachloroaluminate). (1,2,3,4) For Example, we found that F-C alkylation of PSOC 244 high sulfur coal increased its solubility in a 3:1 benzene/methanol solution approximately five fold relative to the untreated demineralized coal. (1,2) We also found that acylating IL #6 coal with acetyl chloride in this medium increased its solubility in 3:1 benz/methanol by about a factor of five. (3,4) The increased solubility is caused by hydrogen ions breaking the methylene chains holding the sub units of the coal macromolecule together. The mechanism for the acylation and accompanying depolymerization is most likely: (3,5,6)



followed by:



The proton then reacts with AlCl_4^- :

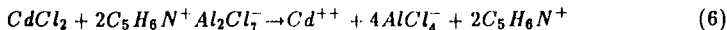


Both AlCl_3 and HCl have been identified as reaction products. The net reaction is



In 1980 Mobley and Bell found that ZnCl_2 catalyzed the removal of sulfur from the model coal compounds dibenzyl sulfide and tetrahydrothiophene and a variety of solid sulfides were identified. The net result of the ZnCl_2 -model compound interaction was the breaking of the aliphatic -C-S bond in each of the model compounds. (7) The ZnCl_2 had little effect on aromatic C-S bonds in thiophene and diphenyl thiophene. The mechanism suggested by Mobley and Bell for the catalytic reaction is somewhat similar to the mechanism for the F-C acylation or alkylation of coal or model compounds in pyridinium heptachloroaluminate. Since CdCl_2 is more soluble in this melt, (8) and also has a great affinity for sulfur, we

decided to dissolve CdCl_2 in the heptachloroaluminate melt. The dissolution reaction is probably,



The $\text{C}_5\text{H}_6\text{NAl}_2\text{Cl}_7$ acts as an acid and the CdCl_2 acts as a base. We then used the Cd^{++} containing melt as both catalyst and reaction medium for the removal of sulfur from model compounds and from coal. We also thought that the scission of C-C- and C-S bonds, as well as the formation of sulfides, would be facilitated by the F-C reactions and by the aluminum ion which forms an extremely stable sulfide. Hydrogen ions, arising from a variety of sources, would also be expected to facilitate the formation of H_2S .

The F-C experimental conditions were similar to those used in earlier studies. (2,3,4)

RESULTS AND DISCUSSION

Reactions of Model Coal Compounds

1. Dibenzyl Sulfide

Dibenzyl sulfide (0.0041 moles) was dissolved in 0.1143 moles of pyridinium heptachloroaluminate to which 0.0071 moles of acetyl chloride and 0.0027 moles of CdCl_2 were added. The mole fraction of CdCl_2 in the slurry was 0.022. The reaction was allowed to proceed under N_2 for 20 hours at 40°C whereupon it was quenched with water. The inorganic compounds $\text{HCl}(\text{g})$, $\text{H}_2\text{S}(\text{g})$ and $\text{AlCl}_3(\text{g})$ were isolated and identified as reaction products. The organic reaction products tentatively identified by GC/MS are listed in Table 1 in order of abundance.

In addition to the compounds listed in Table I, unidentifiable polymeric material was obtained. A second mixture with different concentrations (melt, 0.1200 moles; dibenzyl sulfide, 0.0076 moles; acetyl chloride, 0.0615 moles; CdCl_2 , 0.0081 moles) was allowed to react under N_2 for 20 hours at 40°C . The same products, in different proportions, were identified.

Some of the original cadmium was found in the aqueous layer, and some was incorporated into a black precipitate which formed during the reaction. It is not clear what percentage of the model compound's C-S bonds were broken, but our estimate is that approximately half were cleaved under the reaction conditions used. We think that if reaction conditions were optimized for sulfur removal, all of the C-S bonds in dibenzyl sulfide could be broken.

2. Thiophene

Thiophene (0.0106 moles) was allowed to react with acetyl chloride (0.0625) moles in the Cd^{++} containing melt. $\text{H}_2\text{S}(\text{g})$ was identified along with $\text{HCl}(\text{g})$ and $\text{AlCl}_3(\text{g})$. A yellow filtrate was collected upon filtration of the quenched reaction products. A solid precipitate formed which consisted of brownish-white crystals and a few black crystals. Both Cd and Al were found in the precipitate, as well as some polymeric material that could not be identified. The yellow liquid contained unreacted thiophene, acylated thiophene, and several species which have not been identified yet. Since the H_2S and probably the Cd and Al found in the precipitate arose from a reaction of the thiophene with the melt, aromatic C-S bonds had to have been broken! This was not found to occur with ZnCl_2 even though the reaction conditions were much harsher (250°C , 10 atm pressure). (7)

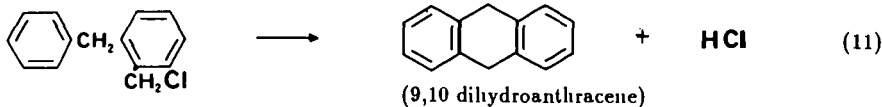
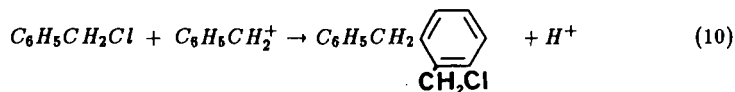
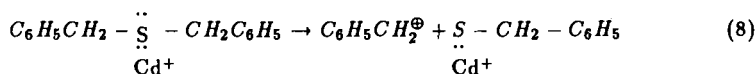
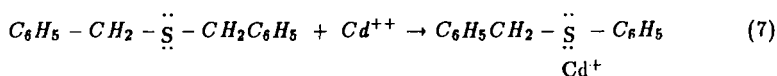
3. Dibenzothiophene

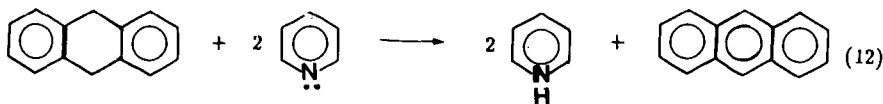
Dibenzothiophene did not react to a measurable degree under the previously described experimental conditions.

II. IL #6 Coal

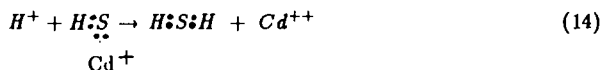
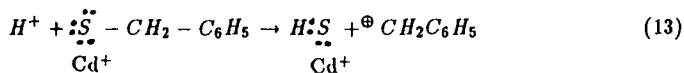
A 1 g sample of HF/HCl demineralized IL #6 coal (batch # I.D. 301.00135) was slurried in 50 ml of Cd^{++} containing heptachloroaluminate molten salt to which 1 g of acetyl chloride was added. The reaction was allowed to continue for 16 hours under nitrogen atmosphere. The procedure is similar to that used in earlier studies. (1,2,3) The coal's solubility was then measured in 3:1 benz/methanol and found to be 11.7%. A small quantity of H_2S was identified as a reaction product of the F-C acylation by allowing the N_2 carrier gas to pass through an aqueous $CdCl_2$ solution and observing the precipitation of CdS . The total sulfur content of the insoluble and soluble portions of the coal were analyzed and compared with the sulfur content of the original demineralized coal. The difference between the sulfur content of the reacted and original coal is assumed to have formed H_2S . The data are shown in Table II. The sulfur containing compounds formed during the reaction will be identified where possible and the results reported at a later date.

The formation of anthracene or phenanthrene from dibenzyl sulfide is perhaps the most unexpected aspect of the model coal compound study. A plausible mechanism that fits all of the data is the following:





In order to substantiate this mechanism, benzyl chloride was added to the melt and allowed to react for 20 hours at 40°C. GC/MS of the precipitate gave the same spectrum as authentic anthracene alone. To establish the presence of 9,10 dihydroanthracene as an intermediate in the reaction, authentic dihydroanthracene was added to the neat melt and allowed to react for 20 hours at 40°C. GC/MS of the precipitate showed the same spectrum as anthracene alone did. The mechanism for H₂S formation is probably as follows:



The Cd⁺⁺ thus serves as a catalyst for the reaction. Al⁺³ also reacts very strongly with sulfur and its role in the desulfurization mechanism is currently under investigation.

CONCLUSION

The extremely mild conditions used for the solubilization and desulfurization of coal and model coal compounds indicate that the molten salt may be an extremely useful medium for coal chemistry. If the soluble coal compounds can be identified, the nature of the sulfur containing fragments of the coal macromolecule can also be determined with some degree of assurance because their structure is the same as, or at least mechanistically related to their structure, in the original coal. Furthermore, if reaction conditions are optimized, a very high percentage of a coal's sulfur can be removed at room temperature and atmospheric pressure.

ACKNOWLEDGMENT

We would like to thank the Alumni Undergraduate Research Program at Bowling Green State University and the Research Challenge Program of the State of Ohio for their support. We would also like to thank the Premium Coal Sample Program at Argonne National Laboratory for contributing the coal samples.

LIST OF REFERENCES

1. D. S. Newman, R. E. Winans, "Proceedings of the Third International Symposium on Molten Salts," G. Mamantov, M. Blander, G. P. Smith, Editors, The Electrochemical Society Softbound Series, p. 425, Pennington, NJ, 1981.
2. D. S. Newman, R. E. Winans, R. L. McBeth, *J. Electrochem. Soc.* **131**, 1079 (1984).
3. D. S. Newman, T. H. Kinstle, G. Thambo, "Proceedings of the Joint International Symposium on Molten Salts," G. Mamantov, M. Blander *et al.* Eds., The Electrochemical Society, Pennington, NJ 1987, p. 991-1001.
4. D. S. Newman, T. H. Kinstle, G. Thambo, R. E. Winans, R. Hayatsu, R. L. McBeth, "Energy and Fuels," submitted for publication, 1988.
5. J. A. Boon, J. A. Levisky, J. L. Pflug, J. S. Wilkes, *J. Org. Chem.* **51**, 480 (1986).
6. J. A. Boon, S. W. Lander, J. A. Levisky, J. L. Pflug, L. M. Skizynecki-Cooke, J. S. Wilkes, "Proceedings of the Joint International Symposium on Molten Salts," G. Mamantov, M. Blander *et al.* Eds., The Electrochemical Society, Pennington, NJ 1987, p. 979-990.
7. D. P. Mobley and A. T. Bell, *Fuel* **59**, 507 (1980).
8. R. R. Rhinebarger, Ph.D. Thesis, Michigan State University (1986).

Table I. Organic Reaction Products of Dibenzyl Sulfide at 40°C

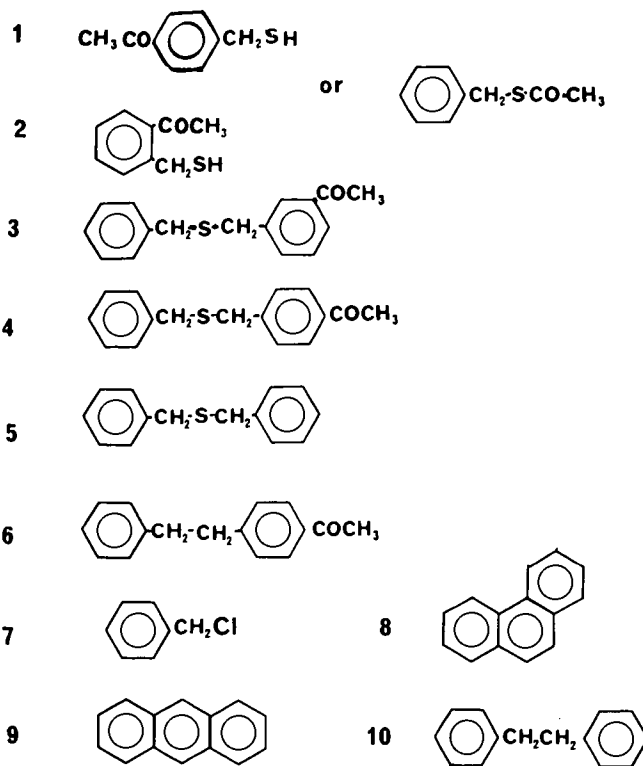


Table II. Weight Percent Sulfur in Coal Samples

Original Coal	Insoluble Portion	Soluble Portion
4.57	3.37	2.42

This page intentionally left blank

THE EFFICIENT, LARGE SCALE SEPARATION OF COAL MACERALS

Gary R. Dyrkacz and C.A.A. Bloomquist

Chemistry Division, Argonne National Laboratory,
9700 South Cass Avenue, Argonne, IL 60439

INTRODUCTION

For fundamental work on the chemical structure of coal, one of the first tasks that should be performed on a coal sample is to ensure that it is as homogeneous as is currently possible. This should require, at the very least, a petrographic analysis, and in many cases a subsequent separation to regulate the quality of the maceral or maceral group, even if the coal sample is optically monomaceral. Dyrkacz et al. have shown that even "pure" vitrinite shows a density distribution, which is, in part, related to differences in chemistry within the vitrinite maceral group.¹⁻³ However, despite the probability that experimental data may suffer from poorly characterized coal samples, it is not traditional practice to be concerned with the maceral separation of coal. The primary reason for this is that maceral separation is considered to be tedious and time-consuming. There is some truth in this statement, but the underlying question which should be asked is what is more important, the credibility and general applicability of the research data, or the additional time required to do a physical separation.

In our continuing efforts in the area of maceral separation, we have recognized the need for a process to supply relatively large amounts of macerals as rapidly as possible. Earlier we reported some initial work using combined sink/float and density gradient centrifugation (DGC) or continuous flow centrifugation and DGC.⁴ These early results indicated that continuous flow separation was somewhat effective, but beset with equipment specific difficulties.

Nevertheless, there are several notable advantages in using continuous flow centrifugation for maceral separation. First, the coal particles can be in a highly dilute suspension, which reduces particle-particle interactions. Second, large amounts of material can be separated; the major limitation being the capacity of the rotor. Third, the separation efficiency is higher. Unlike batch sink/float centrifuge operations, there are less cross-contamination problems with removal of the light and heavy particles, since the light phase is continuously removed. Lastly, the separation is fast. To produce an equivalent amount of purified coal material, much less manipulation is necessary to achieve separation compared to batch sink/float.

With all of these advantages in mind, we have again turned our investigations to continuous flow centrifugation for maceral separations. However, this time we are using a centrifuge specifically designed for such work. We report here our initial investigations on the separation of the maceral groups from Lewiston-Stockton coal from the Argonne Premium Coal Sample Program (APCS-7).

EXPERIMENTAL

Coal Pre-treatment. The APCS-7 coal (-100 mesh) was ground to 1-2 microns average particle size using a Fluid Energy Mill (Sturtevant). The coal was then demineralized using HCl and HF as we have previously reported.⁵

Continuous Flow Centrifugation Procedure. A continuous flow centrifuge (CEPA-LE Laboratory centrifuge, Carl Padberg Zentrifugenbau GmbH; U.S. supplier: New Brunswick Scientific Co., Inc.) with a model "K" clarifier rotor was used for the work reported here. A Sharples model T-1, (PenWalt Corp.), with a 1-H clarifier rotor was also used for some early work. Rotor speed was measured with a Xenon strobe lamp and maintained at 37000 ± 2000 rpm. A peristaltic pump (Masterflex, Model 7520-00, Cole-Parmer) was used to pump the coal slurry through the spinning rotor at a flow rate of 160 mL/min. Before the coal slurry was fed into the rotor, clear solution was used to fill the rotor. Clear solution was also used after the separation to ensure that all the floating coal had been removed. The rotor effluent and deposit were filtered, washed with water, dried and weighed. When the rotor was stopped, fluid that remaining in the spinning rotor drained out. This material was collected and analyzed separately.

DGC Monitoring of the Continuous Flow Separation. Aliquots of the three fractions: effluent (float), deposit (sink) and rotor liquid, derived from the continuous flow centrifuge separation were analyzed by the analytical density gradient centrifugation procedures of ref. [5].

RESULTS

The continuous flow centrifuge that we employed is commonly used for separation of biological materials, such as the harvesting of cells or other biological particulates. This centrifuge is a much simpler design than we used previously.⁴ The heart of the centrifuge is the rotor which consists of a simple rotating hollow cylinder which narrows to an open tube at the bottom and has holes drilled perpendicular to the main axis for the fluid to exit at the top. The expelled effluent is retained by an encircling collector ring. Fluid is injected into the rotor at the bottom through a nozzle centered in a lower bearing assembly. A series of radial vanes within the bottom of the rotor help accelerate the fluid to the rotor velocity. From this description, it is obvious that the CFC process is not truly continuous, since once the rotor deposit nearly fills the rotor, operation must be suspended long enough to empty the rotor. However, this represents only a minor inconvenience when compared to the manipulations involved in a sink/float centrifuge separation.

The coal sample that was chosen for our investigations was the Lewiston-Stockton coal (APCS-7) from West Virginia. This coal is reported to have a high proportion of all three maceral groups. Our own petrographic analysis shows this coal to contain 11.5% liptinite, 72.8% vitrinite and 15.6% inertinite.

There are two ways to analyze the efficiency of the continuous flow procedure. One of the more common approaches is to petrographically analyze the samples generated in the CFC separation. However, we know that the maceral groups have particle density distributions that naturally overlap each other.² Thus, the presence of more than one maceral type in a sink or float fraction does not necessarily translate to a bad separation. Since petrographic analysis is not

able to make such fine distinctions, we chose to use density gradient centrifugation (DGC) to determine the true state of the separated material.

To effectively use DGC, it is first necessary to obtain the density distribution of the unseparated coal. Figure 1 represents the separation and maceral analysis of a two gram sample of APCS-7 coal, using a CsCl/Brij-35 aqueous gradient. This maceral distribution pattern is consistent with other coals of similar rank.^{2,4}

Two CFC separations were done on APCS-7 using separate samples. The density cuts were made at 1.232 and 1.332 g cm⁻³ using CsCl/Brij-35 aqueous solutions. From Figure 1, these densities are near the density points where equal amounts of either liptinite/vitrinite or vitrinite/inertinite particles should be present. The concentration of coal in the feed slurry was 40 g/L. This amount is not the highest slurry concentration that can be used, but instead represents a conservative experiment to demonstrate the separation. However, even this slurry concentration is still much higher than we would recommend for optimum resolution in simple sink/float maceral separations.

Once the separations were completed, the coal in each fraction was isolated by filtration, washed, dried and weighed. Figure 2 represents the sum of all the observations for these two individual separations. The data on the sink/float fractions, as we have already indicated, were derived from analytical DGC on very small amounts (2 mg) of each fraction. The vertical bars on the plots represent the densities of the solutions. Following any particular density distribution of a sink or float fraction (lower two plots), anything passing the vertical line represents cross-contamination. As can be seen some of the fractions are better than 90% disengaged. This result approaches the limit of analytical DGC to probe the CFC separation, since there is some unavoidable maceral band spreading which can give the false impression of contamination. On the other hand, there are some fractions which show substantial cross-contamination. The liptinite/vitrinite+inertinite separation shows a strong bimodal distribution in the float fraction, as does the sink fraction in the liptinite+vitrinite/inertinite separation.

The curves in the lower two plots of Figure 2 oversimplify a more complicated experimental reality, which more critically explains the reason for some fractions showing poorer maceral resolution. The sink data in Figure 2 are actually composed of two separate fractions. Three fractions are actually collected from each run: the float, which exits the rotor during the run, the sink, which is the deposit on the rotor wall, and a third portion, which is obtained from the solution left in the rotor when the run is completed. This additional fraction is collected once the velocity of the rotor decreases below a certain limit. The centrifugal force becomes too low to retain the fluid, and it drains out the bottom of the rotor. It is the sum of this material and the material deposited on the rotor wall, which is shown in Figure 2. Figures 3 and 4 show all three fractions from both density cuts. Each density distribution curve has been normalized to the highest absorbance value (roughly proportional to mass). Notice that all the fractions labeled as sink (material on rotor wall) are actually well separated. The fraction labeled as rotor drainage (Rtr. Drng.) exhibits a high degree of cross-contamination in both runs. Table 1 provides the separation data on the purity of the fractions; the data is derived by integrating the analytical DGC results before and after the solution density cut line shown in either Figures 2 or 3. Without the inclusion of the rotor drainage material (which can account for approximately 50% of the sink material

collected), the material deposited on the rotor wall shows excellent resolution from float material.

We have attributed the behavior of this rotor drainage fraction to the sum of several processes:

1. When the solution in the rotor drains out at the end of the run, some of the material from the rotor wall is unavoidably carried away in this process. At this time we cannot say how much. The level of contamination with sink material may be high because in our tests relatively small amounts of coal (20 grams) are being separated and are being deposited in a narrow area of the rotor.
2. The coal particles have a range of particle size from about 0.5 to 6 microns. The very fine particles may not have time to separate during their passage through the rotor and may be held up in the rotor.
3. Some of the material cannot be separated because it is at or very close to the same density as the solution density.

We have examined several of the float contaminations in our sink fractions under the microscope, and indeed have found that finer material is present in much higher concentration than in the feed. In the case of the liptinite/vitrinite+inertinite separation in Figure 3 the float fraction also shows a large contamination peak. We have determined that the high density peak is due to the presence of extremely fine particles (< 1 micron). This fact suggests that the high density peak does not represent the true amount of material. We have observed previously that fine particles may give rise to a much larger absorbance than larger particles due to greater scattering. The purity in this case should be considered as a minimum enrichment.

DISCUSSION

We believe that the separation of macerals by continuous flow centrifugation offers a simple technique for the large scale separation of macerals. With relatively little cost (~ \$10K), it provides an opportunity for obtaining quite pure maceral fractions. Although we have not completely worked out all the nuances of this separation system, we believe that the problems we have indicated can be minimized to pose only minor inconvenience.

We cannot say that this system completely bypasses the disagreeable tedium or time involved in separating macerals, nor will it by itself overcome the mental inertia required to make maceral separation an accepted necessary fact in fundamental coal science. However, we find our particular brand of continuous flow centrifugation is considerably faster than sink/float separation, can provide a good quality product with even one separation cycle, and permits the handling of more material than a conventional sink/float centrifuge separation.

ACKNOWLEDGMENTS

This work was performed under the auspices of the Office of Basic Energy Sciences, Division of Chemical Sciences, U.S. Department of Energy, under contract W-31-109-ENG-38.

REFERENCES

1. Dyrkacz, G.R., Bloomquist, C.A.A., and Ruscic, L., Fuel, **63**, 1166-1173 (1984).
2. Dyrkacz, G.R., Bloomquist, C.A.A., and Ruscic, L., Fuel, **63**, 1367-1373.
3. Dyrkacz, G.R., Bloomquist, C.A.A., Ruscic, L. and Crelling J., to be published.
4. Dyrkacz, G.R., Bloomquist, C.A.A., and Horwitz, E.P., Sep. Sci. Tech., **16**, 1571-1588 (1981).
5. Dyrkacz, G.R., and Horwitz, E.P., Fuel, **61**, 3-12 (1982).

TABLE 1. Analysis of Continuous Flow Centrifugation Separation by Analytical Density Gradient Centrifugation.

Percent Purity of Fraction from DGC			
Float	Rotor Drainage	Rotor Deposit	Total Sink
Cut Density = 1.232 g cm ⁻³			
47.9	95.7	99.6	98.6
Cut Density = 1.332 g cm ⁻³			
97.4	59.3	97.6	79.4

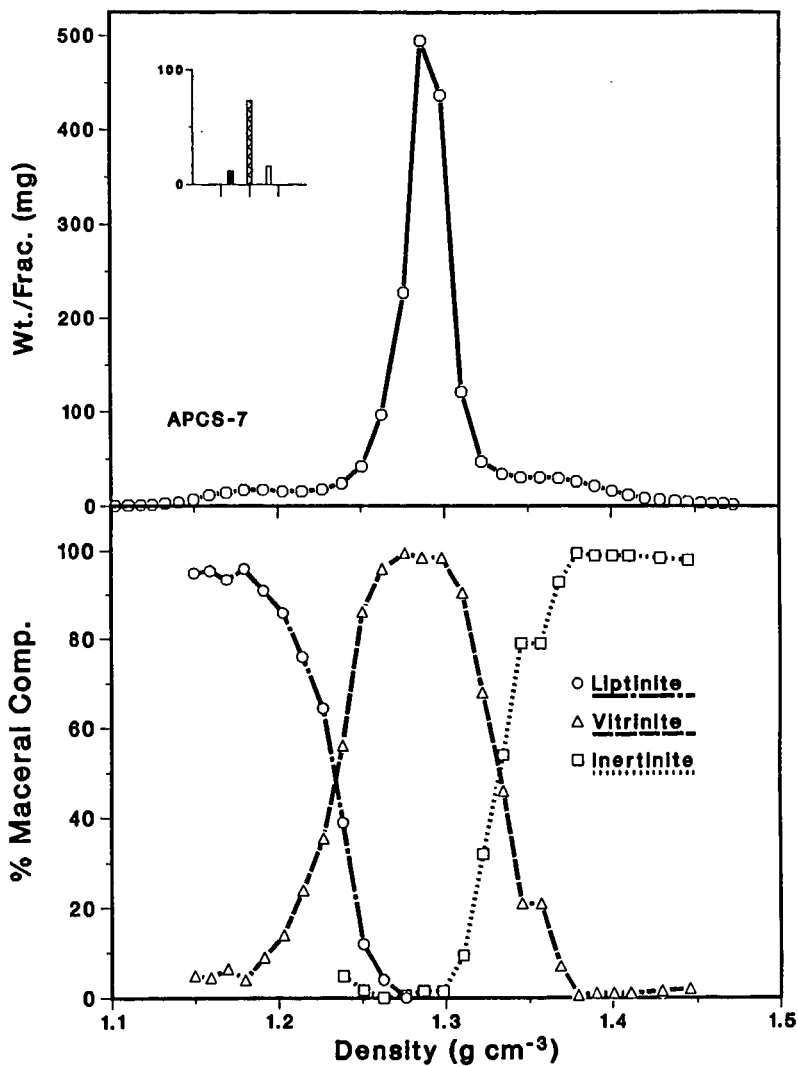


Figure 1. Maceral density distribution of APCS-7 coal obtained by DGC. Lower plot is the maceral analysis of selected density fractions. All densities are at 25°C.

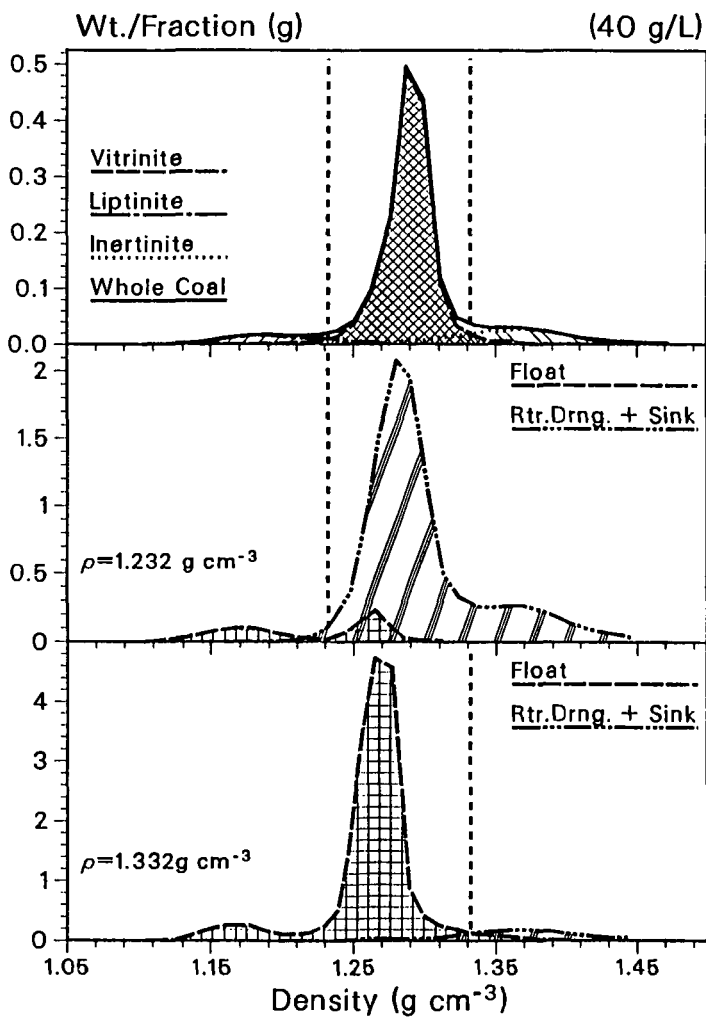


Figure 2. Top: Maceral density distributions of APCS-7 showing the actual weight distribution of each maceral group. Middle: DGC separations of float and sink CFC fractions for removing liptinite from vitrinite + inertinite. Bottom: DGC separations of float and sink CFC fractions for removing vitrinite + liptinite from inertinite. Absorbance is roughly proportional to weight.

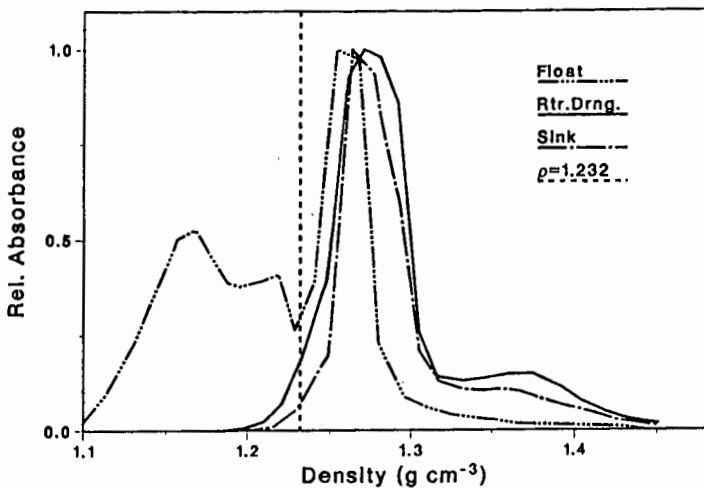


Figure 3. Detailed DGC pattern for the three collected CFC fractions for liptinite removal. All distributions have been normalized to the highest peak in each individual fraction.

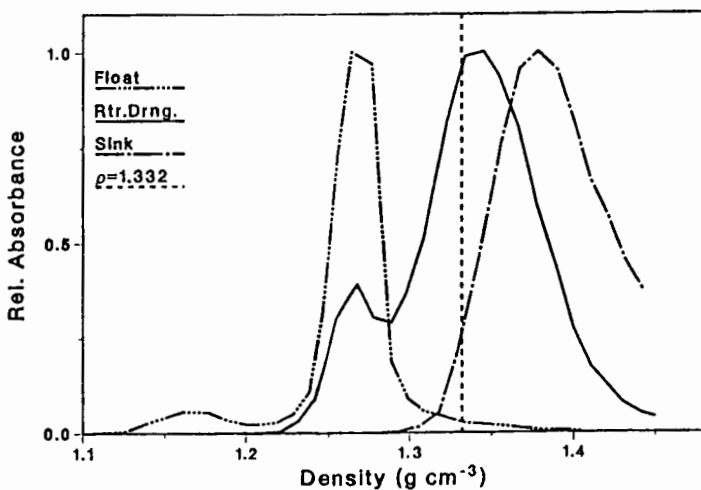


Figure 4. Detailed DGC pattern for the three collected CFC fractions in inertinite removal. All distributions have been normalized to the highest peak in each individual fraction.

WEATHERING STUDY OF ARGONNE PREMIUM COAL SAMPLES
BY FTIR AND MOSSBAUER SPECTROSCOPY

K.A. Martin
S.S. Chao

Institute of Gas Technology
Chicago, Illinois 60616

INTRODUCTION

A considerable number of infrared studies have been done on the low-temperature oxidation of coal with conflicting results. Because the reactions occurring in coal are dependent on a number of factors such as coal rank, particle size, temperature and humidity, a consensus on the oxidation mechanism(s) has not been achieved. Oxidation has been found to produce ethers (1-4), carboxyl groups (2-6), and OH functionalities (5). The formation of a peroxide is generally considered to be the major pathway for the production of new oxygen-containing groups, while at the same time a decrease in the aliphatic CH stretching region is observed (1,5) corresponding to dehydrogenation. The present study is an attempt to use FTIR to follow the effects of mild weathering conditions on a series of standard coal samples. In one part of the study, the room temperature desorption of moisture from these coals was followed using diffuse reflectance spectroscopy (DRIFT), and in the other part, the coals were weathered at room temperature in water-saturated air and sampled at intervals over a three month period for FTIR and Mössbauer analysis.

EXPERIMENTAL

Eight Argonne premium coal samples (-100 mesh) were studied: Pennsylvania Upper Freeport, Wyodak, Illinois #6, Pittsburgh #8, Pocahontas #3, Utah Blind Canyon, West Virginia Stockton-Lewiston, and Beulah-Zap. After thorough mixing, each ampoule of PCSP coal was opened and about 300 mg of the neat sample was transferred to a DRIFT sample cup and enclosed in an environmental chamber in a stream of dry air (2 ml/sec). Infrared spectra were collected at intervals over an eight hour period and again after 24 hours with a Nicolet 60SXB FTIR using 300 scans at 4 cm^{-1} resolution. The same dried KBr reference was used for each series of spectra and, because difference spectra were obtained, the KBr did not contribute to the absorption in the OH region.

For the longer-term study, a second vial of the coal was opened and the coal transferred to a large petri dish which was placed in a large dessicator (without dessicant) through which water-saturated air at 22°C was flowed at a rate of approximately 1 ml/sec. Portions of the coal were removed at intervals of 0, 1, 4, 24, and 48 hours, 1 week, and 1 and 3 months. These samples were dried in a vacuum oven at 40°C for two hours to halt the weathering process and stored under vacuum prior to analysis. Each sample was divided into different portions for infrared, Mössbauer and elemental analysis. Another 0.5 g of the original coal was removed to make the low-temperature ash (International Plasma Machine 1101B, 130 Watts for several days). DRIFT spectra were obtained on the neat coal sample with an environmental chamber for the non-weathered coal and without an environmental chamber for all DRIFT samples. Transmission spectra were obtained on KBr

pellets (about 0.3% coal by weight). All spectra were collected at 4 cm^{-1} resolution using 500 scans for the DRIFT spectra and 128 scans on the KBr pellets. Samples for Mössbauer analysis were prepared by grinding 0.3-0.6 g of the coal with 0.8 g of SOMAR blend, an organic binding agent, and pressing the samples into 32 mm diameter pellets. Mössbauer spectra were obtained on a Ranger Scientific MS-900 spectrometer at room temperature for 1-3 days. Carbon, hydrogen and nitrogen analyses were performed with a LECO CHN-600 analyzer, and oxygen analyses were performed with a Carlo ERBA 1106 elemental analyzer.

RESULTS AND DISCUSSION

Moisture Desorption

The desorption of water from the fresh coal samples was followed by DRIFT in the region $3800\text{-}2800\text{ cm}^{-1}$. DRIFT is especially useful for this type of study because it eliminates the error associated with water which may be trapped in a KBr pellet. This method has been used previously to study water desorption at elevated temperatures (7). The decrease in the integrated area of the OH region from the fresh coal to the vacuum-dried coal can be directly related to the moisture content determined by a separate procedure. In this case, absorbance units were used rather than the Kubelka-Munk units normally used for DRIFT spectra with good results. Table 1 gives the moisture contents of the initial coals and the moisture contents remaining after 1/2 hour and 8 hours of exposure to a stream of dry air at room temperature. Eight hours was found to be sufficient to remove over 90% of the moisture in all but the Illinois and Pittsburgh coals. Between one-third to one-half of the water was removed within the first half-hour of drying with the rate of desorption proportional to the initial moisture level. Spectral subtraction revealed no other changes in the spectrum other than a negative band near 1640 cm^{-1} as water was removed.

Weathering

Weathering under humid conditions over a longer period of time showed other changes in the OH region. DRIFT spectra of the vacuum-dried coals show an increase in the OH band over periods of 1 week and 1 month (Figure 1) with the largest increases found in the Pittsburgh, Illinois, Beulah-Zap and Blind Canyon coals and the least increase in the Pocahontas coal. Simultaneously, a slight increase in absorption centered around 1100 cm^{-1} is observed in all of the KBr pellet coal spectra after 1 week and after 1 month of weathering. An increase in this region after weathering is usually attributed to ethers but may also be due to alcohol groups. Other increases were apparent in the carbonyl region $1800\text{-}1500\text{ cm}^{-1}$ after 1 month (Figure 2). A weak band at 1710 cm^{-1} , not very apparent in the compressed spectra of Figure 2, appears in the subtraction spectra of the Pocahontas and Wyodak coals. All of the coals show an increase near $1660\text{-}1630\text{ cm}^{-1}$, which may be due to highly hydrogen-bonded carbonyls or to water bending modes from water of hydration which is not removed by vacuum. All of the coals except Pennsylvania and Pocahontas show a slight increase in the region $1560\text{-}1540\text{ cm}^{-1}$, which may arise from the formation of carboxylate groups.

In contrast to previous studies which found ether formation the dominant reaction under low temperature oxidation conditions (1-2), these results indicate the formation of an OH group, from either a hydroxyl functionality or water of hydration. This formation is only slightly dependent on coal rank, as the Pennsylvania and Pocahontas coals form the least amount of OH, but the other coals form OH in a manner independent of rank. The formation of ether groups and/or alcohol groups is indicated by the increase near 1100 cm^{-1} . The new bands near 1650 cm^{-1} may be due to water or to a shift in carboxyl group frequency due to increased hydrogen bonding, as might occur with the formation of OH groups, or to oxidation to new carbonyl groups. Carboxylate groups appear to form for all but the highest rank coals. In conclusion, new functional groups are formed on coal after weathering under humid conditions at room temperature for as little as 1 week. These include carboxylate groups on all but the Pennsylvania and Pocahontas coals, carbonyl groups on the Pocahontas and Wyodak coals, and chemisorbed water, alcoholic or ether groups.

ACKNOWLEDGMENT

The authors thank Dr. Karl Vorres of Argonne National Laboratory for the coal samples.

REFERENCES

1. R. Liotta, G. Brons and J. Isaacs, Fuel **62**, 781 (1983).
2. J. S. Gethner, Appl. Spec. **41**, 50 (1987).
3. G. P. Huffman, F. E. Huggins, G. R. Dunmyre, A. J. Pignocco and M. C. Lin, Fuel **64**, 849 (1985).
4. D. C. Cronauer, R. G. Ruberto, R. G. Jenkins, A. Davis, P. C. Painter, D. S. Hoover, M. E. Starsinic and D. Schlyer, Fuel **62**, 1124 (1983).
5. A. G. Pandolfo, R. B. Johns, P. D. Nichols and D. C. White, ACS Preprints, Division of Fuel Chemistry **32**, 171 (1987).
6. B. M. Lynch, L. I. Lancaster and J. A. MacPhee, ACS Preprints, Division of Fuel Chemistry **32**, 139 (1987).
7. N. R. Smyrl and E. L. Fuller, in "Coal and Coal Products: Analytical Characterization Techniques", E. L. Fuller, Ed., ACS Symposium Series 205, American Chemical Society, Washington, D.C., Chap. 5, 1982.

kate

Table 1. Moisture Content of Coals After Room Temperature Air-Drying

	Initial Moisture, %	Moisture Remaining After 1/2 Hour, %	Moisture Remaining After 8 Hours, %
Pocahontas	0.84	0.42	0
Pennsylvania	1.41	1.01	0
Pittsburgh	2.54	1.31	0.32
Lewiston-Stockton	2.70	1.69	0.27
Blind Canyon	5.04	2.38	0
Illinois	8.65	5.83	1.41
Wyodak	24.23*	15.00	0.24
Beulah-Zap	32.84*	25.45	0.92

*From PCSP provided data.

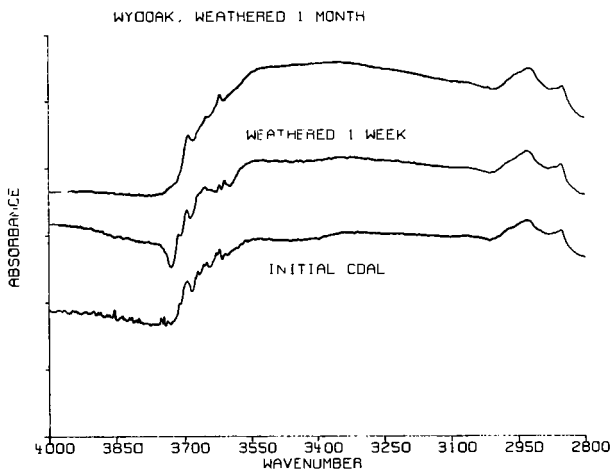


Figure 1. Increase in OH region over one month (Wyodak coal).

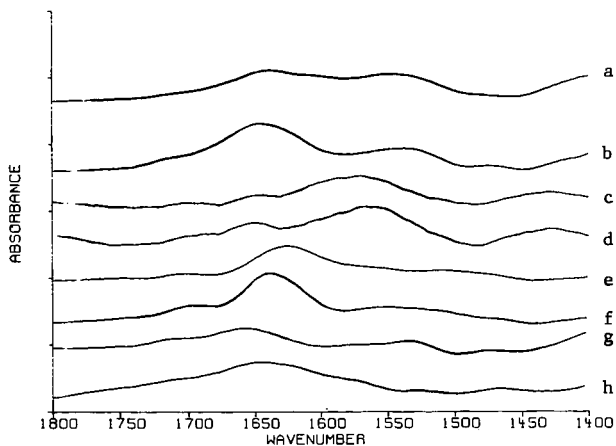


Figure 2. Change in carbonyl region over one month (a = Pittsburgh, b = Illinois, c = Lewiston-Stockton, d = Blind Canyon, e = Pennsylvania, f = Pocahontas, g = Wyodak, h = Beulah-Zap).

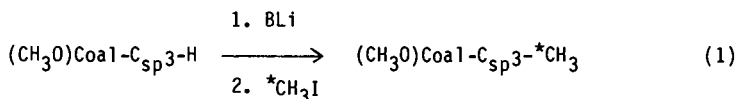
THE IMPORTANCE OF DIPHENYLMETHANE-LIKE STRUCTURAL UNITS
IN AN ARGONNE PREMIUM COAL SAMPLE*

R. Rife Chambers, Jr., E. W. Hagaman and M. C. Woody
Chemistry Division
Oak Ridge National Laboratory
Oak Ridge, Tennessee 37831-6197

INTRODUCTION

The development and application of chemical and spectroscopic techniques for the purpose of evaluating the acidic O-H and C-H sites in coal has received much attention recently (1-8). In general, these studies have relied on the ability of bases to abstract acidic protons from O-H and C-H sites to generate coal anions. These anions can then be alkylated with a variety of reagents which includes alkyl halides (2,5), alkyl tosylates (4) and alkyl sulfates (6,8). The resultant coal derivatives can be studied by using a combination of chemical and spectroscopic probes such as Soxhlet extractability (2,5), pyrolytic behavior (9) and ^{13}C NMR (2,6,7,8).

Our approach (3,6,8) for characterizing the acidic C-H bonds in coal is to treat O-methyl coal with a series of indicator bases, BLi, followed by methylation with C-13,14 double labelled methyl iodide, equation (1).



*C = 13,14C

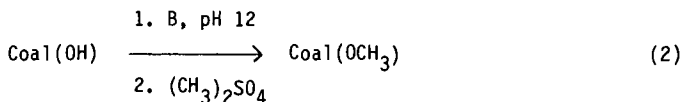
By varying the identity of BLi, and thus the pK_a of the conjugate acid BH, it is possible to evaluate the number of C-H bonds as a function of pK_a . The bases we have used thus far, 9-phenylfluorenyllithium (pK_a , 18.5 (10)), fluorenyllithium (pK_a , 22 (10)) and trityllithium (pK_a , 31 (10)), have allowed us to evaluate the distribution of acidic C-H sites within the three pK_a ranges: $12 < \text{pK}_a < 18.5$, $18.5 < \text{pK}_a < 22$, and $22 < \text{pK}_a < 31$. The application of this approach to two bituminous coals, namely Illinois No. 6 hvCb and PSOC 1197 lvb, led to the discovery of a significant concentration of acidic C-H sites with $18.5 < \text{pK}_a < 22$ which was interpreted as evidence for fluorene-like structural units in coal (6,8).

This approach to coal structure analysis is limited to the evaluation of acidic C-H sites with $\text{pK}_a < 31$. Furthermore, it was shown that PhCH₂Ph (pK_a , 33(11)), the prototypical diarylmethane, is not alkylated to a significant extent upon treatment with trityllithium and methyl iodide (12). For these reasons, we have developed approaches for the evaluation of acidic C-H sites with $31 < \text{pK}_a < 33$. In this article, we illustrate these approaches using Upper Freeport mvb (APCS number 1) as the coal.

*Research sponsored by the Division of Chemical Sciences/Office of Basic Energy Sciences, U.S. Department of Energy under contract DE-AC05-84OR21400 with the Martin Marietta Energy Systems, Inc.

RESULTS AND DISCUSSION

The Upper Freeport coal, empirical formula $C_{100}H_{76}S_{10}O_3$, was O-methylated at pH 12 by using tetrabutylammonium hydroxide as base and natural abundance dimethyl sulfate as previously reported (8), equation (2).



B = nBu₄NOH

Parallel experiments in which ¹⁴C-dimethyl sulfate was employed as the methylating agent established that no more than 0.4 O-methyl groups per 100 coal carbons are formed under these conditions.

The first approach to evaluate the C-H sites with $31 < pK_a < 33$ relies on a comparison of the relative reactivity of the O-methyl coal towards alkylation with base and ^{13,14}CH₃I, where the pK_a of the conjugate acid of the base equals 31 or 33. This was done using trityllithium (pK_a, 31 (10)) and diphenylmethyl-lithium (pK_a, 33 (11)) as the bases. Carbon-14 combustion analysis (13) was used to evaluate the number of methyls introduced with the two bases as a function of the number of repetitive treatments with base and methyl iodide. The data, as shown in Table 1, demonstrate the requirement for a minimum of three multiple treatments to achieve exhaustive methylation. This result parallels our earlier observations on the C-alkylation of O-methyl Illinois No. 6 (3) and O-methyl PSOC 1197 (6,8). This chemical property can be interpreted as evidence for the methylation of structural units which contain multiple acidic C-H bonds such as the methylene group, -CH₂-. The calculation of the number of acidic C-H bonds with $31 < pK_a < 33$ is done by making the difference: number of methyls added with diphenylmethyl-lithium minus number of methyls added with triphenylmethyl-lithium. For O-methyl Upper Freeport, this calculation yields $0.5 \pm 0.2/100$ coal C when the first treatment values are used and $1.1 \pm 0.3/100$ coal C after three treatments.

A second approach was also used to evaluate the number of C-H sites with $31 < pK_a < 33$. This involves the exhaustive methylation of all acidic C-H sites with pK_a < 31 followed by methylation using diphenylmethyl-lithium and ^{13,14}CH₃I. Alkylation of the acidic sites with pK_a < 31 was accomplished by treating O-methyl Upper Freeport with trityllithium and natural abundance methyl iodide a total of six repetitive treatments. Subsequent methylation of this coal derivative with diphenylmethyl-lithium and ^{13,14}CH₃I followed by ¹⁴C combustion analysis yielded a value of 0.9 C-H sites/100 coal C (1 treatment only). Further work is in progress to determine whether this value increases as a result of multiple treatments.

These preliminary data from the two complementary approaches indicate that diarylmethylene units, ArCH₂Ar, and substituted analogs such as ArC(H)R₂Ar which have C-H sites with $31 < pK_a < 33$ are important structural entities in the Upper Freeport coal. Considering only the first treatment data from each approach

where multiple alkylation at $-CH_2-$ groups is assumed to be negligible, then the number of these structural types can be estimated as 0.5 - 0.9 per 100 coal carbons.

REFERENCES

1. L. M. Stock, Coal Science, 1, 161 (1982).
2. (a) R. Liotta, Fuel, 58, 724 (1979). (b) R. Liotta, K. Rose, and E. Hippo, J. Org. Chem., 46, 277 (1981). (c) R. Liotta and G. Brons, J. Am. Chem. Soc., 103, 1735 (1981).
3. R. R. Chambers, Jr., E. W. Hagaman, M. C. Woody, K. E. Smith, and D. R. McKamey, Fuel, 64, 1349 (1985).
4. M. Ettinger, R. Nardin, S. R. Mahassay, and L. M. Stock, J. Org. Chem., 51, 2840 (1986).
5. N. Mallya and L. M. Stock, Fuel, 65, 736 (1986).
6. E. W. Hagaman, R. R. Chambers, Jr., and M. C. Woody, Energy and Fuels, 1, 352 (1987).
7. R. E. Botto, C. Choi, J. V. Muntean, and L. M. Stock, Energy and Fuels, 1, 270 (1987).
8. R. R. Chambers, Jr., E. W. Hagaman, and M. C. Woody, ACS Advances in Chemistry Series No. 217, 'Polynuclear Aromatic Compounds', L. B. Ebert, Ed., 255 (1988).
9. G. R. Rose, R. F. Zabransky, L. M. Stock, C. Huang, V. R. Srinivas and K. Tse, Fuel, 63, 1339 (1984).
10. D. A. Bors, M. J. Kaufman, and A. Streitwieser, Jr., J. Am Chem. Soc., 107, 6975 (1985).
11. A. Streitwieser, Jr., E. R. Vorpapel, and C. Chen, J. Am. Chem. Soc., 107, 6970 (1985).
12. R. R. Chambers, Jr., E. W. Hagaman, and M. C. Woody, Fuel, 65, 895 (1986).
13. V. F. Raaen, G. A. Ropp, and H. P. Raaen, 'Carbon-14', McGraw-Hill: New York, 1968, Chapter 11.

Table 1. C-Methylation of O-Methyl Upper Freeport by using BLi and $^{13,14}\text{CH}_3\text{I}$ in THF at 0°C

Base, BLi (pK_a , BH)	Treatment No.	No. $^{14}\text{CH}_3/100$ Coal C
trityllithium (31)	1	0.61 ± 0.06
	2	0.90 ± 0.09
	3	1.1 ± 0.1
diphenylmethylithium (33)	1	1.1 ± 0.1
	2	1.8 ± 0.2
	3	2.2 ± 0.2